

TECHNISCHE UNIVERSITÄT MÜNCHEN

Lehrstuhl für Biotechnologie

Structure and Function of the Surrogate Light Chain

Natalia Catalina Sarmiento Alam

Vollständiger Abdruck der von der Fakultät für Chemie der Technischen Universität München zur Erlangung des akademischen Grades eines Doktors der Naturwissenschaften (Dr. rer. nat.) genehmigten Dissertation.

Vorsitzender: Univ.–Prof. Dr. M. Feige

Prüfer der Dissertation: 1. Univ.–Prof. Dr. J. Buchner

2. Univ.–Prof. Dr. B. Reif

Die Dissertation wurde am 04.03.2015 bei der Technischen Universität München eingereicht und durch die Fakultät für Chemie am 20.04.2015 angenommen.

Dedicado a mis padres

Contents

Contents	i
Summary.....	1
1. Introduction	3
1.1 Protein folding	3
1.2 Protein folding in the cell and molecular chaperones	5
1.3 Quality control in ER	7
1.4 Folding helpers dedicated to antibody folding	10
1.5 Antibodies	12
1.5.1 Folding pathway of antibodies	15
1.5.2 B cell development	16
1.6 The unique Surrogate Light Chain (SLC).....	19
1.6.1 Function of the SLC and the preBCR.....	19
1.6.2 Structure of the SLC.....	20
1.7 Objective.....	22
2. Materials and Methods	25
2.1 Materials.....	25
2.1.1 Chemicals.....	25
2.1.2 Equipment	26
2.1.3 Computer software, data base and web-base tools.....	28
2.1.4 Consumables	29
2.1.5 Enzymes, Size markers and Kits	29
2.1.6 Antibodies.....	29
2.1.7 Chromatography materials and columns	30
2.1.8 Buffers	30
2.1.8.1 Protein Purification	30
2.1.8.2 Buffers for SDS Polyacrylamide Gel electrophoresis.....	32
2.1.8.3 Buffers for Western Blotting	33
2.1.8.4 Buffers for Molecular Biology.....	33
2.1.8.5 Buffers for Biacore X100	33
2.1.8.6 Buffers for ELISA.....	33
2.1.9 Primers	34
2.1.10 Bacterial strains and Plasmids	36
2.1.11 Media for expression in <i>E. coli</i>	36
2.2 Molecular Biological Methods	37
2.2.1 <i>E. coli</i> cultivation & storage	37
2.2.2 DNA isolation and storage	38
2.2.3 Agarose gel electrophoresis for DNA separation	38

Contents

2.2.4	PCR amplification.....	38
2.2.5	Restriction and ligation protocols	39
2.2.6	Supercompetent <i>E. coli</i> cell preparation	41
2.2.7	Transformation of <i>E. coli</i> cell	41
2.3	Protein chemical methods	41
2.3.1	Expression test	41
2.3.2	Protein expression, harvest and cell disruption	43
2.3.3	Preparation of inclusions bodies for purification of insoluble proteins	44
2.3.4	Methods for protein purification.....	44
2.3.4.1	Affinity chromatography	44
2.3.4.2	Ion exchange chromatography	45
2.3.4.3	Protein refolding	45
2.3.4.3.1	Optimization of refolding conditions	46
2.3.4.3.2	Optimization of refolding buffer	47
2.3.4.4	Size exclusion chromatography (SEC)	47
2.3.4.5	Concentration of proteins	48
2.3.4.6	Protein dialysis	48
2.3.5	SDS-Polyacrylamide Gel Electrophoresis (SDS-PAGE)	48
2.3.6	Western Blotting for His-tagged domains	48
2.3.7	Protein labelling.....	49
2.3.8	Determination of protein concentration with Bradford.....	49
2.4	Spectroscopic methods.....	50
2.4.1	UV-Vis spectroscopy	50
2.4.2	Circular Dichroism (CD) Spectroscopy	51
2.4.3	Fluorescence Spectroscopy	52
2.5	Thermofluor Stability Assay (TSA).....	53
2.6	Quaternary structure and interactions analysis	54
2.6.1	Analytical gel filtration.....	54
2.6.2	Analytical ultracentrifugation.....	55
2.6.3	Nuclear Magnetic Resonance	55
2.6.4	Surface Plasmon Resonance.....	55
2.6.5	Enzyme-linked Immunosorbent Assay (ELISA)	56
3.	Results and Discussion	59
3.1	Expression, purification and characterization of the human SLC	59
3.1.1	Expression of human SLC in <i>E. coli</i>	59
3.1.1.1.	Attempts to produce soluble SLC proteins in <i>E. coli</i>	59
3.1.1.2.	Fermentation of <i>E. coli</i> to increase yields	61
3.1.2	Refolding of SLC proteins derived from <i>E. coli</i>	62
3.1.2.1	Optimization of refolding methods and buffer	62
3.1.2.2	Up-scaling of the refolding procedure	65
3.1.3	Purification of the SLC proteins	65

3.1.4	Characterization of human SLC proteins	68
3.1.4.1	Structural characterization of the SLC proteins	68
3.1.4.2	Chemical and thermal stability of the SLC proteins	70
3.1.4.3	Quaternary structure analysis	72
3.1.5	Discussion	73
3.2	Effect of the unique region in the isolated proteins and the SLC complex.....	75
3.2.1	The role of the unique region in chemical and thermal stability	77
3.2.2	The role of the unique region in SLC complex formation.....	79
3.2.3	Interaction mechanism between V _H and SLC proteins	81
3.2.4	Discussion	83
3.3	Effect of SLC proteins on the folding of the antibody C _H 1 domain	86
3.3.1	Association of the C _H 1 domains with SLC proteins.....	87
3.3.2	Atomic level description of the C _H 1 folding pathway	90
3.3.3	Discussion	91
3.4	Interaction of SLC proteins with F _d fragment of the HC: preliminary results	92
3.4.1	Basic structural characterization of the F _d -SLC.....	93
3.4.2	Structural model of the SLC-Fab	96
3.4.3	Discussion	97
	Conclusion and perspectives	99
	Abbreviations.....	103
	References	105
	Acknowledgements.....	119
	Declaration	121

Summary

The adaptive immune system relies on its ability to recognize diverse infections and foreign pathogens. Antibodies are key players of the adaptative immune response. The production of functionally and structurally intact antibodies depends on the transition of immature B cells from the bone marrow to the spleen. This transition occurs during the B cell development and is tightly linked to several “quality control” check points. During the early stages of B cell development, one receptor molecule, the pre- B Cell Receptor (pre-BCR) determines the viability and proliferation of the pre-B cell. Thus, the production of the pre-BCR is the first checkpoint in the current model of B cell development. The pre-BCR is composed of an immunoglobulin heavy chain molecule associated with an immunoglobulin light chain-like molecule called the Surrogate Light chain (SLC). The SLC is composed by two proteins $\lambda 5$ (constant Ig like) and VpreB (variable Ig like) which are non-covalently linked and possess some particularities. VpreB lacks a β -strand which is provided by the $\lambda 5$ protein allowing the non-covalent interaction essential for formation of the SLC heterodimer. Our understandings of the molecular mechanism of SLC function and assembly are still at an early stage. In particular, we do not know how the unique SLC associates and forms the pre-BCR for the selection of all heavy chains (HCs). This thesis focuses on dissecting the “Fab fragment” of the pre-BCR to study the effect of the unexpected structural features of the SLC to gain insight in HC selection.

To elucidate the complex assembly of Fab fragment of the pre-BCR, the first aim of this project was to acquire a source of functional SLC proteins (VpreB and $\lambda 5$) isolated and in complex that would allow experiments with purified components *in vitro*. After extensive optimization, the expression in *E. coli*, refolding, purification and association of both proteins was established. We also produced variants of VpreB and $\lambda 5$ in which either the unique tail sequences or the additional β -strand was deleted. The characterization of these variants revealed a significant difference between the single domains and the complexes in terms of stability and assembly. Thermal and chemical stability decreased in the presence of the unique regions. In contrast, the complex stability increased in the presence of the unique regions. Follow-up studies on the

Summary

interaction of the SLC proteins with the V_H domain revealed the importance of the unique regions for increasing affinity for its natural partner. The analysis of the interaction of the SLC proteins indicates that the unique regions play a dual role: thus decreasing the stability of the isolated proteins while increasing the complex formation and the affinity for the V_H domain.

The folding behavior of the C_{H1} domain in the presence of the SLC is key for the first quality control mechanism in the endoplasmic reticulum (ER) prior to surface expression. Our results show that the SLC interacts with C_{H1} domain in a similar manner to the C_L domain. Thus, the folding of the naturally disordered C_{H1} domain upon interaction with the SLC releases the HC retention in the ER by BiP. Finally, the formation and purification of the SLC- F_d complex allows the development of a structural model of the Fab fragment of pre-BCR including the unique regions. Our preliminary results of SLC interaction with V_H and its limited antigen recognition in the presence of the $\lambda 5$ unique region, extend our understanding of the mechanism of V_H selection and inactivation by SLC. These results demonstrated that the unique regions are important for the SLC interaction and they may probe the fitness of the respective V_H domain by interacting with its complementary determinant region 3 (CDR3).

Taken together, this dissertation provides new insights into the folding and assembly of the “Fab fragment” of the pre-BCR and paves the way to for a detailed mechanistic understanding of HCs selection by the unique SLC.

Chapter 1

1. Introduction

1.1 Protein folding

Proteins are one of the most abundant macromolecules in all forms of life. They play an important part in nearly all biological processes, including catalysis, DNA replication, transport, storage and immunity. Proteins are linear chains of amino acids (polypeptides), defined by the nucleotide sequence of their genes. To correctly fulfill their biological functions, they have to adopt a functional three-dimensional structure. Following synthesis in the ribosome, each protein molecule folds into a specific conformational state, by a process called protein folding, within the crowded environment of the cell (Ellis & Hartl, 1999; Ellis & Minton, 2003). Exceptions are natively disordered proteins which only obtain their structures upon association with ligands or other proteins in hetero-oligomers (Fink, 2005). The folding process is complex and is driven by many weak non-covalent interactions. Hydrophobic interactions between amino acid side chains seem to play an important role (Walter & Buchner, 2002). Anfinsen showed that protein folding *in vitro* is a spontaneous process governed by the amino acids sequence (Anfinsen, 1973). However, a linear sequence of 100 amino acids protein would need more than a billion years to randomly sample all possible conformations available (Levinthal, 1969). Under physiological conditions the majority of proteins adopt a single, thermodynamically stable structure, on a much faster time scale (Anfinsen, 1973; Baldwin, 1996). These observations were the basis of the Levinthal paradox, which states that proteins must fold by a more directed process. To explain the folding problem, the folding funnel (Figure 1) is used and it describes, from an energy landscape perspective, the process that occurs in a cooperative manner governed by enthalpic and entropic forces (Fersht, 1999). The polypeptide chains moving from the unfolded state (U) to the folded native state (N), explores the funnel-shaped rugged energy landscape towards the global minimum energy (Dill, 1990; Dill & Chan, 1997). Intermediates can be formed during the folding process and might get trapped in local

Introduction

energy minima, when they are not able to overcome certain barriers within the energy landscape (Dobson & Karplus, 1999). The native state of proteins is characterized by defined secondary, tertiary and quaternary structure. During folding, the secondary structure elements, e.g. α -helices and β -strands characterized by defined hydrogen bonds, are formed first, followed by the formation of three dimensional tertiary structure, and, in case of oligomeric states, subsequently assembly into the quaternary structure (Dill, 1990; Kim & Baldwin, 1982). Thus, folding pathways are frequently, described by intermediates which are often a transitory state at local minima on the folding landscape (Radford, 2000) and can accelerate the folding process (Wagner & Kiefhaber, 1999). However, intermediates are only partially folded and expose hydrophobic surfaces which may lead to self-association, polymerization or aggregation (Clark, 2004). In some cases, unfolding and misfolding lead to toxic protein functions. Outstanding examples are many neurodegenerative diseases, such as Parkinson's or Alzheimer's which result from the accumulation of amyloid fibrils formed by misfolded proteins (Scheibel & Buchner, 2006; Selkoe, 2003). To prevent this, the cell has evolved several quality control as well as folding mechanisms that are based on folding-helper proteins, referred to as molecular chaperones (Seckler & Jaenicke, 1992; Walter & Buchner, 2002).

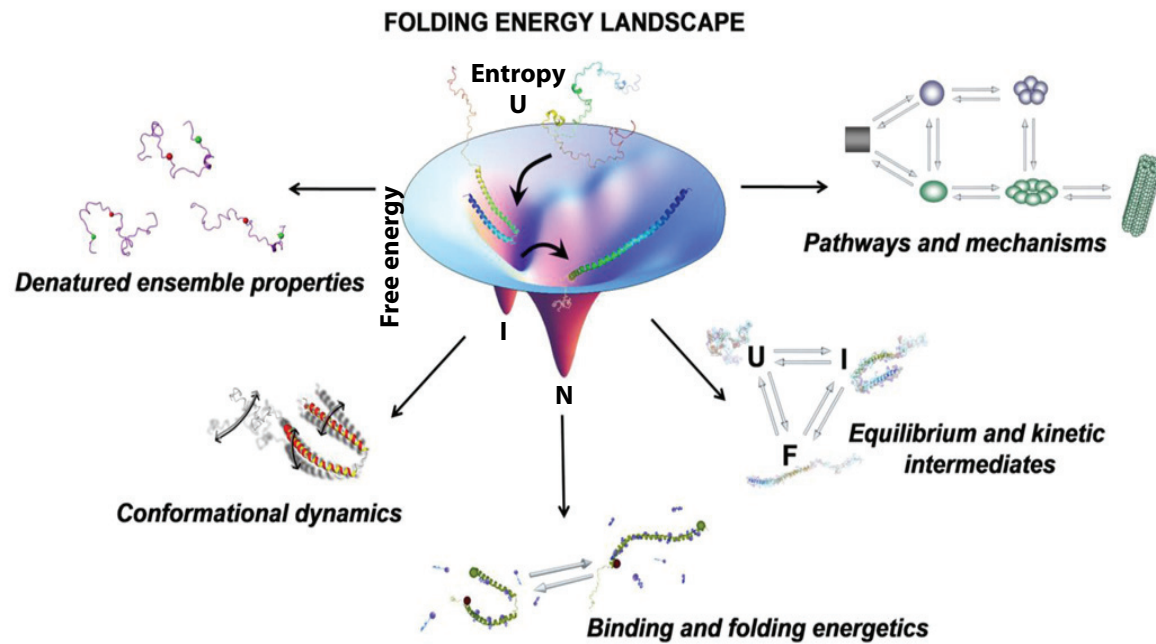


Figure 1: Folding funnel and areas of interest in protein folding. The top of the funnel represents energetic maximum and the protein might be present in many random unfolded states. Protein folding proceeds down the folding funnel towards the native state (N) which corresponds to the energetic minimum. The width of the funnel represents entropy, whereas the depth represents free energy. The inner wall represents the energy potential surface ΔG during folding. Folding intermediates might get kinetically trapped in the ruggedness of the free-energy and have to overcome the free-energy barrier to reach a favorable downhill path. On the sides the different areas of interest in protein folding are schematically added. Adapted from Ferreón and Deniz (2011).

1.2 Protein folding in the cell and molecular chaperones

The cell is a highly viscous and crowded environment with protein concentration in the range of 300 to 400 g/l (Zimmerman & Trach, 1991). Under these complex conditions, intermolecular interactions, protein misfolding and aggregation are strongly favored. Therefore, cells have developed a set of auxiliary proteins to control the proper folding process (Ellis & Hartl, 1999; Hartl, 1996). This highly-conserved protein machinery is called the molecular chaperones. The molecular chaperones are able to interact, assist and assemble newly synthesized proteins and prevent their aggregation (Seckler & Jaenicke, 1992; Walter & Buchner, 2002). As many of them were discovered in correlation with the heat shock response, they are also called heat shock proteins or Hsps (Lindquist & Craig, 1988). There are five major classes of molecular chaperones which are named according to their molecular mass in Kilo Dalton (kDa): the Hsp100 family, Hsp90 family, Hsp70 family, Hsp60 family and the family of small heat shock

Introduction

proteins (sHsps). Although many members are up-regulated upon different stresses such as temperature, ethanol, oxidizing agents and accumulation of unfolded proteins, many molecular chaperones are also constitutively expressed (Richter et al, 2010). In higher eukaryotes, the distinct chaperone classes are interconnected as described in Figure 2. Generally, the mechanism of chaperones involves the controlled binding and release of a wide range of unfolded proteins. This mechanism requires ATP-hydrolysis to fulfill the chaperone function as foldases, with the exception of the family of sHsps. The sHsps form a large oligomeric structure which bind to unfolded substrate preventing aggregation, but their release and refolding require ATP-dependent chaperones (Haslbeck et al, 2005). Another mechanism of protein folding is the substrate encapsulation performed by Hsp60/GroE family. Here, the chaperone not only binds the unfolded protein, but also provides a cavity for folding formed by two ring-like structures providing a physiochemical environment different from the cytosol (Horwich & Fenton, 2009). The most ubiquitously expressed chaperones in eukaryotes are Hsp70 and Hsp90. They form the ATP-driven folding machine which is supplemented by a variety of co-chaperones that can harbor additional functions, such as, regulation of their ATPase activity, peptidyl-prolyl isomerization (PPIase) or oxidoreductase activity (Frydman et al, 1994; Wandinger et al, 2008). Along with molecular chaperones, correct protein folding is achieved by PPIases that catalyze the isomerizations of prolyl peptide bond, and protein-disulfide isomerase (PDI), which catalyzes the formation and isomerization of disulfide bonds (Anfinsen, 1973; Frydman et al, 1994; Gupta & Tuteja, 2011). Despite different modes of action, the chaperones form an organized and dynamic network which allows the transfer of the substrate from one member to the other enabling proteins to refold (Young et al, 2004).

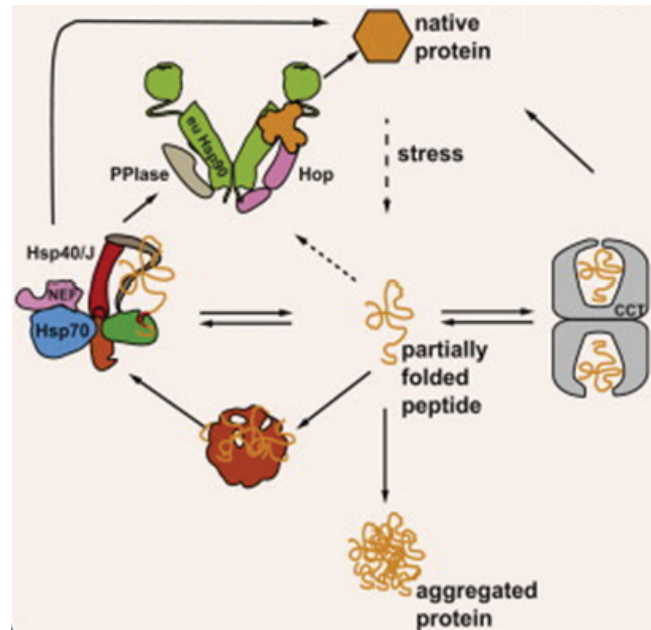


Figure 2: Cytosolic chaperone network of higher eukaryotes. The chaperone system consists of small Hsps shown in red, the Hsp70 system (blue) and its co-chaperones, a member of the Hsp60 family CCT (gray) and the Hsp90 system (green) and its co-factors. Hsp70 protein delivers the substrate to Hsp90 via Hop. A complex network of co-chaperones contributes to the cycling between the different chaperones. The interconnection of the system in folding proteins to their native state is shown by arrows. Adapted from Richter et al (2010).

1.3 Quality control in ER

The protein quality control system has developed in cells of all kingdoms to maintain proteome integrity and homeostasis. In general, proteins have to be transported co-translationally into the endoplasmic reticulum (ER) where they fold and assemble (van Anken & Braakman, 2005; Zimmermann et al, 2011). Thus, the ER is the point of entry of proteins into the secretory pathway, providing a unique environment for protein folding with various folding helpers such as chaperones and oxidoreductase (Wickner et al, 1999). These molecular chaperones and folding enzymes reside in the ER lumen in high concentrations (Stevens & Argon, 1999) and stabilize incompletely folded polypeptide chains, for example by binding to the hydrophobic regions, thus preventing them from aggregating, and also, in many cases, promoting correct folding (Gupta & Tuteja, 2011). Natively folded and assembled proteins leave the ER via vesicular transport for the Golgi complex (Figure 3). In contrast, partially-folded and incompletely-assembled proteins are not transported, but are retained in the ER. Misfolded proteins are either subjected to further folding cycles, or are retranslocated into the cytosol and subsequently

Introduction

degraded by proteasomes, in a process named ER-associated degradation (ERAD) (Figure 3) (Fra et al, 1993; Hellman et al, 1999).

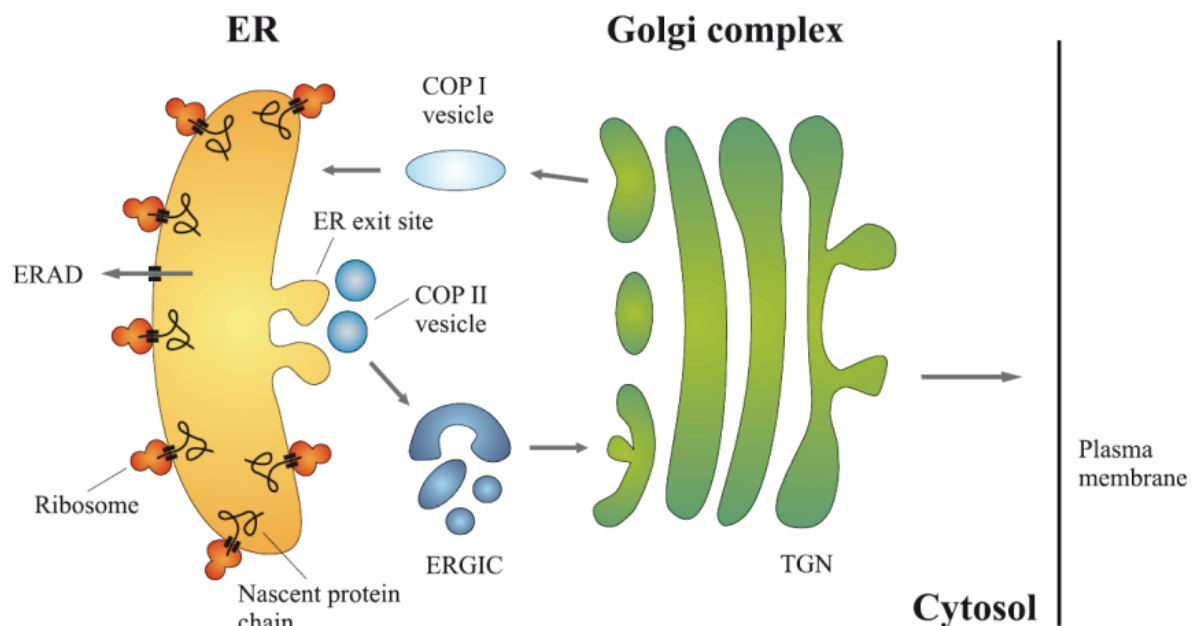


Figure 3 Organelles involved in the secretory pathway. The endoplasmic reticulum (ER) is the site of synthesis and maturation of proteins entering the secretory pathway. Once folded and assembled into the native conformer, the cargo molecules enter the ER exit sites. Vesicles coated with the coatomer protein (COP) II bud off and traffic through the ER-Golgi intermediate compartment (ERGIC) to the cis-face of the Golgi complex. On their way through the Golgi complex, proteins become further modified, e.g. phosphorylated or glycosylated, and are finally sorted according to their function and destination. After the protein passed through the trans-Golgi network (TGN), they proceed to the plasma membrane or beyond. Adapted from Ellgaard and Helenius (2003).

Additionally, a number of biochemical and physiological stimuli can disrupt ER homeostasis, impose stress to the ER, and subsequently lead to accumulation of unfolded or misfolded proteins in the ER lumen. Examples of these stimuli include perturbations in calcium homeostasis or redox status, elevated secretory protein synthesis, expression of misfolded proteins, sugar/glucose deprivation, altered glycosylation, and overloading of cholesterol (Kozutsumi et al, 1988; Rutkowski & Hegde, 2010; Woehlbier & Hetz, 2011). To cope with increases in the ER unfolded secretory protein burden, cells have evolved the Unfolded Protein Response (UPR) (Ron & Walter, 2007; van Anken & Braakman, 2005). The UPR is an ensemble of complex signaling pathways that adapts the ER to the new misfolded protein load, restoring ER homeostasis. This regulatory mechanism is achieved through the action of signal transduction pathways that have sensors facing the ER lumen and effectors that convey

the message to other compartments of the cell. Three transmembrane factors, also known as stress sensors, build up the UPR: protein kinase RNA-like ER kinase (PERK), inositol-requiring protein 1 α (IRE1 α) and activating transcription factor 6 (ATF6) (Harding et al, 1999; Tirasophon et al, 1998; Yoshida et al, 1998). In each case the membrane proteins senses the protein-folding status in the ER lumen and transmit this information across the ER membrane to the cytosol (Figure 4). Upon ER stress the IRE1 α forms a dimer and undergoes trans-autophosphorylation which activates its kinase and endoribonuclease activity which allows excision of X box-binding protein 1 (XBP1) mRNA transcript allowing its translation after religation. Then, the potent transcript factor XBP1 up regulates the ER chaperones (Calton et al, 2002). Additionally, IRE1 α is involved in the activation of the cell death pathways, in response to prolonged ER stress, by associating with the tumor necrosis associated factor 2 (TRAF2) to modulate the activity of the c-Jun N-terminal kinase (JNK) (Hetz, 2012; Maurel et al, 2014) (Figure 4 A). The eIF2 α kinase PERK also dimerize under stress condition inducing its autophosphorylation and subsequently the activation of the cytosolic kinase domain, which activate the PERK-dependant translation via TRAF4, regulating apoptosis and cell cycle (Su et al, 2008) (Figure 4 B). ATF6 is transported to the Golgi apparatus through interaction with the coat protein II (COPII) complex, where it is processed by site protease (S1P) and S2P, to be finally release in the cytosol as ATF6 fragment (ATF6f). The ATF6f up-regulates ER chaperone genes and XBP1 (Yoshida et al, 2001; Yoshida et al, 2000) (Figure 4 C). Therefore, in the ER, sophisticated control mechanism of protein folding referred to as ER quality control exist. ER quality control not only ensures correct folding and assembly of proteins, but also a degradation mechanism to protect the cell from cytotoxic aggregation (Bukau et al, 2006; Wickner et al, 1999). If polypeptides in non-native conformations are not recognized efficiently or the degradation system fails, these proteins aggregate and accumulate in the cell and tissues leading to formation of degradation-resistant amyloids for example (Dobson, 2002) or cell death (Hetz, 2012).

Introduction

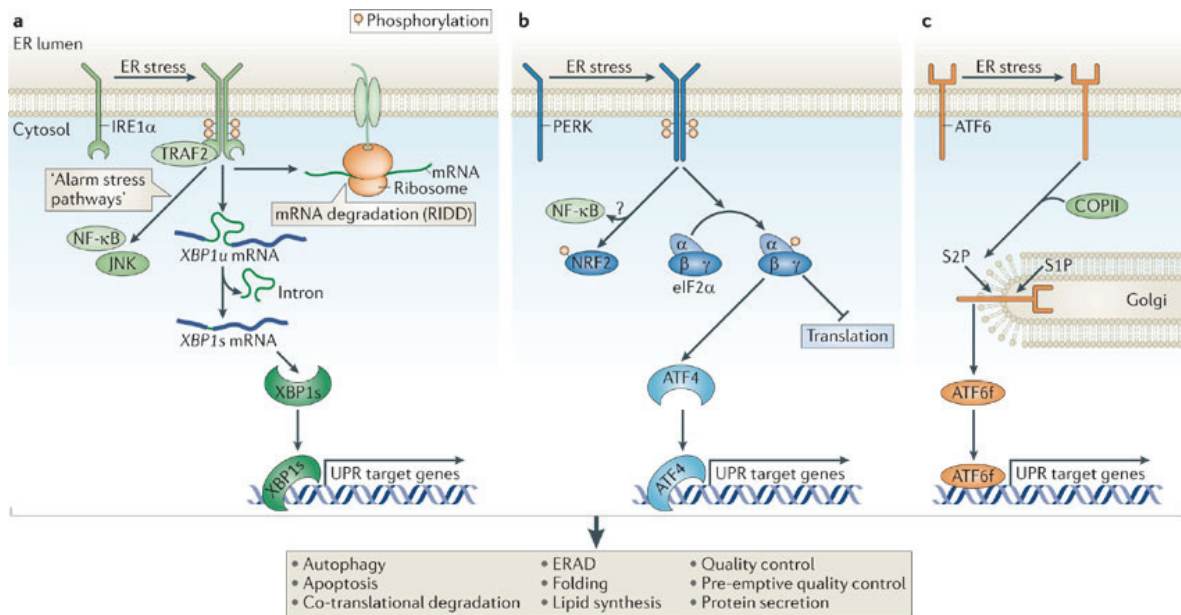


Figure 4: The unfolded protein response (UPR). Stress sensors IRE1 α , PERK and ATF6 transduce information about the folding status of the ER to the cytosol and nucleus to restore protein-folding capacity. In the three cases target genes are activated (e.g. ER chaperones and factor involved in membrane biosynthesis) or a proapoptotic pathway. (A) IRE1 α dimerization, followed by autotransphosphorylation, triggers its RNase activity, which processes the mRNA encoding unspliced XBP1u to produce an active transcription factor, spliced XBP1. XBP1s controls the transcription of genes encoding proteins involved in protein folding, ER-associated degradation (ERAD), protein quality control and phospholipids synthesis. IRE1 α decrease overall protein flux to the ER by enhancing mRNA degradation, activates other cellular pathway such as JNK and nuclear factor- κ B (NF- κ B), through binding to adaptor proteins. (B) Upon activation, PERK phosphorylates the initiation factor eIF2 α to decrease the overall translation while increasing the specific translation of genes including ATF4, which encodes a transcription factor controlling the transcription of genes involved in autophagy, apoptosis, amino acid metabolism and antioxidant responses. (C) ATF6 is localized at the ER in unstressed cells. Under ER stress, ATF6 is transported to the Golgi through interaction with COPII, where it is processed by S1P and S2P, releasing its cytosolic domain fragment ATF6f. ATF6f controls up-regulates genes encoding ERAD components and also XBP1. At the bottom of the figure, general UPR outcomes, which may or may not require transcription, are presented. Figure taken from Hetz (2012).

1.4 Folding helpers dedicated to antibody folding

The ER chaperone BiP (immunoglobulin heavy chain binding protein) is the only Hsp70 family member present in the ER of eukaryotes (Haas & Wabl, 1983; Karlin & Brocchieri, 1998) and is retained in the ER (along with associated proteins) by virtue of its C-terminal KDEL tetrapeptide (Munro & Pelham, 1987). BiP has an important role in the folding and assembly of immunoglobulins (Igs), and it was the first component of the eukaryotic ER quality-control mechanism to be identified in association with unassembled heavy chains (HCs) and light chains (LCs) (Haas & Wabl, 1983; Hendershot

et al, 1996). The ER is the location for oxidative folding in the cell as a more oxidizing environment than the cytosol is provided by a redox system consisting of the small peptides GSH and GSSG (Montero et al, 2013). This system allows the formation of covalent intra- or intermolecular disulfide bridges between cysteine residues. Disulfide bonds are a very important feature in antibody folding as the internal disulfide bond is a conserved feature of the so called immunoglobulin fold in antibodies (Feige et al, 2007). Additionally, most of the Igs first assemble as HC dimers to which LC are added covalently via a disulfide bond between the C_L and C_{H1} domains (Baumal et al, 1971). This reaction is limited by prolyl-isomerization, catalyzed by the PPIase CypB and rendered irreversible by the formation of the HC-LC inter-chain disulfide bond (Feige et al, 2009; Hendershot, 1990; Lee et al, 1999) (Figure 5). BiP is the major cause of retention of HC in the ER via the unfolded first constant domain of the HC (C_{H1}) in the absence of LC synthesis (Hendershot et al, 1987b). The LCs are able to displace BiP and induce folding of the C_{H1} domain (Figure 5) this being a critical step in antibody quality control mechanism in the ER (Feige et al, 2009). Besides LC involvement, the BiP chaperone cycle is modulated by the soluble J-domain protein ERdj3 at several steps, being the main BiP co-chaperone in antibody folding in mammalian cells (Marcinowski et al, 2011; Shen & Hendershot, 2005). Furthermore, the ER provides the environment for glycosylation of proteins, such as asparagines residues of the sequence N-X-T/S (X not being a proline), further increasing the stability and allowing the interaction and assembly of proteins via their covalently attached sugar residues (Helenius & Aebi, 2004). Achieving glycosilation is an important step for many biological antibody functions (Arnold et al, 2007; Dalziel et al, 2014). The ER machinery, especially BiP, and its quality control mechanism, provides the optimal conditions, for example in terms of oxidizing capabilities or post-translational modifications, for the assembly and transport of functional antibodies (Feige & Hendershot, 2011; Feige et al, 2010a).

Introduction

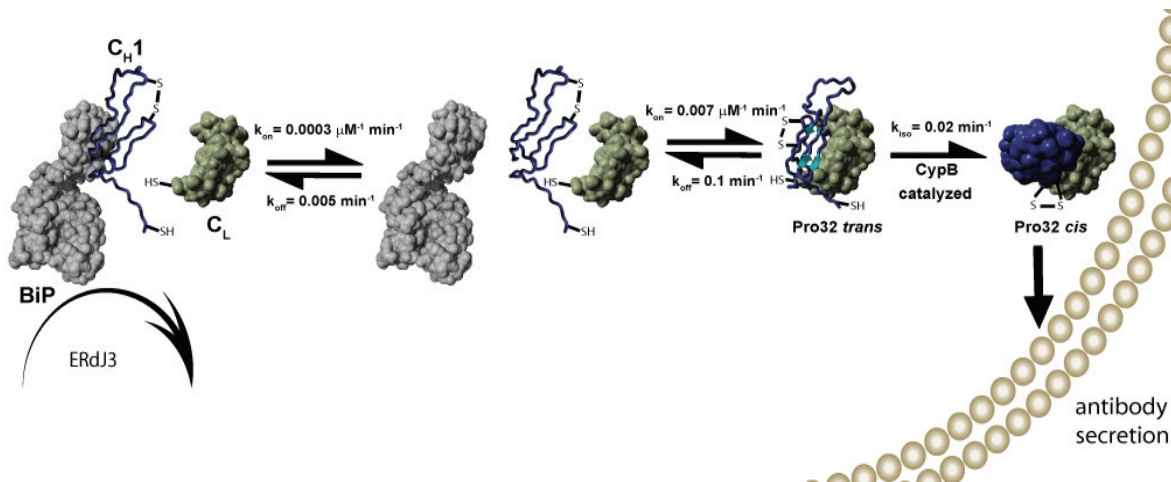


Figure 5: Secretion control mechanism of antibodies in the ER. After synthesis of the polypeptide chain by the ribosome, the C_{H1} domain of the heavy chain (blue) enters the ER in a reduced state. Due to its intrinsically unfolded nature, the C_{H1} domain stably binds to the ER-specific chaperone BiP. This interaction involves cycles of binding and release from the chaperone which enables the assembly with the C_L domain of the light chain (green) during the release cycle. Since reduced C_{H1} does not associate with C_L nor does C_L interact with BiP-bound C_{H1}, the oxidation of the internal disulfide bridge is most likely controlled by additional components of the Ig assembly machinery. After release from the chaperone BiP, the oxidized C_{H1} domain can complete its folding in association with the C_L domain. Once C_{H1} is properly folded, the intermolecular disulfide bridge is formed, which covalently cross-links the C_L domain and the C_{H1} domain. The isomerization reaction can be accelerated by cyclophilin B. Adapted from Feige et al (2009).

1.5 Antibodies

The adaptive immune system relies on its ability to recognize diverse infections and foreign pathogens. The mediators of this humoral response are the immunoglobulins (Igs) whose large variety results from the somatic DNA recombination during B cells development. Immunoglobulins can either exist as membrane-bound receptor complexes thereby playing an essential role in the development and activation of B lymphocytes or as secreted effector molecules, known as antibodies (Casadevall & Pirofski, 2012). Antibodies are able to directly neutralize pathogens and pathogen-derived products and are as well recruiting molecular and cellular immune effectors to eradicate infections and tumor cells (Xu et al, 2012).

The immunoglobulin superfamily is a large group of functionally diverse proteins that share the immunoglobulin fold as a common structural feature (Williams & Barclay, 1988). In higher vertebrates five different classes of immunoglobulins (Igs) exist: IgA, IgD, IgE, IgG and IgM. The antibody classes are identified by the different constant

regions in their heavy chains (α , δ , ϵ , γ , and μ chain), while two different types of LC exist (λ and κ) which can be combined with all types of HCs. They differ in their biological properties, functional locations and ability to confront different antigens. Within a given cell, only one allele for a light chain and one allele for a heavy chain are expressed which ensures a single specificity of the produced antibody (Murphy, 2008).

IgM molecules are secreted as pentameres or hexameres, and they are the first immune response after the contact with an antigen. Thanks to its structure, IgM has a high avidity for antigens leading to the lysis of microorganisms as a consequence of binding and activation of the complement response (Thomas & Morgan-Capner, 1990). However, they cannot pass into the extravascular space owing to their large size (Boes, 2000). In contrast, monomeric IgG is the predominant isotype with the longest serum half life. Four IgG subclasses (IgG1 – IgG4) are distinguished based on structural differences (Schroeder & Cavacini, 2010). IgG1, the most common class, is a heterotetrameric glycoprotein assembled from two light chains (LCs), consisting of V_L and C_L domain, and two heavy chains (HCs), with the V_H and C_{H1-3} domains (Figure 6 A). The “Y” shaped molecule is covalently linked via disulfide bridges between the HC and LC and can be subdivided into fragments crystallizable (F_c) composed of homodimers of C_{H2} and C_{H3} domains and two Fab fragments composed of the heterodimer of LC and the V_H and C_{H1} domains of the HC (Figure 6 A) (Huber et al, 1976). The immunoglobulin domains which belong to the variable region of the antibody molecule, namely V_L and V_H , constitute together the antigen binding site that provides the exquisite binding specificity of the antibody molecule. Within each variable domain, three hypervariable regions (complementary determining regions or CDRs), constitute the residues interacting with antigens. The variability in sequence and site of the CDRs causes a large diversity of the topography of this surface. Therefore, the specificity and affinity of the binding sites for the enormous variety of distinct antigens are governed by the structure of the six CDRs which are embedded into a scaffold of conserved sequences and structure (Kabat et al, 1977; Wu & Kabat, 1970) (Figure 6 A). The hinge region between the first C_{H1} and the second C_{H2} enables segmental flexibility essential for the binding of the Fab region to antigen while the F_c region remains accessible to effector ligands (Saphire et al, 2002). Despite diverse amino acid sequences, the topology of the

Introduction

antibody domain structure is highly conserved. It is a β -barrel structure composed of seven β -strands (a, b, c, d, e, f, g) for the constant domains and nine β -strands (a, b, c, c', c'', d, e, f, g) for the variable domains, distributed between two sheets with typical topology and a disulfide bridge connecting the strands b and f, known as "Ig fold" (Bork et al, 1994) (Figure 6 B).

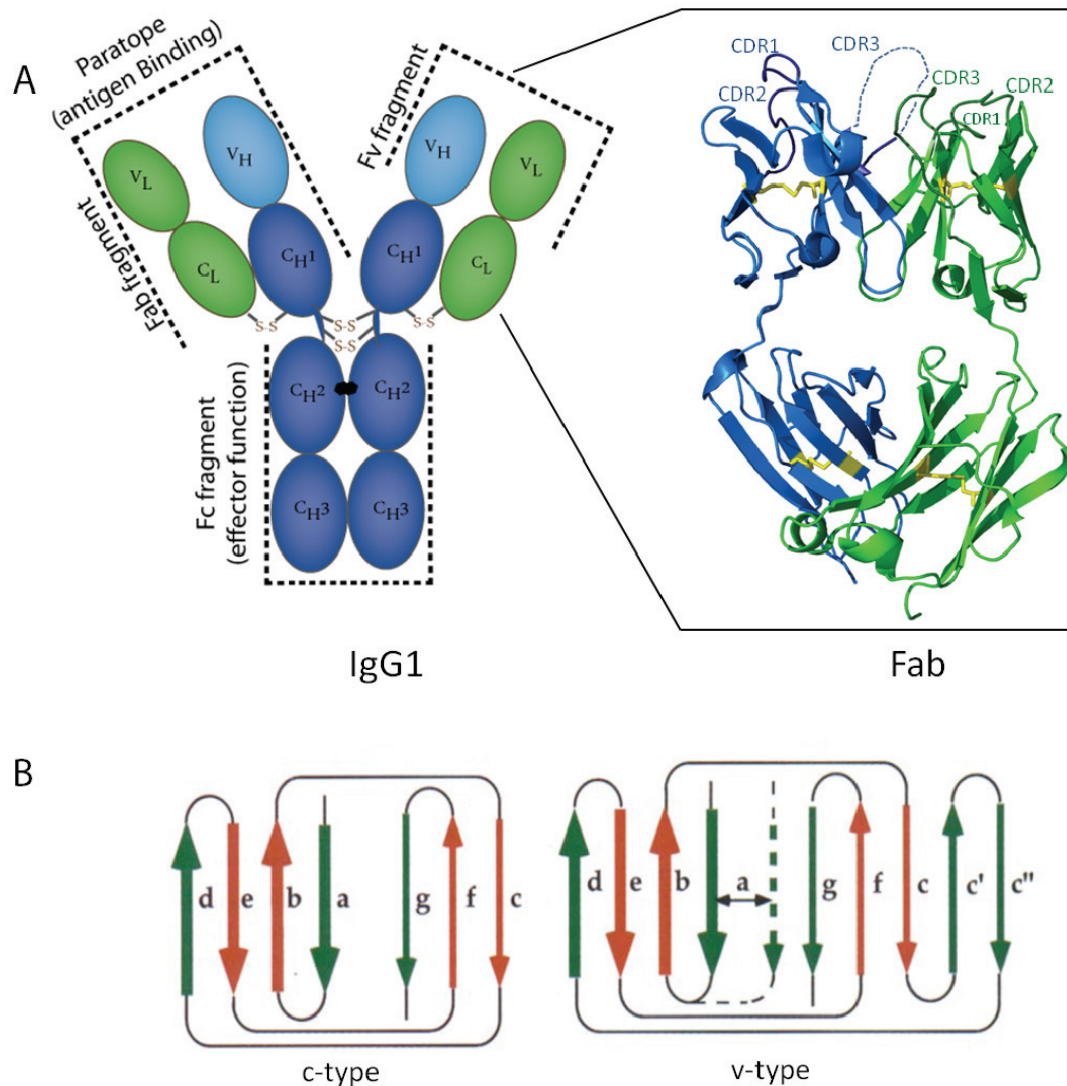


Figure 6: Schematic of an IgG antibody molecule and its Fab fragment structure. (A) Schematic diagram of an IgG antibody. LCs are depicted in green, HCs in blue (constant domains dark blue and variable domains light blue), sugar moieties are represented by black hexagon and S-S indicates a disulfide bridge. Figure adapted from Feige et al (2010a). The cartoon of the Fab fragment shows the conserved Ig fold including the disulfide bonds (yellow sticks). The two variable domains, V_L and V_H , that form the antigen binding site, also known as the Fv-region, contains the hypervariable regions known as the complementary determining regions (CDRs), which are highlighted in dark green and dark blue for V_L and V_H , respectively. The structure is based on PDB 1FH5 and CDR-H3 is indicated as dashed line as it is not resolved in this structure. (B) Two-dimensional topology diagrams of the observed hydrogen bonding patterns. Ig constant domains have a seven strands in general in a c-type topology, variable domains have in total nine strands in general in v-type topology, figure taken from Bork et al (1994).

1.5.1 Folding pathway of antibodies

The detection of differences in the folding of the highly similar structure of antibody domains was only possible by studying of the individual domains. Pioneering studies from Goto and co-workers on immunoglobulin folding focused on denaturing and refolding LCs (Goto et al, 1979). The study of isolated domains started with the C_L domain (Goto & Hamaguchi, 1982) and C_{H3} domains (Isenman et al, 1979) and revealed their autonomous fold as well as the importance of the rate-determining peptidyl-prolyl isomerization reaction. This reaction can be catalyzed and accelerated by peptidyl-prolyl *cis-trans* isomerases (PPIases) (Lang et al, 1987; Lilie et al, 1993). The C_{H3} folding showed that the prolyl-isomerisation has to take place before the formation of the homo-dimer (Isenman et al, 1979; Thies et al, 1999). In the folding pathway of the C_L domain, a small helix connecting two strands is the first element that adopts its native structure upon refolding and seems to guide the orientation of the rest of the protein (Feige et al, 2008). A special observation was made for the C_{H1} domain, as already described in section 1.4. It is intrinsically disordered and can fold only upon binding to its native partner interaction, the C_L domain (Feige et al, 2009). Dissecting antibodies into individual domains allowed the mechanistic description of how antibodies fold (Feige et al, 2010a). Shortly, antibodies fold and assemble in the ER lumen where the HCs are retained until they are correctly assembled with the LCs (Mains & Sibley, 1983) or eventually degraded by ERAD. The intrinsically unfolded C_{H1} is bound to the molecular chaperone BiP (Hendershot et al, 1987b) until the C_L domain induces its folding and the formation of the interdomain disulfide bond (Feige et al, 2009). Afterwards, the assembled IgG molecule is released from the ER and secreted (Feige & Buchner, 2014; Feige et al, 2010a) (Figure 7).

Introduction

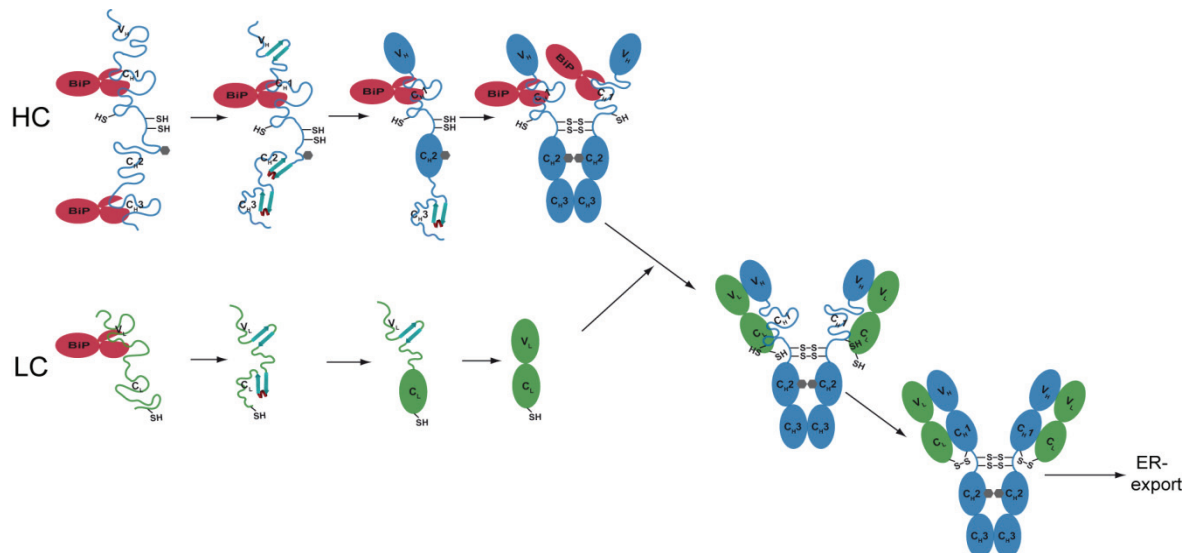


Figure 7: Folding assembly of the IgG molecule. Folding of the LC (green) and HC (blue) begins cotranslationally in the ER, with the formation of disulfide bridges and glycosylation. The unfolded C_{H1} domain remains bound to the molecular chaperone BiP until correctly folded LC interacts and induces its folding. Folding of the C_{H3} domains induces dimerization of the HCs that are stabilized by disulfide bonds in the hinge region. Once the C_{H1} domain is folded, by the presence of the LC, the HCs and LCs are stabilized via disulfide bonds and the assembled IgG molecule can be secreted. Chaperones and folding catalysts, such as protein the disulfide isomerase (PDI) and peptidyl-prolyl-isomerase cyclophilin B contribute to the individual steps in Ig biogenesis. Figure taken from Feige et al (2010a).

1.5.2 B cell development

The B cell development from pluripotent hematopoietic stem cells takes place in the bone marrow and proceeds throughout life. The differentiation of precursor cells along the developmental pathway from B lineage-committed progenitor to the mature antigen-sensitive BCR-expression B cells is characterized by changes in the expression pattern of molecular markers. Along this pathway different checkpoints guarantee that competent B cells develop. Thus B cell development occurs through several stages, where the differentiation of precursor cells into progenitor (pro-) B, precursor (pre-) B, and immature B cells are linked to the recombination of various gene segments encoding the heavy chain (HC) and light chains (LC) of Ig (Melchers et al, 2000) (Figure 9). This mechanism of somatic DNA recombination is also known as V(D)J recombination, has to produce a unique Ig in each individual mature B cell and it combines a single variable (V) gene segment with one diversity (D) and one joining (J) gene segment (Tonegawa, 1983) (Figure 8).

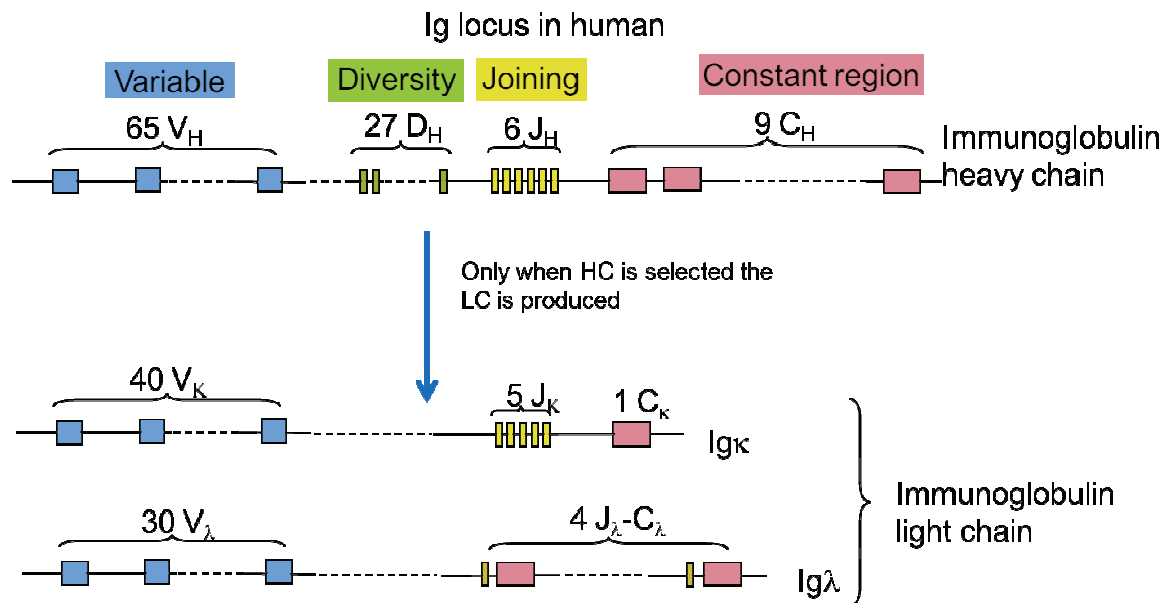


Figure 8: Schematic representation of the VDJ genes segments. Immunoglobulin genes are assembled from gene segments during B cell maturation. Ig of HC (H) and LC (λ and κ) loci contain variable (V), diversity (D), joining (J) and constant region (C) gene elements. First the coding sequence for IgH variable region is assembled from V_H , D_H and J_H gene segments by V(D)J recombination. Productive V(D)J recombination leads to the expression of Ig HC. If the produced HC is selected by the SLC, the HC gene rearrangement is stopped and the LC gene rearrangement starts. Figure modified from Janeway (2005).

The earliest B cell progenitor, the pre/pro-B cell, is phenotypically defined by the pan B cell marker B220, CD43, IL-7R chain and c-kit (Allman et al, 1999; Ogawa et al, 2000). At the pro-B cell stage, cells start to express the BCR component CD19, which is then expressed on all later B cell stages, except the plasma cells (Kozmik et al, 1992; Nutt et al, 1999). Pro-B cells start the Ig-gene rearrangement machinery (Rag1 and Rag2), to rearrange their D_H and J_H gene elements in their IgH loci and eventually develop into preB1 cells, which have DJ_H rearrangements, often on both IgH alleles (Rolink & Melchers, 1991). Furthermore, the pre-B cell receptor (pre-BCR) components VpreB and $\lambda 5$ are expressed. Large pre-B II cells undergo a limited clonal expansion phase of four to six cell divisions which results in the selective expansion of HC-expressing pre-B cells (Decker et al, 1991). The transition from the late pro-B to the large pre-B stage is known as the pre-BCR checkpoint (Burrows et al, 2002). The surface expression of the pre-BCR is dependent on the successful pairing interaction with the surrogate light chain (SLC) components, VpreB and $\lambda 5$ (Karasuyama et al, 1990; Tsubata & Reth, 1990). At this stage pre-BII cells gain IL-2R chain (CD25) expression but lose c-kit expression and are therefore not expandable any longer (Rolink et al, 1994; ten Boekel et al, 1997). After

Introduction

exit from the cell cycle, large pre-B cells differentiate into small, non cycling pre-B cells. These cells rearrange their IgL locus (V_L to J_L) and they develop into surface-IgM positive immature B cells, provided they produce a LC capable of pairing with the HC (Ehlich et al, 1993; Reth et al, 1987; Reth et al, 1985). Some of the immature B cells express a BCR with affinity for autoantigens and consequently may become negatively selected and die in the bone marrow (Avalos et al, 2014; Pelanda et al, 1997). Cells surviving this negative selection leave the bone marrow via the blood stream to the spleen where most of them become mature B-cells (Cooper, 2015) (Figure 9).

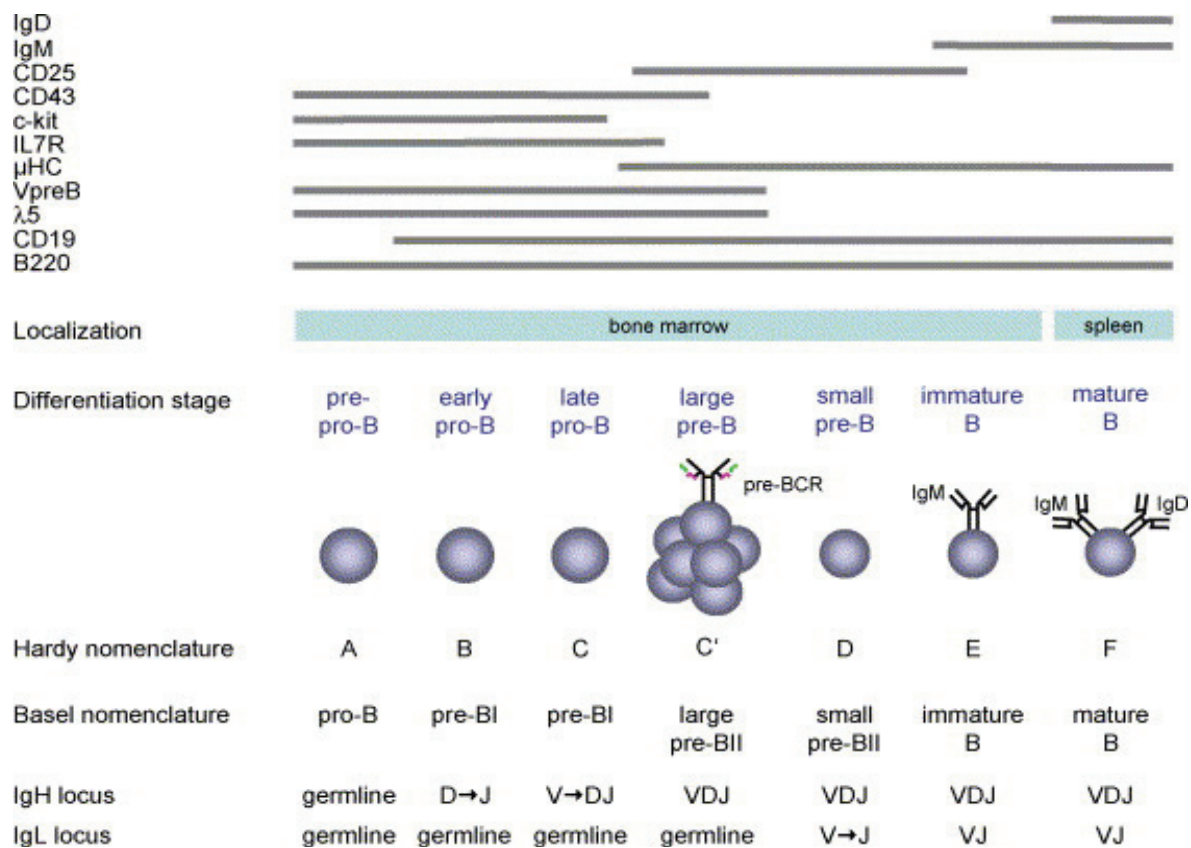


Figure 9: The different stages of B cell development. Scheme of murine B cell development stages characterized by their various surface markers expression (shown in grey) and rearrangement status at the IgH and IgL loci (indicated below). VpreB and $\lambda 5$, SLC components are expressed until the stage of large, pre-B cells. At the small preB II cell stage, SLC expression ceases and pre-BCR disappears from the cell surface. Then LCs become available to assemble to μ HCs, small pre-B cells develop into IgM positive immature B cells. After selection against self reactive BCR, immature B cells leave the bone marrow and differentiate en route to peripheral lymphatic organs into mature and antigen-dependant responsive B cells (surface IgM and IgD). Figure taken from Vettermann et al (2006).

1.6 The unique Surrogate Light Chain (SLC)

1.6.1 Function of the SLC and the preBCR

The pre-B cell Receptor is an essential check point in B cell development. The Ig HC and LC rearrangement is temporally separated during B cell development (Burrows et al, 1979). The V(D)J recombination is initiated at the HC locus resulting in pro-B and pre-B cells expressing a pre-B Cell receptor (pre-BCR). The correctly rearranged HC is expressed on the cell surface as part of the pre-BCR (Karasuyama et al, 1990; Wang et al, 1998) composed of two HCs and two λ LC-like surrogate light chain (SLC). The HCs are associated with the membrane-bound signaling subunits $Ig\alpha$ and $Ig\beta$ via their membrane domains (Figure 10). The $Ig\alpha$ - $Ig\beta$ dimer is non-covalently associated with membrane Ig through polar residues in the transmembrane domain of the HC and it initiates pre-BCR signaling through immune receptor tyrosine activation motifs (ITAMs) (Gazumyan et al, 2006). The SLC is composed of the VpreB and $\lambda 5$ proteins, which are non-covalently associated into an Ig-light chain like structure. Both VpreB and $\lambda 5$ proteins have a non Ig sequence (unique region) at their N- and C- terminal region, respectively (Melchers et al, 1993). HCs pair with the unique SLC forming the pre-BCR. This binding allows for the receptor to be expressed on the cell surface as a prerequisite for the B cell development to continue and the LC rearrangement to start. Thus, the SLC is responsible for the pre-BCR selection and is also involved in its signaling. It should be noted that approximately 50 % of rearranged HC are SLC-incompatible and therefore cannot be expressed as part of pre-BCR (ten Boekel et al, 1997). However, once the pre-BCR is expressed on the cell surface, pre-BCR signaling induce B cell proliferation and by activation of the recombination of the IgL gene B cell differentiation occurs (Herzog et al, 2009). The signaling cascade downstream of the preBCR is important to submit signals inside the cell to initiate the process for large pre-BII transition to small pre-BII. The molecular mechanisms by which the pre-BCR promotes these processes is still not fully understood. However, similar signaling complexes are formed following the engagement of the BCR and the pre-BCR, which suggests that the two receptors use the same main signal transduction pathways (Guo et al, 2000). The $Ig\alpha$ - and $Ig\beta$ -domain mediated signaling leads to down regulation of Rag1/2 recombinases (Melchers, 2005) through a

Introduction

cascade of phosphorylation where the spleen tyrosine kinase (SYK) plays a central role (Hauser et al, 2013; Herzog et al, 2009) and the activation of the IL-7 dependent proliferation in large pre B cells. Therefore, expression of the pre-BCR emerges as an important check point for IgH genes as there must be a suitable fit of the μ HC protein and the components of the surrogate light chain (SLC) in order for a cell to progress through the pre-BCR positive stage (Kline et al, 1998; Reth et al, 1987).

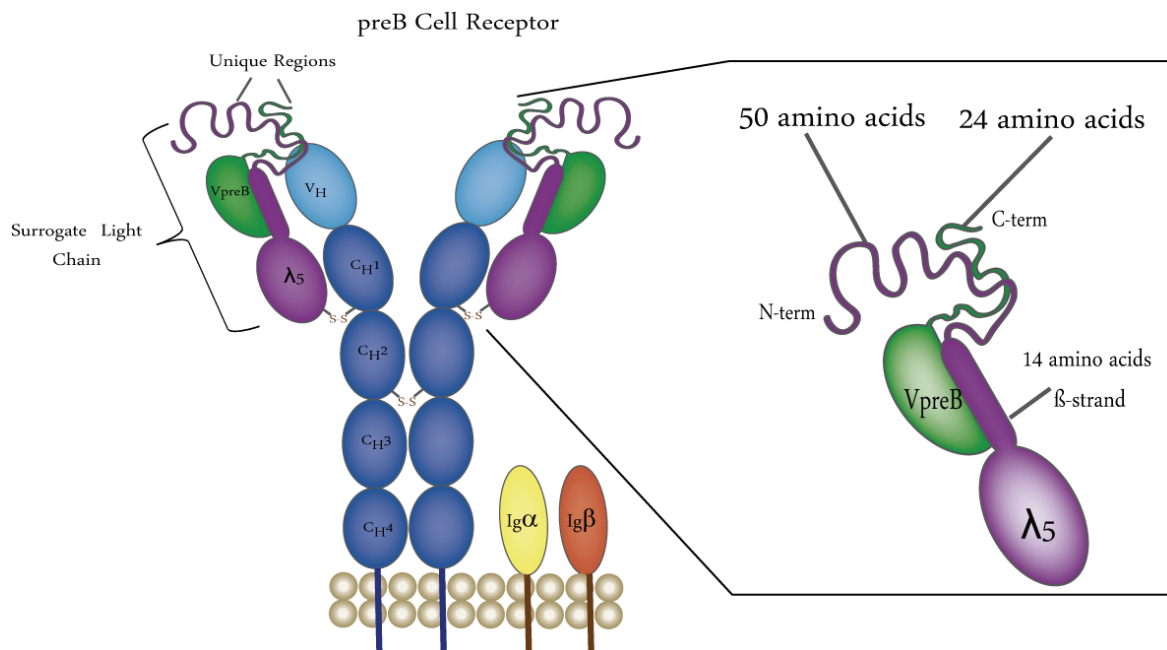


Figure 10: Scheme of a preB cell receptor and his SLC. Schematic of PreB cell receptor with the SLC components VpreB (green) and λ 5 (violet). The pre-BCR is composed of two HCs (blue), two SLCs and the signal-transducing Ig α and Ig β dimer. SLC is a heterodimeric molecule consisting of the non-covalently associated and invariant VpreB and λ 5 proteins. VpreB is lacking a β -sheet, which is provided by λ 5, allowing the non covalent interaction. The unique regions of VpreB and λ 5 at the C- and N-terminus, respectively, protrude from the SLC molecule at the position, where the CDR3 region would reside in a conventional LC.

1.6.2 Structure of the SLC

The pre-BCR is composed of two heterodimeric SLC molecules consisting of two heavy chains to which invariant VpreB and λ 5 proteins are bound. VpreB, a V λ -like domain, is composed of only eight β -strands instead of the nine β -strands observed in conventional V domains, and λ 5, a domain homologous to C λ -like domains, contains one additional β -strand connected to the seven found in conventional C λ domains (Figure 11 A). The missing β -strand in VpreB provided by the λ 5 domain (Bankovich et al, 2007) (Figure 11 B) is essential for the binding of λ 5 to VpreB (Minegishi et al, 1999). The crystal structure

of pre-BCR indicates the interaction of the C-terminal unique region of VpreB, which is situated nearby the HC complementary determining region 3 (CDR3). These unique regions showed a plasticity that could permit them to adapt to diverse CDR3 sequences and loop lengths (Bankovich et al, 2007). Moreover, the study of the CDR3 length and its amino acid composition establish a specific structural requirement for a functional HC to be able to bind the SLC (Martin et al, 2003). Unexpectedly, the addition of this particular β -sheet from $\lambda 5$ to a recombinant VpreB allowed to produce a protein that resembles the V-domain of Ig in its native conformation (Morstadt et al, 2008). Further structural characterization has shown that VpreB and $\lambda 5$ possess at their C- and N-terminal ends, respectively, unique non-Ig tails, also known as unique regions, which are negatively and positively charged. The 24-aa unique tail of VpreB contains six negatively charged residues and the 50-aa unique tail of $\lambda 5$ contains eight positively charged arginine/lysine residues (Bradl et al, 2003; Guelpa-Fonlupt et al, 1994). It could be expected that their opposite charges may be necessary for the SLC assembly; however, their deletion did not inhibit SLC formation (Minegishi et al, 1999). Contrary to initial belief, this unique region was shown to be important for the phosphorylation and signaling of the pre-BCR (Ohnishi & Melchers, 2003), limiting the number of pre-BCR molecules on the cell surface (Herzog et al, 2009). In the same direction, a recent study showed the opposite role played by the unique regions in the surface representation of the receptor. The VpreB non-Ig part fixes the pre-BCR on the surface while the non Ig-part of $\lambda 5$ crosslinks pre-BCRs for down-regulation and stimulation (Knoll et al, 2012). Further studies have demonstrated that the $\lambda 5$ domain and its unique region are sufficient to select and discriminate SLC-incompatible HCs (Smith & Roman, 2010). Additionally, the $\lambda 5$ unique region interacts with stroma cells (Bradl et al, 2003) as well as with galectine-1 (Espeli et al, 2009; Gauthier et al, 2002). The complex of 24 amino acids from the unique region of $\lambda 5$ (22 to 45) and galectine 1 was recently resolved demonstrating the importance of the unique region for the preBCR signaling, which relies in a ligand-induced activation (Elantak et al, 2012). However, there are aspects of the pre-BCR that still remain unclear. The presence of tryptophan (Trp) residues in the unique regions, three in $\lambda 5$ unique region and one in the VpreB one, has not being study. As an aromatic and hydrophobic amino acid, tryptophan is preferentially buried in protein hydrophobic cores. The unique region being surface expose their presence can be explained by the capacity of the Trp

Introduction

aromatic side chain in stacking interaction with other aromatic side-chains, most likely the one present in the CDR3 of V_H domain, as well as interactions with ligands as stroma cell and galectine-1 (Vettermann et al, 2006). Deficient $\lambda 5$ mice still produce a small number of B cells, which increases up to almost 20 % with age (Kitamura et al, 1991). On the other hand, humans with mutations in $\lambda 5$ have severe deficiencies in B cell development that lead to deficiency in B cell and even agammaglobulinemia [patients who do not generate mature B cells] (Minegishi et al, 1998). This difference between species suggest that instead of generating a decreased pre-BCR signal, the L chain-independent HC may evoke a signal that in humans results in negative selection which is somehow better tolerated in mouse (Conley & Burrows, 2010).

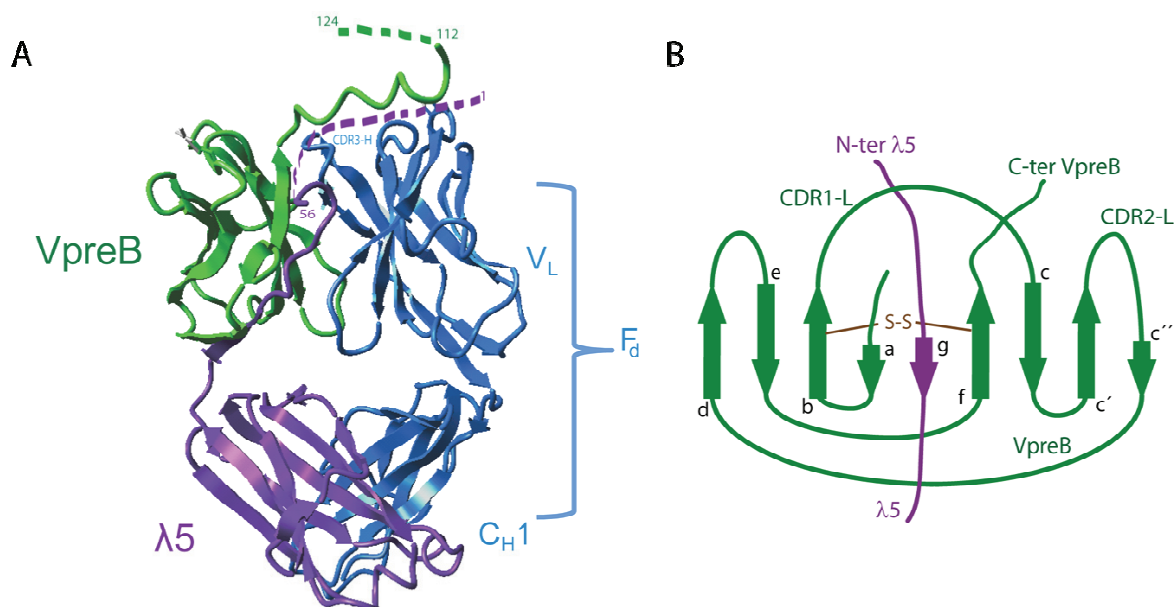


Figure 11: Structure of the SLC. (A) The Fab-like part of the pre-BCR was crystallized by Bankovich et al (2007). It shows a classical Ig λ C-domain structure for $\lambda 5$, followed by a $\beta 8$ strand which completes the lacking β strand of VpreB. The missing portions of the unique regions are indicated with residues numbers and dashed lines at the N-terminus of $\lambda 5$ (48 aa missing) and the C-terminus of VpreB (15 aa missing). The unique regions are positioned where the CDR3 region would be in a conventional LC (PDB ID: 2H32). (B) Schematic representation of V-type Ig fold formed by VpreB and $\lambda 5$ β strands are designated by arrows labeled a to g. VpreB loops that are homologous to Fab CDRs are labeled. The brown line with S-S indicates the intramolecular disulfide bond. Figure modified from Bankovich et al (2007).

1.7 Objective

The pre-BCR receptor clearly plays a major role in the clonal expansion of pre-B cell populations, allelic exclusion, and repertoire selection. Thus, the pre-BCR is an important

check point to ensure the production of structurally intact antibodies, a prerequisite for adaptive humoral immunity. Therefore, efforts have been made to elucidate the pre-BCR formation and signaling. However, the molecular details of this mechanism remained elusive and were thus focus of the present thesis.

The first aim of this work was to establish a robust expression and purification system for the SLC proteins VpreB and $\lambda 5$ as well as variants in which the unique tail sequences were deleted or in which the β -strand involved in intermolecular β -sheet complementation was deleted. Recombinant expression analysis using *E. coli* and refolding experiments were carried out to explore the possibilities to obtain the SLC complexes as well as isolated proteins VpreB, $\lambda 5$ and mutants. A protocol of purification and general conformation of the recombinant proteins should be obtained. Once the recombinant and functional proteins were available, reconstitution experiments with V_H , C_H1 and F_d were performed to dissect the essential parameters for the formation of Fab like complex of the pre-BCR.

The non-Ig part of the VpreB and $\lambda 5$ proteins are not essential for the complex formation (Minegishi et al, 1999) but play an important role in the pre-BCR signaling (Herzog et al, 2009; Melchers, 2005). The effects of their deletion with respect to structure, stability and complex formation were studied. The determination of kinetics of acquisition of the secondary, tertiary and quaternary structure could provide to a better understanding of the role of the two non-Ig regions and aid in elucidating the long-term questions of why two non covalently link proteins form the SLC while LC is in a single chain.

The $\lambda 5$ domain is able to form a disulphide bridge with the C_H1 domain only when it is noncovalently associated with VpreB. This suggests that VpreB and $\lambda 5$ have to be co-expressed to change the $\lambda 5$ conformation to an Ig domain-like structure (Melchers et al, 1999). Following the identification of assembly and secretion control mechanism of IgG antibodies by its unfolded first constant region C_H1 (Feige et al, 2009), it could be assumed that SLC has the same effect and therefore helps to fold C_H1 . The folding mechanism and association of C_H1 with the SLC complex and its isolated domain was studied. These experiments provided a detailed understanding of the effect of SLC on

Introduction

C_H1 folding and allowed us to compare the different steps to those previously determined for the C_L-mediated process.

The refolding and purification of the SLC-F_d complex, with or without unique region, was established. The ability of the SLC-V_H complex to recognize its antigen and interaction was tested with the different mutants. These results provide us with detailed insight of the position and function of this unique region in the pre-BCR complex.

Chapter 2

2. Materials and Methods

2.1 Materials

2.1.1 Chemicals

Name	Origin
$^{15}\text{NH}_4\text{Cl}$	Cambridge Isotope Laboratories (Andover, USA)
1,4-Dithiothreitol (DTT)	Roth (Karlsruhe, Germany)
5,5 Dithio-bis-Nitrobenzoic acid (DTNB)	Sigma (St. Louis, USA)
2-Mercaptoethanol	Sigma (St. Louis, USA)
Acrylamid Bisacrylamide solution 38:2 (40 % w:v)	Serva (Heidelberg, Germany)
Agarose, ultra pure	Roth (Karlsruhe, Germany)
Ammoniumperoxodisulfate (APS)	Roche (Mannheim, Germany)
Ampicillin	Roth (Karlsruhe, Germany)
Agar Agar	Serva (Heidelberg, Germany)
Agarose	Serva (Heidelberg, Germany)
Bacto Agar	Difco (Detroit, USA)
Bacto Tryptone	Difco (Detroit, USA)
Bacto Yeast Extract	Difco (Detroit, USA)
Bromphenol blue	Serva (Heidelberg, Germany)
Coomassie Brilliant-Blue R-250	Serva (Heidelberg, Germany)
Coomassie Protein Assay Reagent	Pierce (Rockford, USA)
Deoxynucleoside triphosphates (dNTPs)	Roche (Mannheim, Germany)
Dimethyl sulfoxide (DMSO)	Sigma (St. Louis, USA)
ECL-Westernblot Detection System	GE Healthcare (Munich, Germany)
Ethylendiamintetraacidic (EDTA)	Merck (Darmstadt, Germany)
Ethanol	Merck (Darmstadt, Germany)
Ethidiumbromide	Sigma (St. Louis, USA)
Glucose	Sigma (St. Louis, USA)
Glutathione, oxidized (GSSG)	Sigma (St. Louis, USA)
Glutathione, reduced (GSH)	Sigma (St. Louis, USA)
Glycerol	Roth (Karlsruhe, Germany)
Guanidinium Chloride (GdmCl)	Sigma (St. Louis, USA)
HCl 32 %	Merck (Darmstadt, Germany)
HEPES (N-(2-Hydroxyethyl)-piperazin-N'2-ethansulfonic acid)	ICN (Costa Mesa, USA)
Imidazole	Sigma (St. Louis, USA)

Materials and Methods

Isopropanol	Roth (Karlsruhe, Germany)
Isopropyl-β-D-thiogalaktopyranosid (IPTG)	Roth (Karlsruhe, Germany)
Kanamycin	Roth (Karlsruhe, Germany)
KCl	Roth (Karlsruhe, Germany)
KH ₂ PO ₄	Merck (Darmstadt, Germany)
L-Arginine	Sigma (St. Louis, USA)
LB medium	Serva (Heidelberg, Germany)
Milk powder	Roth (Karlsruhe, Germany)
NaCl	Merck (Darmstadt, Germany)
Na ₂ HPO ₄ * 2H ₂ O	Merck (Darmstadt, Germany)
NaH ₂ PO ₄ * H ₂ O	Merck (Darmstadt, Germany)
Protease inhibitor Mix G, HP	Serva (Heidelberg, Germany)
Sodium dodecylsulphate (SDS)	Serva (Heidelberg, Germany)
Stain G	Sigma-Aldrich (Hamburg, Germany)
TCEP	Pierce (Rockford, USA)
Tetramethylethylenediamine (TEMED)	Roth (Karlsruhe, Germany)
Tris-(Hydroxymethyl)-aminomethane (Tris)	Roth (Karlsruhe, Germany)
Triton X-100	Merck (Darmstadt, Germany)
Polyoxyethylen-Sorbitan-monolaurat (Tween 20)	Merck (Darmstadt, Germany)
Urea	Merck (Darmstadt, Germany)

All other reagents were p.a. quality and purchased from Merck (Darmstadt, Germany), except fluorescence labels, which were provided by Atto-tech (Siegen, Germany). For the preparation of buffers, only deionised water (TKA GenPure, Thermo Scientific, Niederelbert, Germany) was used.

2.1.2 Equipment

Device	Origin
<u>Analytical Ultracentrifuge</u> XL-A equipped with absorbance and fluorescence detections system	Beckman Coulter (Krefeld, Germany) and AVIV biomedical (Lakewood, USA)
<u>Analytical Balance</u> BP 121 S BL 310	Satorius (Göttingen, Germany) Satorius (Göttingen, Germany)
<u>Centrifuges</u> Avanti J25 and J26 XP Optima XL-A (equipped with FDS) Optima XL-I Rotina 46R Rotina 420R Universal 320R	Beckman Coulter (Vienna, Austria) Beckman Coulter (Aviv, Lakewood, USA) Beckman Coulter (Lakewood, USA) Hettich (Tuttlingen, Germany) Hettich (Tuttlingen, Germany) Hettich (Tuttlingen, Germany)

Benchtop centrifuge 5418 Benchtop centrifuge Mikro R200	Eppendorf (hamburg, Germany) Hettich (Tuttlingen, Germany)
<u>Chromatography systems</u> ÄKTA Prime ÄKTA Purifier + REC 112 FPLC + REC 112 Frac-900/950 fraction collectors Superloops (various volumes)	GE Healthcare (Freiburg, Germany) GE Healthcare (Freiburg, Germany) GE Amersham (Freiburg, Germany) GE Healthcare (Freiburg, Germany) GE Healthcare (Freiburg, Germany)
<u>Circular dichroism spectropolarimeters</u> J710 (with PFD-350S Peltier device) J715 (with PTC 348 WI Peltier device)	Jasco (Großumstadt, Germany) Jasco (Großumstadt, Germany)
<u>Temperature controlled incubator</u> Digital heat block Eppendorf-Thermomixer TB1 Thermoblock	VWR (Darmstadt, Germany) Eppendorf (Hamburg, Germany) Biometra (Göttingen, Germany)
<u>Fluorescence spectrophotometers</u> FluoroMax-2 FluoroMax-4	Jobin Yvon Spex (Edison, USA) Horiba Jobin Yvon (München, Germany)
<u>Gel documentation system</u> Biodoc II ImageQuant 300 Image Scanner III Gel electrophoresis and blotting devices: Hoefer Mighty SamII II	Biometra (Göttingen, Germany) GE Healthcare (Freiburg, Germany) GE Healthcare (Freiburg, Germany) GE Healthcare (Freiburg, Germany)
<u>Magnetic stirrer</u> MR2000 MR3001 MR80	Heidolph (Kelheim, Germany) Heidolph (Kelheim, Germany) Heidolph (Kelheim, Germany)
<u>HPLC devises</u> HPLC-Device Pump System: PU-1580 Flourescence Detector: FP-920 UV-Detector: UV-1575 Auto-sample: A5 1555	Jasco (Großumstadt, Germany)
<u>Fermenter</u> Biostat C	B. Braun Biotech International / Satorius (Göttingen, Germany)
<u>Additional Equipment</u> Membrane vacuum pump Autoclave Varioclav EP-Z Cell Disruption Apparatus Basic Z pH meter Power amplifiers EPS 3500, 3501 and 1001 Homogeniser Ultra Turrax DIAX900 Ice maker	Sartorius (Göttingen, Germany) H+P (Oberschleißheim, Germany) Constant Systems (Warrick, UK) WTW (Weilheim, Germany) GE Healthcare (Freiburg, Germany) Heidolph (Staufen, Germany) Zieger (Cheshire, UK)

Materials and Methods

Incubator	New Brunswick Scientific (Nürtingen, Germany)
Thermal cycler MJ Mini 48 well	Biorad (München, Germany)
Ultra filtration cell 8050	Amicon (Witten, Germany)
Ultraflex II MALDI ToF/ToF	Bruker Daltonics (Bremen, Germany)
Vortex MS2	IKA (Staufen, Germany)
Water bath F6-K	Haake (Karlsruhe, Germany)
Vortex MS2	IKA (Staufen, Germany)
X-ray film processor Optimax TR	MS Laborgeräte (Dielheim, Germany)
<hr/>	
<u>UV-Vis spectrophotometers</u>	
UltroSpec 1100 pro	Amersham (Freiburg, Germany)
Nanodrop	Peqlab (Erlangen, Germany)

2.1.3 Computer software, data base and web-base tools

Computer Programs	
Adobe CS2 Adobe system	Adobe Systems (San Jose, USA)
BioEdit	Ibis Biosciences (Carlsbad, USA)
MMass V2.4.0	Open Source (Martin Strohaln)
EndNote X6	Thomson Reuters
Microsoft Office 2007	Microsoft (Unterschleißheim, Germany)
Origin 8.6	OriginLab (Northampton, USA)
ProtParamToolExpansy	(http://expasy.hcuge.ch/)
Pymol	Schrödinger
Sedfit	Peter Schuck
SedView	Hayes and Stafford, 2010
Yasara	Elmar Krieger
<hr/>	
Data Base	
PDB	www.rcsb.org/pdb
PubMed	www.ncbi.nlm.nih.gov/pubmed
UniProt	www.uniprot.org
<hr/>	
Web-base tools	
Clustal W sequence alignment	http://www.ebi.ac.uk/Tools/msa/clustalw2/
Denaturant Calculator	http://mcb.berkeley.edu/labs/krantz/tools/gdmcl.html
Kabat numbering	http://www.bioinf.org.uk/abs/
NCBI Blast	http://blast.ncbi.nlm.nih.gov/
NEBcutter V 2.0	http://tools.neb.com/NEBcutter2/
OligoAnalyzer 3.1	http://eu.idtdna.com/analyzer/applications/oligoanalyzer
ProtParam	http://web.expasy.org/protparam/
Reverse complement	http://www.bioinformatics.org/sms/rev_comp.html

2.1.4 Consumables

Device	Origin
Amicon Ultra-15 Centrifugal Filter Units	Millipore (Bedford, USA)
Amicon Ultra-4 Centrifugal Filter Units	Millipore (Bedford, USA)
Blotting paper	Whatman (Maidstone, UK)
Disposable cuvettes, plastic, 1 ml	Brand (Wertheim, Germany)
Dialysis tubes Spectra/Por (6-8 kDa)	Spectrum (Huston, USA)
Immobilon-P membrane (PVDF)	Roth (Karlsruhe, Germany)
Membrane discs	Sartorius (Göttingen, Germany)
PCR tubes	BioRad (München, Germany)
PE tubes, 15 and 50 ml	Greiner & Söhne (Nürtingen, Germany)
Petri dishes, PS, 94 mm	Greiner & Söhne (Nürtingen, Germany)
pH indicator strips	Roth (Karlsruhe, Germany)
Reaction tubes, various volumes	Sarstedt (Nümbrecht, Germany)
Sterile filter 0.2 µm	Zefa (München, Germany)
X-ray film X-OMAT AR kodak	Sigma-Aldrich (Hamburg, Germany)
Zip Tip	Millipore (Bedford, USA)

2.1.5 Enzymes, Size markers and Kits

Antarctic phosphatase	New England Biolabs (Beverly, USA)
ECL plus Western Blotting Detection System	GE Healthcare (Freiburg, Germany)
Lysozyme from chicken egg white	Sigma-Aldrich (Hamburg, Germany)
Low Range molecular weight standard	Biorad (München, Germany)
PeqGold 1 kb ladder Orange G	Peqlab (Erlangen, Germany)
Peqlab Protein Marker IV	Peqlab (Erlangen, Germany)
Pfu DNA polymerase	Promega (Madison, USA)
Phusion HF DNA polymerase	New England Biolabs (Beverly, USA)
Restriction enzymes	New England Biolabs (Beverly, USA) and Promega (Madison, USA)
Roti Mark, prestained	Roth (Karlsruhe, Germany)
T4 ligase	Promega (Madison, USA)
Wizard Plus SV Minipreps DNA Purification System Protocol	Promega (Madison, USA)
Wizard SV Gel and PCR clean-up system	Promega (Madison, USA)

2.1.6 Antibodies

Anti-His ₆ -Peroxidase	Roche (Mannheim, Germany)
Anti-FLAG M2-peroxidase (HRP)	Sigma-Aldrich (St. Louis, USA)

Materials and Methods

2.1.7 Chromatography materials and columns

HisTrap Fast Flow	GE Healthcare (Freiburg, Germany)
PD-10 Desalting Columns	GE Healthcare (Freiburg, Germany)
Q Sepharose Fast Flow	GE Healthcare (Freiburg, Germany)
Ressource Q	GE Healthcare (Freiburg, Germany)
SP Sepharose Fast Flow	GE Healthcare (Freiburg, Germany)
Superdex 75 Prep Grade (26/60)	GE Healthcare (Freiburg, Germany)
Superdex 200 Prep Grade (26/60)	GE Healthcare (Freiburg, Germany)
Superdex 75 HR (10/300GL)	GE Healthcare (Freiburg, Germany)
Superdex 200 HR (10/300GL)	GE Healthcare (Freiburg, Germany)
TSK G3000PW HPLC gel filtration	Tosoh Bioscience (Yamaguchi, Japan)
YMC-Pack Diol	YMC (Dinslaken, Germany)

2.1.8 Buffers

2.1.8.1 Protein Purification

Lysis buffer for fermentor cells (5x)	Tris/HCl pH 7.5	50 mM
	NaCl	500 mM
Inclusion Bodies preparation buffer (5x)	Tris/HCl pH 7.5	50 mM
	EDTA	5 mM
	NaCl	5 mM
Denaturant Inclusion Bodies preparation buffer for fermentor cells (5x)	Tris/HCl pH 7.5	50 mM
	EDTA	5 mM
	NaCl	5 mM
	Urea	5 M

SP/Q-Sepharose:

Denaturing condition:

Inclusion Bodies dissolving buffer	Tris/HCl pH 7.5 - 8.0	25 mM
	EDTA	5 mM
	Urea	8 M
	β -mercaptoethanol	10 mM
Buffer A low salt buffer	Tris/HCl pH 7.5 - 8.0	25 mM
	EDTA	5 mM
	Urea	5 M
Buffer B high salt buffer	Tris/HCl pH 7.5 - 8.0	25 mM
	EDTA	5 mM
	Urea	5 M
	NaCl	1 M

His Trap FF Ni-affinity chromatography

Denaturing condition:

Buffer A	Na-P (Na ₂ HPO ₄ 2H ₂ O/NaH ₂ PO ₄ H ₂ O) pH 7.5	40 mM
	Guanidinium Chloride (GdmCl)	5 M
	Imidazole	20 mM
		40 mM

Buffer B	Na-P (Na ₂ HPO ₄ 2H ₂ O/NaH ₂ PO ₄ H ₂ O) pH 7.5	40 mM
	GdmCl	5 M
	Imidazole	500 mM

Native condition:

Buffer A	Na-P (Na ₂ HPO ₄ 2H ₂ O/NaH ₂ PO ₄ H ₂ O) pH 7.5	40 mM
	NaCl	300 mM
	Imidazole	20 mM

Buffer B	Na-P (Na ₂ HPO ₄ 2H ₂ O/NaH ₂ PO ₄ H ₂ O) pH 7.5	40 mM
	Imidazol	500 mM

Resource Q

Buffer A low salt	Tris/HCl pH 8.0	20 mM
-------------------	-----------------	-------

Buffer B high salt	Tris/HCl pH 8.0	20 mM
	NaCl	1 M

Size Exclusion Chromatography (SE)

PBS	NaCl	137 mM
	KCl	2.7 mM
	Na ₂ HPO ₄ H ₂ O	10 mM
	KH ₂ PO ₄	2.0 mM
	pH 7.4	

Hepes	Hepes/KOH pH 7.5	50 mM
	KCl	150 mM

Denaturing SEC	GdmCl	3 M
	Tris/HCl pH 7.5	50 mM
	EDTA	10 mM
	DTT	1 mM

Refolding buffers

Refolding buffer SLC single domain and variants	Tris/HCl pH 8.0	100 mM
	NaCl	150 mM
	EDTA	5 mM
	L-Arginine	350 mM
	GSH	0.5 mM

Materials and Methods

Refolding buffer C _H 1	GSSG	1 mM
	Tris/HCl pH 8.2	250 mM
	EDTA	5 mM
	L-Arginine	200 mM
	GSH	0.5 mM
Refolding buffer V _H	GSSG	1 mM
	Tris/HCl pH 8.0	250 mM
	EDTA	5 mM
	L-Arginine	400 mM
	GSH	0.5 mM
Thrombin restriction buffer	GSSG	1 mM
	Na-citrate	50 mM
	NaCl	200 mM NaCl
	PEG 1000	0.1 % (v/v)
	Glycerin	50% (v/v)
	pH 7.5	

2.1.8.2 Buffers for SDS Polyacrylamide Gel electrophoresis

Fairbanks A (Coomassie staining)	2-Propanol	25 % (v/v)
	Acetic acid	10 % (v/v)
	Coomassie Blue R	0.05 % (w/v)
Fairbanks D (destaining solution)	Acetic acid	10 % (v/v)
Laemmli sample buffer (5x)	Tris/HCl, pH 6.8	0.3 M
	SDS	10 % (w/v)
	Glycerol	50 % (v/v)
	2-Mercaptoethanol	5 % (v/v)
	Bromophenol blue	0.05 % (w/v)
SDS running buffer (10x)	Tris/HCl, pH 8.0	0.25 M
	Glycine	2 M
	SDS	1 % (w/v)
Separation gel buffer (2x)	Tris/HCl, pH 8.8	1.5 M
	SDS	0.8 % (w/v)
Stacking gel buffer (4x)	Tris/HCl, pH 6.8	0.25 M
	SDS	0.4 % (w/v)

2.1.8.3 Buffers for Western Blotting

Transfer buffer	Tris/HCl, pH 7.5	50 mM
	Glycine	40 mM
	SDS	0.04 % (w/v)
	Methanol	20 % (v/v)
PBS-T	1x PBS	
	Tween 20	0.1% (w/v)

2.1.8.4 Buffers for Molecular Biology

TAE (50X):	Tris/acetate, pH 8.0	2 M
	EDTA	50 mM
Loading buffer (10X) :	Glycerol	50 % (v/v)
	Tris/HCl , pH 8.0	10 mM
	Orange G	0.2 % (w/v)
	Xylencyanol	0.2 % (w/v)

2.1.8.5 Buffers for Biacore X100

HBS-P+ (10 X)	HEPES	0.1 M
	NaCl	1.5 M
	Surfactant P20	1.5 % (v/v)
	pH 7.4	

2.1.8.6 Buffers for ELISA

Reaction Mix I Creatine kinase	human creatine kinase	25 µg pre-dissolved in
	(biotinylated)	2 ml H ₂ O
	blocking reagent in H ₂ O	5 %
Reaction Mix I IgG	human IgG	25 µg pre-dissolved in
	(biotinylated)	2 ml H ₂ O
	blocking reagent in H ₂ O	5 %
Reaction Mix II	Na ₂ HPO ₄ / NaH ₂ PO ₄ pH 7.5	100 mM
	NaCl	50 mM
	EDTA	0.5 mM
	Tween-20	0.1 %
	Blocking Reagent	0.5 g/50 ml
Reaction Mix III	ABTS-Buffer	0.835 g/50 ml
	APTS	1 tablet

Materials and Methods

Blocking reagent for ELISA, ABTS Tablets, ABTS Buffer Powder, as well as the Streptavidine-coated microwell plates were purchased from Roche Diagnostics.

2.1.9 Primers

QC-PCR	Name	Sequence (5`-3`)	
VpreB	VpreBWT_forg	GGTACCATGGGTCAGCCGGTTCTGCAT	
	VpreBWT_rev	AGCTCAAGCTTTTATTACGGAACACGGGTACG T	
	VpreBDU_rev	ATATATAAGCTTTTATTAGCTACGTGCACCCAT	
	VpreB+B_forg	ATGGGTGCACGTAGCACCCATGTTTTTGGTAGCGGC AC CCAGCTGACCGTTCTGAGCAGCGAAAAAGAAGAA	
	VpreB+B_rev	TTCTTCTTTTTCGCTGCTCAGAACGGTCAGCTGGGTG CCGCTACCAAAAACATGGGTGCTACGTGCACCCAT	
	VpreBDU+B_rev	ATATATAAGCTTTTATTAGCTCAGAACGGTCAGCTG	
	VpreBWT_forg_hist	TATATTCATATGGGTCAGCCGGTTCTGCAT	
	VpreBWT_rev_hist	TATTATCTCGAGTTATTACGGAACACGGGTACG	
	VprBWT_hisperi_For	ATTTTCCATGGGCAGCAGCCATCATCATCATCAC AGCAGCGCCTGGTGCCGCGCGGCAGCCACGGTCA GCCGGTTCTGCATCAG	
	VBU-15r_HindIII	GCTCAAGCTTTCATTATTCAGTTCACGTTCTTC	
	8_NS_Ncol_for	ATTTCCATGGCACATCATCATCAC	
	8_NS_HindIII_rev	TAAATTATTAGCTCAGAACGGT	
	8_2NS_HindIII_r	GGTACCAAGCTTTTATTAGCTCAGAACGGTCAG	
	λ5	L5WT_forg	AGGTACCATGGGTCTGCTGCGTCCGAC
		L5WT_rev	AGCTCAAGCTTTTATTAGCTACATTCTGCCGGTGCAA
L5WT_forg_hist		TATATTCATATGGGTCTGCTGCGTCCGACAGCTG	
L5WT_rev_hist		ATATATCTCGAGTTATTAGCTACATTCTGCCGGTGCA A	
L5DB_forg		CATAATAGCGTTCAGCCGAAAGCA	
L5DB_rev		TGCTTTCGGCTGAACGCTATTATG	
L5DU_forg		TATATCCATGGGAACCCATGTTTTTGGTAGC	
L5DUDB_forg		ATATCCATGGGACAGCCGAAAGCAACC	
L5WT_hisperi_For		ATTTTCCATGGGCAGCAGCCATCATCATCATCAC AGCAGCGCCTGGTGCCGCGCGGCAGCCACGGTCT GCTGCGTCCGACAGCT	
L5U-11_f_Ncol		TTTTCCATGGGCAGCAGCCATCATCATCATCAC	

		GCAGCGCCTGGTGCCGCGCGGCAGCCACGCACTG GGTCCGGGTGCACCGGGT
	L5U-21_f_Ncol	TTTTCCATGGGCAGCAGCCATCATCATCATCACA GCAGCGCCTGGTGCCGCGCGGCAGCCACAGCCGT AGCAGTCTGCGTAGCCGT
	L5U-27_f_Ncol	TTTTCCATGGGCAGCAGCCATCATCATCATCACA GCAGCGCCTGGTGCCGCGCGGCAGCCACAGCCGT TGGGGTCGTTTTCTGCTG
	L5U-38_f_Ncol	TTTTCCATGGGCAGCAGCCATCATCATCATCACA GCAGCGCCTGGTGCCGCGCGGCAGCCACAGCTGG ACCGGACCGGTTGTTGG
	L5U-45_f_Ncol	TTTTCCATGGGCAGCAGCCATCATCATCATCACA GCAGCGCCTGGTGCCGCGCGGCAGCCACTGGCCT CGTGGTTTTAGAGCAA
	L5DC_For	CCGGACCGCGTAGCTGGCCTCGTGG
	L5DC_Rev	CCACGAGGCCAgctACGCGGTCCGG
	L5_r_HindIII	ATATATAAGCTTTTATTAACATTCTGCCGGTGCAACG GT
C_H1 1HEZ	CH1HZ_Xhol_rvNF	TAAACTCGAGCTATTAAGGCAGCGGAAC
	CH1HZ_Ncol_for	ATTTCCATGGCAAGCGCACCGACC
	CH1HZ_Xhol_rv	TAAACTCGAGCTATTATTTGTCATCATC
C_H1 1HEZ C12S	1HEZC12S_FOR_QC	CCGCTGGTTAGCAGCGAAAATAGCAATCCG
	1HEZC12S_rev_QC	CGGATTGCTATTTTCGCTGCTAACCAGCGG
F_d 1HEZ	Fd_1HEZ_for	AGCAGCGGTAGCGCAAGC
	Fd_1HEZ_rev	GCTTGCCTACCGCTGCT
	Fd_1HEZ_2for	AGCAGCGGCAGCGCAAGC
	Fd_1HEZ_2rev	GCTTGCCTGCCGCTGCT
V_H 1HEZ	VH1HEZ_for_Ncol	ATTTCCATGGCACAGGTTGAGCTG
C_H1 2H32	CH12H32_Ncol_fr	ATTTCCATGGCAAGCGCACCG
	CH12H32_Xhol_rv	ATAACTCGAGCTATTATTTGTCATCATC
	CH12H3_Xhol_rvNF	ATAACTCGAGCTATTAAGGCAGCGGAAC
C_H1 2H32 C12S	2H32C12S_FOR_QC	CCGCTGGTTAGCAGCGAAAATAGCCCGTC
	2H32C12S_REV_QC	GACGGGCTATTTTCGCTGCTAACCAGCGG
V_H 2H32	VH2H32_Ncol_for	ATTTCCATGGCAGAAGTTGAG
	VH2H32_HindIII_rev	AATAAAGCTTCTATTAGCTGCTAACGGT

Materials and Methods

All primers were purchased from Eurofins MWG Operon (Ebersberg, Germany).

2.1.10 Bacterial strains and Plasmids

All constructs for expression in *Escherichia coli* were cloned into pET28-b and pET22-b plasmids (Novagen, Darmstadt, Germany).

Strain	Genotype	Origin
<i>E. coli</i> BL21 (DE3) codon plus	F ⁻ <i>ompT hsdS</i> (rB ⁻ mB ⁻) <i>dcm</i> ⁺ Tetr <i>gal endA Hte</i> (<i>argU proL Camr</i>)	Stratagene
<i>E. coli</i> BL21 star (DE3)	F- <i>ompT hsdS</i> _B (r _B ⁻ m _B ⁻) <i>gal dcm rne131</i> (DE3)	Invitrogen
<i>E. coli</i> Mach1	Δ recA1398 <i>endA1 tonA</i> Φ 80 Δ lacM15 Δ lacX74 <i>hsdR</i> (r _k ⁻ m _k ⁺)	Invitrogen

E. coli Mach1 were used for cloning and amplification of plasmids. *E. coli* BL21 (DE3) Codon Plus and *E. coli* BL21 star (DE3) were used for gene expression in order to obtain recombinant protein.

2.1.11 Media for expression in *E. coli*

LB ₀ (Serva, Heidelberg, Germany)	LB medium for plates: Bacto Agar	20 g/l 15 g/l
SOB (Serva, Heidelberg, Germany)	Yeast extract Tryptone NaCl KCl MgCl ₂ MgSO ₄	0.5 % (w/v) 2 % (w/v) 10 mM 2.5 mM 10 mM 10 mM
TB solution (for supercompetent cells)	HEPES CaCl ₂ KCl pH 6.7 with KOH or HCl MnCl ₂	10 mM 15 mM 250 mM 55 mM
<u>Fermentor</u> Media (6L)	K ₂ HPO ₄ MgSO ₄ Glucose Yeast extract NH ₄ Cl	13,2 % w/v (0.5 L) 1,6 % w/v (0.25 L) 6 % w/v (0.25 L) 300 g 3 g

Feeding solution (2L)	Antifoam	1 ml
	Yeast extract	500 g
	Glucose	250 g
M9	Na ₂ HPO ₄	6 g/l
	KH ₂ PO ₄	3 g/l
	NaCl	0.5 g/l
	pH 7.3 (NaOH)	
	add before use:	
	D-(+)-glucose (¹³ C or ¹² C)	0.2 g/ml; 10 ml / l
	¹⁵ NH ₄ Cl	0.1 g/l; 10 ml/l
	MgSO ₄	1 M; 1 ml/l
	CaCl ₂	1 M; 0.3 ml/l
	Thiamine HCl	1 mg/ml; 1 ml/l
	100X trace elements	
Antibiotics (1000x stocks)	Ampicillin	100 µg/l (in ddH ₂ O)
	Kanamycin	50 µg/l (in ddH ₂ O)

100x trace elements contain per 1L: 5 g EDTA, 0.83 g FeCl₂*6 H₂O, 84 mg ZnCl₂, 10.25 g CuCl₂*2 H₂O, 10 mg CoCl₂*6H₂O, 10 mg H₃BO₃, and 1.35 mg MnCl₂*4H₂O. Solution was sterile filtered before use.

All media and TB solutions were sterilised using an autoclave at 121 °C for 20 min. Antibiotic stocks were passed through a sterile filter (0.22 µm) and stored at -20 °C.

2.2 Molecular Biological Methods

For the growth of microorganisms and for all molecular biological methods, the solutions were autoclaved or sterile filtered. If not state otherwise, work was performed at room temperature (RT).

2.2.1 *E. coli* cultivation & storage

E. coli cultures were prepared from glycerol stocks or by adding a single colony from plates into LB liquid media, containing the appropriate antibiotic, and grown at 37 °C, 200 rpm. The antibiotic addition assures the selection of cells containing the corresponding resistance gene in their plasmid. Bacterial growth was monitor by measuring the optical density (OD) at 600 nm with the Vis spectroscopy (OD₆₀₀ = 1

Materials and Methods

corresponding to approximated 8×10^8 cells). For long-term storage, 800 μ l of fresh overnight culture was mixed with 200 μ l of 80 % glycerol, shock-frozen in liquid nitrogen and stored at -80 °C.

2.2.2 DNA isolation and storage

DNA plasmids for analytical and preparative purposes were isolated from 5 ml overnight cultures with the Wizard® Plus SV Mini-Prep kit following their recommended protocol (Promega, Madison, USA). PCR products and restricted fragments were purified using the Wizard® SV Gel and PCR Clean-Up System. Isolated DNA was stored in sterile nuclease free H₂O at -20 °C. Sequencing of DNA plasmid, (concentration of 50 to 100 ng/ μ l), was performed by GATC Biotech AG (Kontanz, Germany).

2.2.3 Agarose gel electrophoresis for DNA separation

Isolation of PCR products or digested fragments by gel extraction was performed in 1 % (w/v) agarose gel prepared in TAE buffer containing Stain G (Serva, Heidelberg, Germany). Electrophoresis was carried out in TAE buffer with a constant voltage of 120 mV for 20-30 min. DNA was detected with UV light (Biodoc II system, Biometra, Göttingen, Germany) and the size determination was achieved by comparison to a 1 kb ladder (Peqlab, Erlangen, Germany).

2.2.4 PCR amplification

To selectively amplify DNA fragments; the polymerase chain reaction (PCR) was performed using Pfu polymerase (Promega, Madison, USA) or Phusion polymerase with the provided buffer. For *E. coli* expression all codon optimized templates were purchased from GeneArt® (Thermo Fisher Scientific). Primers were design with a melting temperature of approximately 60 °C, controlled with the OligoAnalyzer and order from Eurofins MWG (Ebersberg, Germany). The following standard mixture and protocol were used for PCR reaction:

Template DNA	1 μ l
10X Pfu buffer	5 μ l
Forward and Reverse Primers (100 pmol/ μ l)	1 μ l
dNTPs (100 mM)	1 μ l
Pfu polymerase	1 μ l
Nuclease free H ₂ O	Ad 50 μ l

Reaction protocol:

Melting	95 °C, 1 min	
Denaturation	95 °C, 1 min	
Annealing	55 - 64 °C, 1 min	X30
Amplification	70 °C, 1 min	
Amplification (short end)	68 °C, 1 min	
Storage	4 °C, for ever	

Single point mutation Quick change mutagenesis was performed after the protocol of the QuickChange® Site-Directed Mutagenesis Kit (Stratagene, La Jolla, USA) with small modifications of the standard protocol. After PCR, the DNA template was digested with DpnI (NEB, Beverly, USA) for 1 hour at 37 °C and subsequently transformed into competent cells which were plated into LB plates with the appropriated antibiotic for selection.

For introduction of sequences in between a template the linker PCR were used. For this method three PCR reactions were performed: amplification of insert part 1 with template DNA, amplification of insert part 2 with same template. Then, the two PCR products, with their overlapping ends, were purified prior to the last PCR in which there were added in 1:1 ratio, using the overlaps between insert 1 and 2 and forward primer of PCR 1 and reverse primer of PCR 2. PCR product formation was controlled by agarose gel.

2.2.5 Restriction and ligation protocols

Restriction digestions were performed using the restriction protocol shown below. The digested fragments were verified by agarose gel electrophoresis and purified from the gel when needed. Prior to ligation, in order to avoid religation of the cut vectors, vectors

Materials and Methods

were treated with shrimp alkaline phosphatase. After digestion, the DNA insert was ligated into the corresponding vector using T4 DNA ligase and quick ligation vector for 10 min at room temperature or overnight (ON) at 4 °C. The reaction mixture was then transformed into *E. coli* cells for selection and final sequencing. The mixtures used are described as followed:

Restriction protocol:

PCR product or plasmid (100 ng)	40 µl
10X NEB/Promega buffer	5 µl
High fidelity enzyme I (NEB/Promega)	1 µl
High fidelity enzyme II (NEB/Promega)	1 µl
Nuclease free H ₂ O	Add 50 µl
Incubation	at 37 °C overnight

Dephosphorylation of DNA ends protocol:

Plasmid	40 µl
10X buffer	5 µl
Alkaline phosphatase	2 µl
Nuclease free H ₂ O	Add 50 µl
Incubation	at 37 °C for 2 hours

After desphosphorylation, plasmids were purified from the agarose gel for ligation.

Ligation protocol:

Vector: digested DNA plasmid (100 ng)	7 µl
Insert: digested PCR product	1:3 or 1:5 ratio
Quick ligation buffer	1.5
Ligase T4	1 µl
Nuclease free H ₂ O	Add 10 to 20 µl
Incubation	at RT for 10 min or at 4 °C overnight

Quick ligation buffer	
Tris-HCl, pH 7.5	50 mM
MgCl ₂	10 mM
ATP	1 mM
DTT	10 mM

2.2.6 Supercompetent *E. coli* cell preparation

Ten large colonies were transferred from a freshly plated overnight culture into 250 ml SOB medium and incubated at 19 °C at 200 rpm until OD₆₀₀ of 0.5 was reached (approx. 24 h). The culture was then cooled down on ice for 10 min, centrifuged for 10 min at 4000 rpm at 4 °C. Cells were gently resuspended in 80 ml ice-cold TB medium and kept on ice for 10 min. After the second centrifugation step, cells were resuspended in 20 ml ice-cold TB medium containing 1.4 ml DMSO, aliquoted in 100 µl, frozen in liquid nitrogen and stored at -80 °C (Sambrook & Russell, 2011).

2.2.7 Transformation of *E. coli* cell

For transformation, 100 µl of cells were incubated with 50 ng of DNA plasmid or 10 µl of ligation reaction, on ice for 15 min. Cells were subsequently heat shocked at 42 °C for 45 sec, followed by a cooling down on ice for at least 1 min. Afterwards, 1 ml of liquid LB medium was added and the cells were incubated at 37 °C for 1 hour in a shaker incubator 200 rpm to let the resistance genes be transcribed and the antibiotics converting enzymes be synthesized. Cells were thereafter centrifuged at 8 000 rpm for 3 min and plated on the respective selective media. Plates were incubated overnight at 37 °C.

2.3 Protein chemical methods

2.3.1 Expression test

Expression tests were performed, before large scale expression, in order to obtain the important hints for optimization of culture conditions and therefore increase the protein yield. *E. coli* strain BL21star (DE3) and BL21 (DE3) codon plus were transformed with pET27b and pET22b and grown in LB supplemented with the respective antibiotics. Individual colonies were picked and cultured in 5 ml of LB that was supplemented with antibiotic and were grown overnight at 37 °C with shaking 200 rpm. 50 ml LB media containing appropriated antibiotic was inoculated with 1/1000 preculture and grown to

Materials and Methods

an optical density at 600 nm of 0.6. Protein expression was tested using different IPTG concentrations (0.5 or 1 mM), length of induction (4 h or overnight) and temperature (30 or 37 °C) with shaking 200 rpm. For the expression analysis, 1 ml samples were collected after 4 h of induction and after overnight expression, then harvested by centrifugation at 8 000 x g for 5 min at 4 °C and frozen at -20 °C.

For pET22b expression, three fractions were separated:

- Periplasmic: cells were resuspended in 100 µl of periplasmic buffer and incubated for 1 h at 4 °C, so the polymyxin B sulphate can bind to the lipid A portion of bacterial lipopolysaccharides, inducing pore formation in the membranes of cortex cells and therefore releasing only the periplasmic fraction. The sample was then centrifuged for 8 min at 14 000 rpm at 4 °C and the soluble fraction was isolated as periplasmic fraction (40 µl) and added to 10 µl of laemmli buffer.
- Soluble: complete cells lysis was performed using an osmotic shock. 100 µl of buffer was added to the pellet, followed by centrifugation at 14 000 rpm at 4 °C for 10 min. The supernatant was recovered as the soluble fraction and laemmli buffer was added.
- Insoluble: the remaining cell pellet, which represents the insoluble fraction, was resuspend in 40 µL of insoluble buffer which allows the solubilisation of the fraction and laemmli was added to load into the polyacrylamide gel.

For pET28b expression, only soluble and insoluble fractions were studied and treated as described for pET22b expression.

Finally, all samples were analyzed by SDS-PAGE gel. This procedure allowed us to determine the optimal condition used for protein expression in large scale growth.

Buffers:

Periplasmic fraction buffer:

Tris/HCl, pH 7.5	20 mM
EDTA	1 mM
Protease inhibitor	10 µl (in 100 µl)
Polymyxin B sulphate (Sigma)	1 mg/ml

Osmotic shock buffer:	1 mM
Tris/HCl, pH 8.0	
EDTA	2 mM
Protease inhibitor	5 μ l
Incubation	on ice for 45 min
<hr/>	
Insoluble fraction buffer:	
Tris/HCl, pH 8.0	100 mM
Urea	8 M
EDTA	1 mM

2.3.2 Protein expression, harvest and cell disruption

Large scale production of SLC WT and deleted region constructs were performed in 10 l fermenter (Biostat-C Fermenter, Sartorius, Göttingen, Germany) with 6 l media (see 2.1.11). First, 5 liters of media with 60 g/l yeast extract, 0.6 g/l NH_4Cl and 1 ml antifoam were sterilized for 30 min at 121 °C in the fermenter. After setting the temperature to 37 °C, 1 liter of buffer containing 13.2 % (w/v) K_2HPO_4 , 1.6 % (w/v) MgSO_4 and 6 % (w/v) D(+)-glucose, previously autoclaved, was added. After addition of the corresponding antibiotic, the media was inoculated with 400 ml of a stationary *E. coli* overnight culture. To monitor the OD_{600} and glucose concentration, 1 ml samples were collected at different time points. As soon as the glucose was consumed, the feeding solution was added with increased flow. Induction was performed at OD_{600} of approximately 30 and expression was induced for 4 h. All other proteins were produced in shaker flasks by growing the *E. coli* in 2.5 l of LB with the respective antibiotic, at 37 °C 200 rpm until an OD_{600} of 0.8 was reached. The expression was induced with 1 mM IPTG and incubated overnight at 37 °C 200 rpm. Cells were harvested by centrifugation at 6 000 rpm for 15 min at 8 °C. The cells were resuspended in the respective buffer, supplemented with DNase I, protease inhibitor cocktail, and processed using a Basic Z cell disruption system at 1.8 Kbar (Constant system, Warwick, UK). Fermented culture cells were resuspended in cell lysis buffer supplemented with lysozyme (200 $\mu\text{g}/\text{ml}$) and left 30 min at RT previously to cell disruption.

Expression of ^{15}N -labelled protein was performed in *E. coli* BL21 star in M9 minimal medium containing $^{15}\text{NH}_4\text{Cl}$ (Cambridge Isotope Laboratories, Andover, USA) and

Materials and Methods

glucose. Before inoculation of the main culture, the overnight pre-culture in LB was harvested and washed once in PBS to remove LB traces.

2.3.3 Preparation of inclusions bodies for purification of insoluble proteins

After cell disruption, described in section 2.3.2, insoluble over expressed proteins were isolated. 2 % Triton X-100 was added to the cell lysate and stirred at 4 °C for 30 minutes in order to solubilise membrane fragments. The inclusion bodies (IB) were obtained by centrifugation (20 min at 20 000 rpm at 4 °C) and were washed twice with the IB buffer. For IB obtained from fermented culture, an additional wash with denaturing IB buffer was performed. The IB pellet was directly dissolved in denaturing buffer for purification or stored at -20 °C.

2.3.4 Methods for protein purification

The detailed purification schemes developed in this thesis are given in section 3.1.3.

In general, all purification steps described in this thesis, were carried out at ~ 8 °C. Wild type C_L, C_{H1}, V_L, and V_H were purified according to published protocols by Feige and Simpson (Feige et al, 2007; Feige et al, 2010b; Feige et al, 2004; Simpson et al, 2009). The final protein preparations, were dialyzed against the desired buffers, and stored at -80 °C. The purity was assessed by SDS-PAGE analysis combined with Coomassie staining. The identity and correct molecular mass of each sample was confirmed using MALDI-TOF mass spectrometry (MS).

2.3.4.1 Affinity chromatography

Affinity chromatography is based on the specific and reversible binding of a protein to a matrix-bound affinity ligand. The interaction between the ligand and the absorbent allows a selective separation of the target protein from a complex mixture of different molecules. The elution of the target protein is achieved by competitive displacement or by induced conformational changes for example a change of pH. In this work, 5 ml HisTrapFastFlow Ni-affinity (GE Healthcare, Freiburg, Germany) chromatography

columns were used. The HisTrap column is based on the formation of chelate complex between a His₆-tag protein and the matrix bound cations (Ni-ions). Elution is obtained by increasing the concentration of imidazole in the running buffer which competes with the His₆-tag protein for binding to the matrix. This column was employed for the purification of soluble and insoluble His₆-tag proteins, as well as for the refolding experiments. The protein was loaded with a flow rate of 2 ml/min and washed with 10 column volumes of equilibration buffer (A). Elution was achieved by a gradient elution of 15 column volumes from 0 to 100 % of buffer B (containing 500 mM imidazole). Fractions containing the target protein were pooled and its purification continued with SEC column for insoluble proteins. Screening for the optimal refolding buffer was also performed in 96-well HisMultiTrap plates.

2.3.4.2 Ion exchange chromatography

The ion exchange chromatography principle is based on the reversible absorption of oppositely charged molecules to the ion exchange groups immobilized on the matrix. Net charges of a protein are determined by its side-chains and can be negative or positive. This characteristic is used with the isoelectric point (pI) of a protein, which defines the pH at which the protein has a net charge of 0. Depending on the pH of the buffer, the protein will bind to an oppositely charged carrier material. Elution of a bound protein is achieved by change of the ionic strength of the running buffer. The pH of the running buffer is determined by the pI of the target protein. In this work, the anion exchange Q-sepharose FF column (GE Healthcare, Freiburg, Germany) was used with a flow rate of 3 ml/min. The inclusion bodies were dissolved in IB buffer added with 10 mM β-mercaptoethanol for 2 hours at room temperature. After centrifugation (20000 rpm, 25 min) supernatant was loaded on the column. Once the protein was loaded, the column was washed with 10 column volumes of equilibration buffer A, followed by 15-20 column volumes of buffer B (containing 1M of NaCl).

2.3.4.3 Protein refolding

Purification of insoluble proteins was performed from IBs obtained as described in (2.3.3). In order to obtain complete denaturation of the IBs, 5 M guanidinium hydrochloride or 8 M

Materials and Methods

urea was used in combination with the reducing agent 2-Mercaptoethanol (10 mM). The buffer was chosen according to the first purification: GdmCl for Histag proteins and urea for non-tag proteins in order to use an anion exchange column. To obtain complete solubilisation, samples were incubated for at least 2 h at RT. After purification in denaturing conditions, the refolding was initiated.

Denatured samples were incubated at RT for 3 h. Refolding was initiated by rapid dilution (1:100) into the respective refolding buffer in a microwell plate to a final volume of 1 ml, with final protein concentration of 0.1 mg/ml. The refolding samples were incubated ON at 8 °C with the exception of the Fab fragment and SLC variants, which were incubated at 10 °C for 72 h. Native and refolding controls were treated identically.

2.3.4.3.1 Optimization of refolding conditions

For refolding screening, three methods were tested: on column, by rapid dilution and by dialysis into the respective refolding buffer. For all methods and buffers tested the final refolding yields were assayed with the Thermofluor Stability Assay (2.5). All data shown represent the average of at least 3 independent experiments.

In column, the refolding was performed using HisMultiTrap FF 96 well plates (GE Healthcare, Freiburg, Germany), handled according to the manufacturer's protocol. After pre-equilibration in the denaturing buffer, 100 µl of protein solutions were applied to the respective well, and incubated for 3 min. Thereafter, 500 µl of the respective refolding buffer were added subsequently to each well and the plates were centrifuged for 2 min at 100 x g. 500 µL of refolding buffer were subsequently applied to each well and incubated for 1 h at 8 °C. The elution of the refolded proteins was performed by adding 200 µl of 40 nM Na-P, 500 mM imidazol, pH 7.5 to each well.

Refolding by rapid dilution was performed in a 96 microwell plate where the protein solution was diluted to a final concentration of 0.1 mg/ml in a final volume of 1 ml of the corresponding refolding buffer. The samples were incubated over night, 2 and 3 days at 8 °C. Then, samples were concentrated and the refolding yield was determined.

Refolding by dialysis was performed in 50 ml falcon tubes containing the corresponding refolding buffer. The protein solution was added to the dialysis membrane with a final

concentration of 0.1 mg/ml and incubated ON, 2 and 3 days at 8 °C. Once the refolding was completed, the samples were concentrated and the refolding yield was measured.

2.3.4.3.2 Optimization of refolding buffer

In order to optimize the yield of refolding different buffers were tested using the step wise refolding protocol described by Dashivets et al (2009). The refolding screening was then realized in different buffers for which the pH was first optimized followed by the salt concentration. For the last step of optimization, the additives were varied at the best buffer, pH and salt concentrations. The different buffers, pH, salts and additives tested are summarized in the following tables.

Buffer	pH	mM NaCl	mM KCl	mM L-Arg	mM L-Gln
40 mM Hepes	7.5 - 9.0	25 - 150	25 - 50	50 - 500	0 - 50
100 mM Tris	7.5 - 9.0	25 - 150	25 - 50	50 - 500	0 - 50
250 mM Tris	7.5 - 9.0	25 - 150	25 - 50	50 - 500	0 - 50
40 mM NaP	7.5 - 9.0	25 - 150	25 - 50	50 - 500	0 - 50

Additive	Concentration
Glutathione reduced	0.5 - 5 mM
Glutathione oxidized	1 - 5 mM
Glycerine	0 - 15 %

2.3.4.4 Size exclusion chromatography (SEC)

To complete the protein purification, a size exclusion chromatography was performed. The matrix of this column is composed of a three-dimensional network of defined pore size which allows the separation of proteins according to their hydrodynamic radius. Proteins larger than a pore are not capable to penetrate the pores of the material and are the first ones to be eluted from the column within the void volume. On the other hand, smaller proteins can penetrate the pores and thus elute later. Therefore the separation range of a SEC is defined by the pore size of the stationary phase. In order to avoid unspecific ionic interaction between proteins and the matrix, buffer with higher ionic strength were used. In this work, Superdex 75 Prep Grade and Superdex 200 Prep Grade (Healthcare, Freiburg, Germany) were used depending on the required separation range.

2.3.4.5 Concentration of proteins

To obtain the desired concentration or volume protein solutions were concentrated using 15 ml volume Millipore Ultr-15 concentrators (Darmstadt, Germany). Depending on the size of the proteins, 3 or 10 KDa molecular weight cut-offs membranes were used in this work. The protein solution was concentrated by centrifugation at 3500 x g at 8 °C until the desired concentration or volume was reached.

2.3.4.6 Protein dialysis

Dialysis was used to change the buffer composition of the protein sample. Protein was poured into the dialysis bag with defined molecular weight cut-off and dialyzed against 100 to 1000 fold volume of the original buffer, at 8 °C for at least 4 h or ON.

2.3.5 SDS-Polyacrylamide Gel Electrophoresis (SDS-PAGE)

Proteins were separated by SDS-PAGE using the general procedure according to Laemmli (1970). Polyacrylamide gels were casted to a final concentration of 15 % or 18 % of acrylamide depending on the size of the proteins. Polymerization of the solution was induced by adding ammonium persulfate (10 % w/v in H₂O) and tetramethylethylenediamine (TEMED). Before loading, all samples were mixed with 5 X Laemmli buffer (added with 5 % β-mercaptoethanol) and heated at 95 °C for 5 min. The gels were running in SDS-PAGE buffer at a constant current of 35 mA per gel for 60 min. Then, they were stained with Coomassie buffer using the modified protocol from Fairbank.G et al (1971). To estimate the molecular weight of the proteins, LMW or prestained marker were loaded on the gel.

2.3.6 Western Blotting for His-tagged domains

Proteins were separated by SDS-PAGE and transferred onto polyvinylidene difluoride (PVDF) membrane as described by standard procedures (Sambrook & Russell, 2011) using a FastBlots system (Biometra, Göttingen, Germany). Prior to the blotting, 6 Whatman 3 MM filter papers and methanol-activated PVDF were incubated for 5 min in western blot transfer buffer. A stack of 3 Whatman 3MM filter paper, PVDF membrane,

SDS-PAGE gel and 3 Whatman 3 MM filter paper was prepared. The transfer was performed applying 72 mA per gel for 60 min. After blotting, the membrane was incubated in blocking buffer (PBS-T with 5 % milk powder) for 60 min or ON at 8 °C. The peroxidase coupled antibody, Anti-His₆-HPR, was added in a 1:10000 dilution in 10 ml PBS-T (1 % milk powder) and incubated for 1 hour at RT. After three washing steps with PBS-T, of 15 min each, the antibody-enzyme conjugate was detected by chemoluminescence with ECL detection kit (GE Healthcare, Freiburg, Germany). Light emission was detected on a photographic film (GE Healthcare, Freiburg, Germany) and developed using an Optomax TR (MS-Laborgeräte, Dielheim, Germany).

2.3.7 Protein labelling

Proteins were labelled specifically on cysteine residues using maleimide Atto 488 or Atto 550 (Atto-tech, Siegen, Germany). The labelling reaction was carried out by incubating the proteins 20 min at RT with 1 mM TCEP for reducing the free cysteine, followed by an ON incubation with 2-3 fold excess of the fluorescence dye. Separation of free label was achieved by extensive dialysis (2 times exchange and ON) against buffer or using PD10 columns (GE Healthcare, Freiburg, Germany). Labelling efficiency was determined using UV spectroscopy following the manufacturer's protocol.

2.3.8 Determination of protein concentration with Bradford

Imidazole buffers interfere with the determination of protein concentration using UV-spectrometer. In this case, the protein concentration was determined using Bradford, which relies on binding of chromophore to basic and aromatic amino acids of proteins (Bradford, 1976). This binding results in a shift of the absorption maximum of the chromophore from 465 nm to 595 nm, which can be measured spectroscopically. Chromophore solution (Coomassie Proteins Assay Reagent, Pierce, Rockford, USA) was used according to manufacturer's protocol. A calibration curve was generated with different concentration of BSA. Samples to analyse were diluted and incubated for 10 min at RT prior to measure the absorption at 595 nm. Concentrations were determined using the calibration curve and taking in account the dilution factor.

2.4 Spectroscopic methods

All spectra were corrected with the respective buffer spectra as reference.

2.4.1 UV-Vis spectroscopy

Peptide bonds absorb in the range of 180 - 240 nm, whereas aromatic amino acids tyrosine, tryptophan and phenylalanine, as well as disulfide bonds are capable of absorption of the UV light from 280 to 230 nm (see table).

	λ_{\max} (nm)	ϵ_{\max} ($M^{-1} \text{ cm}^{-1}$)
Trp	280	5700
Tyr	274	1400
Phe	257	200
Disulphide bond	250	300

To determine protein concentrations, UV absorption was used according to the law of Lambert-Beer (Equation 1).

$$A = \epsilon \cdot c \cdot d \leftrightarrow c = \frac{A}{\epsilon \cdot d}$$

Equation 1: Beer-Lambert law.

A = Absorbance, ϵ = molar extinction coefficient ($M^{-1} \text{ cm}^{-1}$), c = molar protein concentration (M), path length (cm)

The theoretical molar extinction coefficients were determined using the ProtParam tool and spectra were recorded with Ultrospec 1100 (Amersham bioscience, Freiburg, Germany) in quartz cuvettes or nanodrop (PeqLab, Erlangen, Germany) at room temperature. If necessary, proteins were diluted in order to get an absorption between 0.5 - 1 and ensure linearity of the Lambert-Beer's law.

2.4.2 Circular Dichroism (CD) Spectroscopy

Circular dichroism (CD) refers to the differential absorption of left (L) and right (R) circularly polarized light by optical active (chiral) molecules. The optical activity of proteins is the result of asymmetric carbon atoms and/or aromatic amino acids which leads to a mutual influence of the fields and therefore to a different absorption of L and R. The resulting radiation can be assessed as elliptical polarization (Equation 2). CD is measured as ellipticity (Θ) in degrees (Kelly et al, 2005).

$$\Delta A(\lambda) = A_L(\lambda) - A_R(\lambda)$$

Equation 2: Absorption between left and right handed circularly polarized light.

A= absorption, λ = wavelength, R and L subscripts describe left- and right-handed circular polarized.

Far-UV (FUV) measurement (180 - 250 nm) provides useful information regarding the secondary structure of proteins as distinctive signals are caused predominantly. α -helices show typical minima at 208 nm and 222 nm, while β -sheets display a signal with a single minimum at 218 nm and random coil structures show one characteristic minimum at 200 nm. The signals in the near-UV (NUV) region (320 - 260 nm) determine a characteristic fingerprint of a defined tertiary structure within a protein by measuring the chiroptical characteristic of the aromatic amino acids. The molar ellipticity is the quantitative measure of the CD ellipticity in relation to the average molecular weight of the amino acids of the protein Θ_{MRW} , and is calculated in equation 3:

$$\Theta_{MRW} = \frac{\Theta \cdot 100 \cdot M}{d \cdot c \cdot N_{aa}}$$

Equation 3: Determination of the mean residue ellipticity.

Θ_{MRW} = mean residue ellipticity ($\text{deg cm}^2 \text{d mol}^{-1}$), Θ = ellipticity (deg), M = molecular mass (g/mol), d = path length (cm), c = concentration (M), N_{aa} = number of amino acid residues.

In this work, far-UV spectra were recorded to monitor the secondary structure of proteins, as well as following the folding reaction of C_H1 domain or determining thermal stability of different constructs. Measurements were carried out in quartz glass cuvettes using a thermostable cuvette holder and a peltier unit (Jasco, Groß-Umstadt, Germany). For determination of thermal stability, samples were heated with 20 °C/h and changes in CD signal at a defined wavelength were observed. The midpoint of the transition was

Materials and Methods

determined by a Boltzmann fit. To follow the C_{H1} folding CD signal changes were followed at a defined wavelength and the midpoint was determined by exponential decay fit.

Parameter	FUV
Wavelength (nm)	250 - 200
Scan speed (nm/min)	20
Data pitch (nm)	0.2
Band with (nm)	1.0
Response (sec)	4
Temperature (°C)	20
Accumulations	16
Concentration (μM)	10

2.4.3 Fluorescence Spectroscopy

Fluorescence is defined by the emission of light by a substance after excitation with electromagnetic radiation. During excitation, the absorption of photons goes along with the excitation of a molecule from its ground state (S_0) to a higher energy state (S_1). The return of the electron to the S_0 state is accompanied by the emission of electromagnetic radiation, and the molecule has ample time to relax into the lowest accessible vibrational and rotational state. Consequently, the different degree of energy dissipation leads to a continuous emission spectrum. The aromatic amino acid residues in proteins (tryptophan, tyrosine and phenylalanine) are responsible for the so-called intrinsic fluorescence of a protein because of their delocalized π -electron system. Additionally, numerous extrinsic fluorescence probes with different binding characteristics are available for specific applications.

Folding and interaction studies were performed by following the intrinsic fluorescence of at least one tryptophan. Antibody domains possess at least one conserved tryptophan residue which is buried in the folded state. Upon unfolding, this residue becomes surface exposed, resulting in an increase of the fluorescence signal. For GdmCl-induced equilibrium unfolding transition, samples were incubated ON at 20 °C at different GdmCl concentrations, which were determined refractometrically (Schmid, 2005). Measurements were carried out in a Spex FluoroMax IV fluorimeter (Horiba Jobin-yvon, Edison, USA). All experiments were performed at 20 °C, at protein concentration of 1 μM

using a 1 cm quartz cuvette, if not stated otherwise. Intrinsic tryptophan fluorescence spectra were recorded from 300 nm to 450 nm, exciting the sample at 280 nm, excitation and emission slits widths set to 2 nm and 5 nm, respectively. Samples with different GdmCl concentrations were excited at 280 nm and the signal was monitored at the wavelength with the largest signal/spectra difference between native and unfolded state using equation 4.

Data were evaluated with Origin (OriginLab, Nothampton, USA); for urea-induced unfolding transitions, a two-state model was applied (Bolen & Santoro, 1988).

$$y(D) = y_N^0 + m_N \cdot [D] - \frac{(y_N^0 + m_N \cdot [D]) - (y_U^0 + m_U \cdot T)}{1 + \exp\left(-\frac{\Delta G_{stab} + m_c \cdot [D]}{R \cdot T}\right)}$$

Equation 4: Two-state model with the assumption of linear dependency of emission from native and unfolded protein.

y(D) = fluorescence or CD signal; *y* = *y*-intercepts; *N* = data of native protein; *U* = data of unfolded protein; *m* = slope of the best fit straight line; *m_c* = cooperativity; [*D*] = denaturant concentration; *T* = temperature in Kelvin (20 °C (RT) ~ 293.1 K); ΔG_{stab} = free enthalpy of denaturant induced unfolding; *R* = universal gas constant (8.314 J mol⁻¹ K⁻¹).

For interaction studies exponential changes in fluorescence were fitted using Origin (OriginLab, Nothampton, USA). Different exponential functions (single, double and triple exponential) were tested and the residual compared. The fit with the best residuals was chosen.

2.5 Thermofluor Stability Assay (TSA)

The thermal unfolding and refolding efficiencies of proteins was performed using the thermofluor stability assay (Ericsson et al, 2006), with the fluorescence dye Sypro Orange (Invitrogen, Carlsbad, USA). This dye interacts with the hydrophobic stretches of a polypeptide chain which greatly enhances its fluorescence. This characteristic is exploited by monitoring the thermal denaturation, a procedure by which the protein unfolds and exposes its hydrophobic residues, which become solvent-exposed (Ericsson et al, 2006; Pantoliano et al, 2001). The fluorescence emission is detected during the heating of the sample by a real-time PCR machine (Mx3000P QPCR system, Stratagene,

Materials and Methods

La Jolla, USA), using the melting curve protocol with defined heating rate of 1 °C/min between every detection step. In this work the TSA was used to measure the stability of the refolded proteins which showed a difference in the thermal transitions depending on the refolding yield of the analyzed sample. Refolded proteins were used to a final concentration of 1 to 10 µg in 10 µL, mixed with 10 µL of a 1:5000 dilution of the ready to use dye, for a final dilution of 1:1000 of Sypro Orange. Additionally, this method is fast and can be carried out in a 96-well format, it does not require large amounts of proteins per assay and more importantly, it can be directly applied to the refolded samples.

2.6 Quaternary structure and interactions analysis

2.6.1 Analytical gel filtration

Gel filtration is based on the separation of proteins according to their molecular size. Here, HPLC was used as analytical gel filtration chromatography for determination of quaternary structure of proteins. Thus, whether a protein exists in monomer, homodimers or homooligomers as well as heterodimers can be calculated. To this end a calibration curve was drawn by plotting log(molecular weight) against the retention time. This curve allows apparent molecular weight of proteins to be calculated base on the correlation of retention time and molecular weight. For detection, a Jasco HPLC (Großumstadt, Germany) with UV and fluorescence detection or a Shimadzu HPLC (Columbia, USA) system was used. Different columns were used depending on the theoretical molecular weight of proteins analyze: superdex 75 10/300 GL column (GE Healthcare, Freiburg, Germany), TSK3000PW column (Tosoh bioscience, Yamaguchi, Japan) or YMC-Pack Diol-SEC 300 (YMC, Dinslaken, Germany). Columns were equilibrated in Hepes buffer, unless stated otherwise. The flow rate was set to 0.5 ml/min at RT and detection was carried out at 280 nm and 350 nm (intrinsic fluorescence).

2.6.2 Analytical ultracentrifugation

Analytical ultracentrifugation (aUC) is a powerful method that allows the precise and selective observation of sedimentation of macromolecules in solution. AUC allows the calculation of the sedimentation coefficient from proteins or complexes under strong centrifugal force in solution. The advantage of this method is the study of protein complexes and interactions without interference of matrix or surface interaction. In this work we used sedimentation velocity experiments in a Beckman ProteomeLab XL-A (Beckman Coulter, Krefeld, Germany) equipped with a fluorescence or absorbance detection system. To determine the protein-protein interaction and the apparent K_D of complex formation, labelled protein (200 nM of labelled species) was added to increasing concentration of the unlabelled protein and complex formation was determined by the shift of the sedimentation coefficient. Experiments were performed by Katrin Christiane Back (TUM) and data analysis was carried out using SEDFIT software (Schuck, 2000).

2.6.3 Nuclear Magnetic Resonance

NMR experiments were performed in collaboration with Professor Bernd Reif (TUM). Diana Carolina Rodriguez performed all measurements. All samples were recorded in a NMR- spectrometer from Bruker 600 MHz at 12.5 °C, if not stated otherwise.

For C_H1 folding in presence of the C_L domain or $\lambda 5\Delta U\Delta\beta$, a 2D spectrum were recorded as described by Feige (Feige et al, 2009). All ^{15}N 2D spectra are SOFAST-HMQC, allowing fast pulsing by using selective proton flip-back technique (Schanda & Brutscher, 2005).

2.6.4 Surface Plasmon Resonance

Surface Plasmon Resonance (SPR) spectroscopy is a common method used to analyze protein-protein interactions. The method is based on the reflection of polarized light in an electrically conducting gold layer which leads to the excitation of surfaceplasmons at a certain angle. Reflective light is detected within the system. The protein is immobilized on the sensor (ligand) and the second protein is passed under continuous flow (analyte).

Materials and Methods

Under these conditions the total reflection at the interface between buffer with different refractive index and the glass sensor surface is reduce. The resonance angle at which the intensity minimum occurs is a function of the refractive index of the solution close to the gold layer on the opposing face of the sensor surface. The signal measured in resonance units (RU) is directly correlated to the amount of protein bound. In this work a BiacoreX100 (GE, Healthcare, Uppsala, Sweden) system was used and proteins were bound to a CM5, SA and NTA SPR chip following the manufacture protocol. The analytes were flushed in HBSP+ buffer for measurements at 20 °C with a flow rate of 10 μ L/min. Single and multicycle kinetic assays were performed with different ligand and analyte concentrations and regenerations were done with 1.5 M NaCl. The experimental data was analysed with the Biacore x100 Evaluation Software.

2.6.5 Enzyme-linked Immunosorbent Assay (ELISA)

Enzyme-linked Immunosorbent Assay (ELISA) is a plate-based assay designed for example for the detection and quantification of antibodies binding to their antigen. Here we used the ELISA established by Dr. Eva-Maria Herold to test the functionality of the mutated V_H and V_L domains. The complex of antibody domain and antigen can then be immobilized to a solid surface and detected with the linked enzyme antibody. Detection is accomplished by assessing the conjugated enzyme activity via incubation with the substrate. In this study the interaction of V_H , SLC constructs and antigen were tested with the experimental setup depicted in Figure 12.

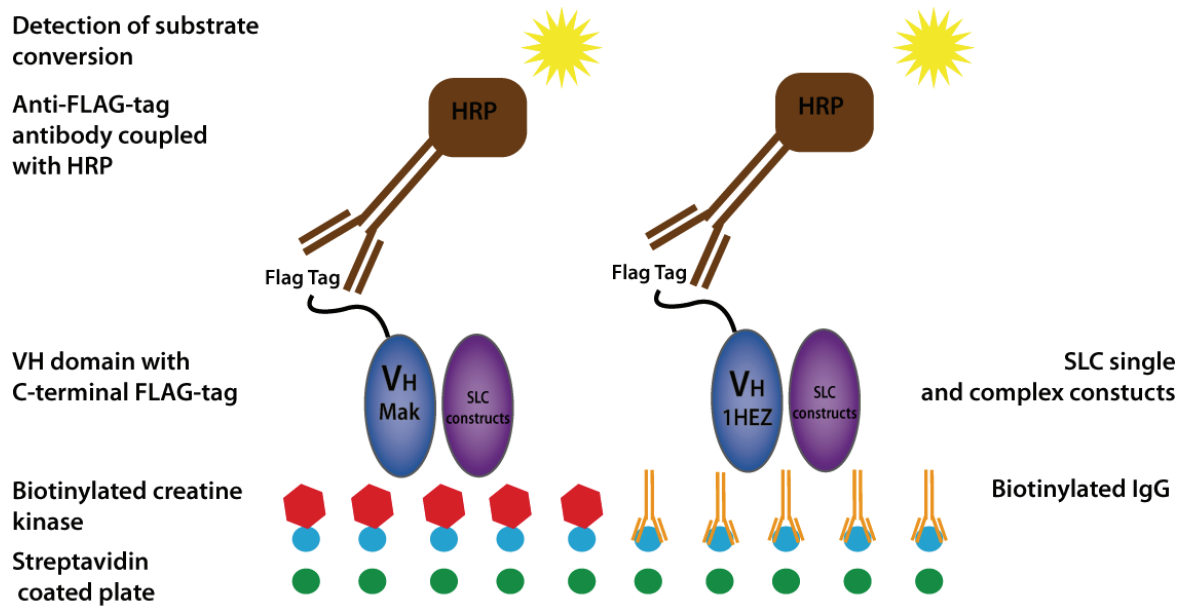


Figure 12: ELISA set-up to test binding affinities of isolated domains. Biotinylated human creatine kinase or IgG antibody is coupled to a streptavidin coated microwell plate; V_H wild type with C-terminal Flag-tag domains and the SLC constructs interaction partner are incubate and detection is enabled via a Horseradish peroxidase (HRP) coupled Anti-Flag-tag antibody.

Microwell streptavidin-coated plates were used to immobilize the V_H Mak 33 or V_H 1HEZ biotinylated antigen creatine kinase or F_c part of IgG, respectively. The assay was performed according to the manufacturer's recommendations. First 10 µl of the mixture V_HFlag-tag-SLC construct (1:1 ratio) was added to the biotinylated antigen solution (90 µL). Then, the mixture was incubated in the streptavidin well for 45 min at 4 °C at 300 rpm. After washing with water, the horseradishperoxidase-conjugated detection antibody was added in a 1:15000 dilution and incubated as previously described. The second washing step was followed by the addition of the synthetic peroxidase substrate to initiate the colorimetric reaction, which was instantly monitored in a Tecan (Männedorf, Switzerland) genios plate reader. Absorption was measured at 405 nm for 30 min.

Chapter 3

3. Results and Discussion

3.1 Expression, purification and characterization of the human SLC

3.1.1 Expression of human SLC in *E. coli*

The Surrogate light chain (SLC) is crucial for B cell development. For obtaining the crystal structure of truncated SLC-F_d fragment (PDB: 2H32), the fragment was expressed in baculovirus-infected cells by triple co-infection of recombinant virus encoding for F_d, VpreB and λ5 (Bankovich et al, 2007). The established SLC-HC model as we know it today originates mainly from FACS, immunoblotting from different cells lines or mouse models (Gauthier et al, 2002; Guelpa-Fonlupt et al, 1994; Melchers et al, 1999; Minegishi et al, 1999; Seidl et al, 2001). Thus, many molecular and mechanistic aspects of the SLC proteins VpreB and λ-like (λ5) including their unique region are not known. For detailed *in vitro* analysis, the production of functional SLC proteins separately and in complex is an important prerequisite. This chapter describes various methods employed to optimize the production of recombinant human SLC proteins in *E. coli*.

3.1.1.1. *Attempts to produce soluble SLC proteins in E. coli*

The human SLC protein λ-like and VpreB are difficult to express in cells as they are down-regulated in preB cells (Hauser et al, 2013). Thus another source for SLC production is a key prerequisite for *in vitro* analysis. There is no established protocol for the soluble expression SLC WT proteins in *E. coli* cells preserving their unique region. Their similarity to the antibody domains C_L and V_L allows planning different approaches to facilitate the expression of human proteins in bacteria including host strain selection, using an optimized codon sequence for *E. coli* and/or secretion into the oxidizing periplasmic space (Sone et al, 1997). In addition, the co-expression of thioredoxin can significantly enhance soluble expression of antibodies domains as their internal disulfide

Results and Discussion

bridge formation is essential for their proper folding (Feige et al, 2007; Yasukawa et al, 1995).

In a first attempt to express the SLC WT proteins, their human sequences, kindly provided by Prof. Dr. Hendershot (St. Jude Children's Research Hospital, Memphis), were cloned in a pET28b vector and expression was tested in BL21 and Rosetta cells. Unfortunately, despite modifying the environmental conditions, such as temperature and IPTG concentration, the cells did not express the SLC WT. Thus the SLC WT sequences were synthesized by GeneArt® (Thermo Fisher Scientific) with codon optimization for expression in *E. coli* in pET28b vector. An N-terminal his-tag was also added to facilitate the expression and purification of the proteins. An expression study was performed as described in 2.3.1, but VpreB WT was only expressed in an insoluble form. To enhance the soluble expression of SLC WT proteins, a pET22 vector was also tested as the pelB signal sequences assure secretion into the oxidizing periplasmic space, as well as the co-expression of thioredoxin. In both cases, the soluble expression was not obtained, although both proteins were found in the insoluble fraction as you can see in the western blot (Figure 13). It turns out that, after 4 hour of expression, SLC recombinant proteins were only found in the insoluble fraction, but after overnight expression, they were no longer detectable by western blot. However, the insoluble expression was only visible by western blot which required efforts to improve the protein yield described below (3.1.1.2).

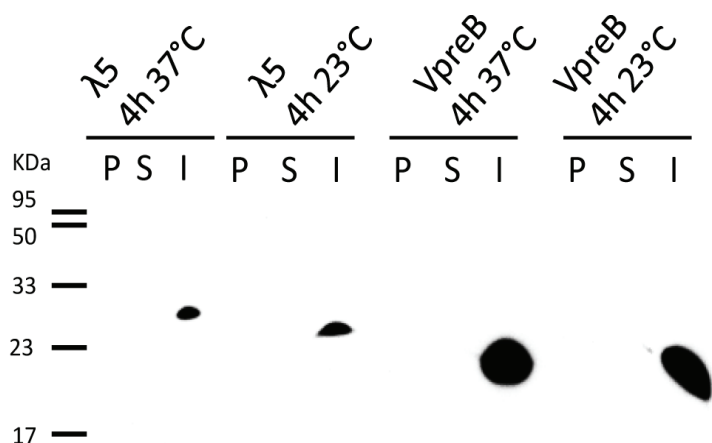


Figure 13: Expression analysis of humans SLC proteins $\lambda 5$ and VpreB. Plasmid-carrying *E. coli* BL21 Codon Star cells were grown in 50 ml volumes for 4 h at 37 °C. Then cultures were induced with 1 mM IPTG and incubated at 23 °C or 37 °C. Samples were taken at different time points and treated as described in 2.3.1, here the results after 4 h of expression are shown. P: periplasmic fraction; S: soluble fraction and I: insoluble fraction. Fractions were loaded on a SDS-gel and further analyzed by Western blot (2.3.6) using a His-POD conjugate at a dilution of 1:10 000.

3.1.1.2. Fermentation of *E. coli* to increase yields

As described in 3.1.1.1, the expression of the SLC WT construct only produced insoluble protein.

In order to increase the protein yield and to obtain soluble SLC proteins, we first tried different media for expression: enbase media (biosilta, Cambridgeshire, UK). This media can support growth with controlled pH and glucose availability in a fermenter-like environment. Unfortunately, changing the media did not increase the protein. So we decided to continue to use fed-batch fermentation. This allows cell growth in a more controlled environment, adjusting the oxygen and glucose levels according to the cells' needs. In such environment, the cell growth was optimized (we obtained approximately one kilo of cells per 6 liters of media) leading to higher protein yield.

As proteins were expressed in the insoluble fraction, in order to purify them after cell lysis, the pellet was used for the preparation of inclusion bodies. For the fed-batch fermentation expression, contaminations from the yeast extract were still present after cell lysis, which decreased the purity of the inclusion bodies. We established an

Results and Discussion

additional 2 M urea washing step, in order to purify the inclusion bodies as described in 2.3.3. This step increases the quantity of proteins obtained, as cell grew in an optimal environment, and the optimization of the inclusion body preparation led to a high and purer amount of insoluble protein which can be refolded as previously described (Rudolph & Lilie, 1996).








3.1.2 Refolding of SLC proteins derived from *E. coli*

3.1.2.1 Optimization of refolding methods and buffer

Unfortunately, the soluble expression of the WT SLC proteins was not successful. As large amounts of insoluble proteins accumulated during expression in *E. coli* (3.1.1.1), a refolding strategy (Feige et al, 2007) was applied to obtain functional proteins. First, the inclusion bodies were solubilized in buffer containing 5 M GdmCl. The denatured protein was then purified with a his-tag binding column and refolded in a refolding buffer established by Feige et al (2007). This buffer was not successful in refolding the SLC proteins in complex, which lead to a screening of different buffers and conditions using a stepwise protocol (Dashivets et al, 2009). Three different conditions were investigated as described in Figure 14 A: refolding by dilution, refolding by dialysis and matrix-assisted refolding. To determine the folding and stability of the refolded proteins, the Thermo Fluor stability assay (TSA) was used (see section 2.5 for details). This is a fast method which allows the screening of different buffers in a 96 well format with a low amount of protein. Once the screening was set up, the refolding buffer was applied for optimization of buffer components and pH. The buffer conditions with the highest refolding efficiencies were chosen to optimize ionic strength. NaCl concentrations from 50 mM to 150 mM were tested. Analysis of the TSA showed an increase in soluble protein stability at a NaCl concentration of 150 mM. The buffer composition 100 mM or 250 mM Tris-HCl, 150 mM NaCl and pH 8 gave the best results (Figure 14 A and B). Subsequently, in the third optimization step, different concentrations of Arg alone or in equimolar combination with Gln (50 mM) were tested. This third step resulted in a further increase in the overall refolding yield for the dialysis refolding. Refolding in a matrix or by dilution techniques were then discontinued as

their efficiency was lower than the dialysis approach. In a further optimization step, glycerol was added as a stabilizer and tested in combination with a redox system composed by glutathione reduce (GSH) and oxidize (GSSG) (Figure 14 B). The best conditions were determined by the highest thermal transition which correlates with the proper folding of the proteins. It is important to note that the redox systems differs in their GSH/GSSG ratio, which is an important component in antibody domain folding as their internal disulfide bond is essential to assure the so called immunoglobulin fold (Feige et al, 2007). In Figure 14 B we can observe an example of the melting curves obtained from the TSA. Each curve corresponds to a specific buffer as described in Table 1 using a Tris (100 or 250 mM) base buffer with 150 mM NaCl at pH 8. The additives L-Arg with equimolar Gln or only 350 mM L-Arg, as well as 0 or 10 % glycerol are shown. The melting temperature is higher in presence of 350 mM of L-Arg compare to the equimolar mixture L-Arg/Gln, and no significant increase was observed with or without glycerol (Figure 14 B).

Table 1: Example of refolding buffers screening.

	250 mM Tris, 50 mM L-arg/Glu, pH 8, 10 % glycerol, 0.5/1 mM redox, 1 mM EDTA, 150 mM NaCl, 20 µl protein
	100 mM Tris, 50 mM L-arg/Glu, pH 8, 0 % glycerol, 0.5/1 mM redox, 1 mM EDTA, 150 mM NaCl, 30 µl protein
	100 mM Tris, 50 mM L-arg/Glu, pH 8, 10 % glycerol, 0.5/1 mM redox, 1 mM EDTA, 150 mM NaCl, 30 µl protein
	250 mM Tris, 50 mM L-arg/Glu, pH 8, 10 % glycerol, 0.5/1 mM redox, 1 mM EDTA, 150 mM NaCl, 30 µl protein
	100 mM Tris, 350 mM L-arg, pH 8, 0 % glycerol, 0.5/1 mM redox, 1 mM EDTA, 150 mM NaCl, 30 µl protein
	250 mM Tris, 350 mM L-arg, pH 8, 10 % glycerol, 0.5/1 mM redox, 1 mM EDTA, 150 mM NaCl, 30 µl protein
	100 mM Tris, 350 mM L-arg, pH 8, 0 % glycerol, 0.5/1 mM redox, 1 mM EDTA, 150 mM NaCl, 20 µl protein

Refolding buffers used in the TSA assay shown in Figure 14 B with their respective symbol.

Results and Discussion

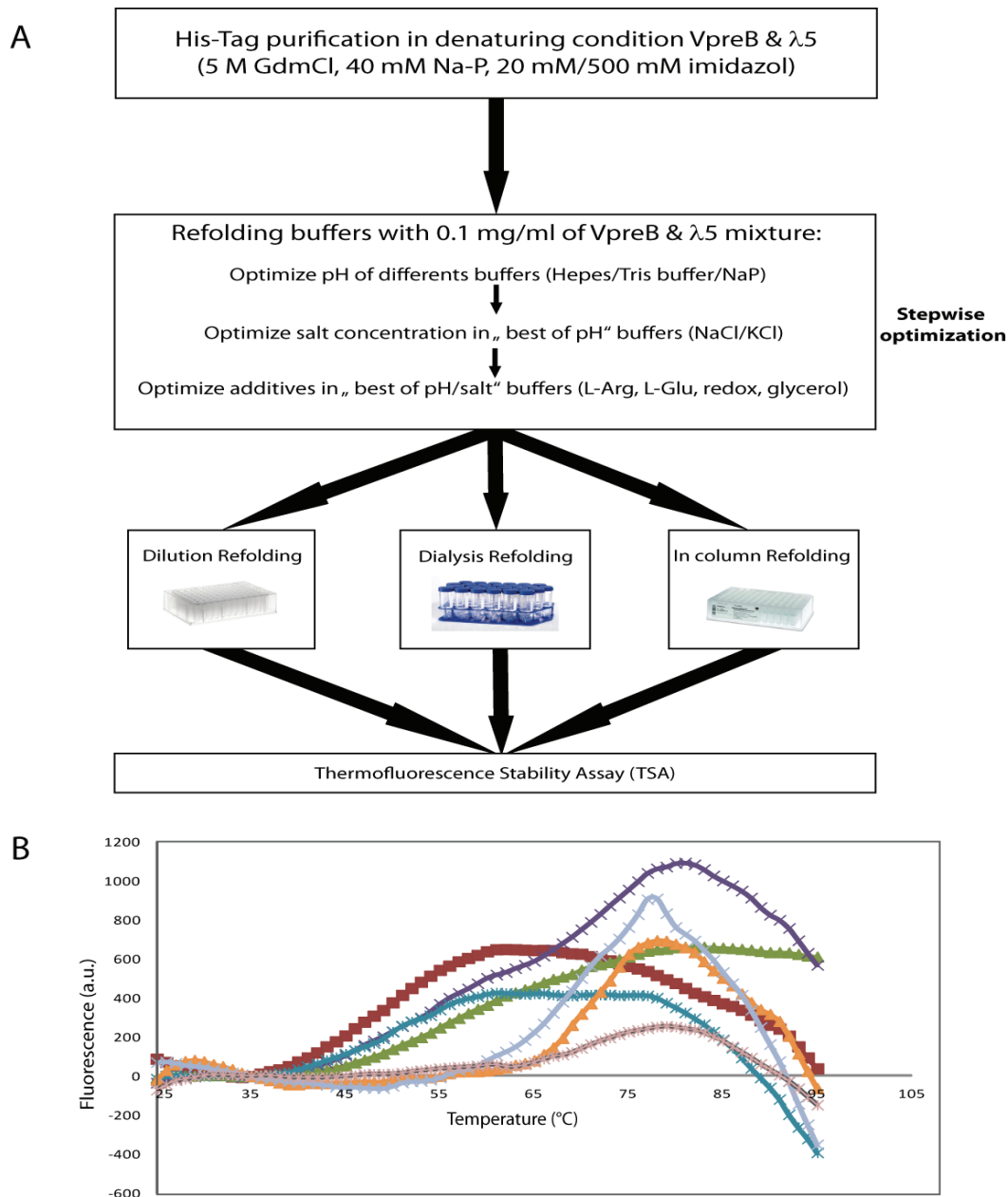


Figure 14: Refolding stepwise optimization. (A): Methods and buffers for protein refolding optimization. After purification with His affinity chromatography, proteins at 0.1 mg/ml were refolded with different methods (2.3.4.3.1) and buffers (2.3.4.3.2): refolding by dilution, by dialysis or on column. For the last method purification and refolding were performed in 96 well HisMultitrap FF plates. (B): TSA of best hits before the final buffer determination. The fluorescence signal increases with temperature increase, allowing the melting temperature determination in correlation with the folding degree.

Taken together, these results show that the stepwise optimization approach, in combination with the TSA, was an efficient screen which allowed different parameters and methods to be tested in parallel. The optimal buffer, method and time for SLC proteins refolding were determined to be: 100 mM Tris-HCl, 350 mM L-Arg, 150 mM

NaCl, 0.5 mM GSH, 1 mM GSSG, 1 mM EDTA pH 8 for 3 days by dialysis with a final protein concentration of 0.1 mg/ml and a dilution factor of 1:30.

3.1.2.2 *Up-scaling of the refolding procedure*

Having determined the optimal refolding conditions for the SLC protein complex, scaling-up of the refolding procedure was carried out using bigger volume of refolding dialysis buffer for the complex and single domains followed by purification through a prepacked SEC column. This strategy was not successful for WT proteins, and therefore further optimization of the purification protocol was necessary as described below.

3.1.3 Purification of the SLC proteins

The SEC after refolding the SLC proteins was disappointingly not working as no protein peak was observable. Though the over expression in the feed batch fermentor provided enough unfolded proteins, which combined with the optimal refolding buffer allowed us to develop a purification strategy. Several different purification procedures and conditions were tested until an optimal purification protocol was established. This protocol enabled us to obtain pure SLC proteins separated and in complex which is depicted schematically in Figure 15. Briefly, harvested cells were lysed (2.3.2) and inclusion bodies produced (2.3.3), 5 M GdmCl buffer was used to dissolve the IB and the solution was loaded onto a His Trap FF column. Ni-affinity chromatography was performed in buffer A (2.1.8.1), protein bounded to the column was eluted with a linear increasing concentration of imidazole in the running buffer up to 500 mM over 15 column volumes. Because some contaminating proteins were found in the fractions eluted from the His Trap FF column, and in order to increase the refolding yield, a size exclusion column was performed in the denaturing conditions with 3 M GdmCl buffer (2.1.8.1). Then, refolding was achieved by dialysis in the determined optimal buffer for 3 days at 8 °C. Part of the protein and contaminants precipitated in the dialysis tube. To avoid further precipitation, a centrifugation step (20 000 x g, 20 min, and 8 °C) was carried out. Subsequently, the protein solution was loaded on a His Trap FF column with native buffers, and fractions containing the proteins were collected and dialyzed against 50 mM Hepes buffer. As contaminating protein was observable in VpreB samples

Results and Discussion

(Figure 15 B), a resource Q sepharose column and SEC were tested. However, the low salt buffer exchange to load in the resource Q column caused a high precipitation of the proteins and no protein was detected in the elution. To the same end, no protein peak was detected after the SEC run. These attempts did not result in a purer protein preparation. Therefore, for the WT proteins, no further purification steps were established. On the other hand, the mutant single domains or in complex elute from the SEC resulting in pure proteins (Figure 20). For this reason, after refolding, they were applied to the SEC column. The presence of the purified proteins was verified by western blot and mass spectroscopy.

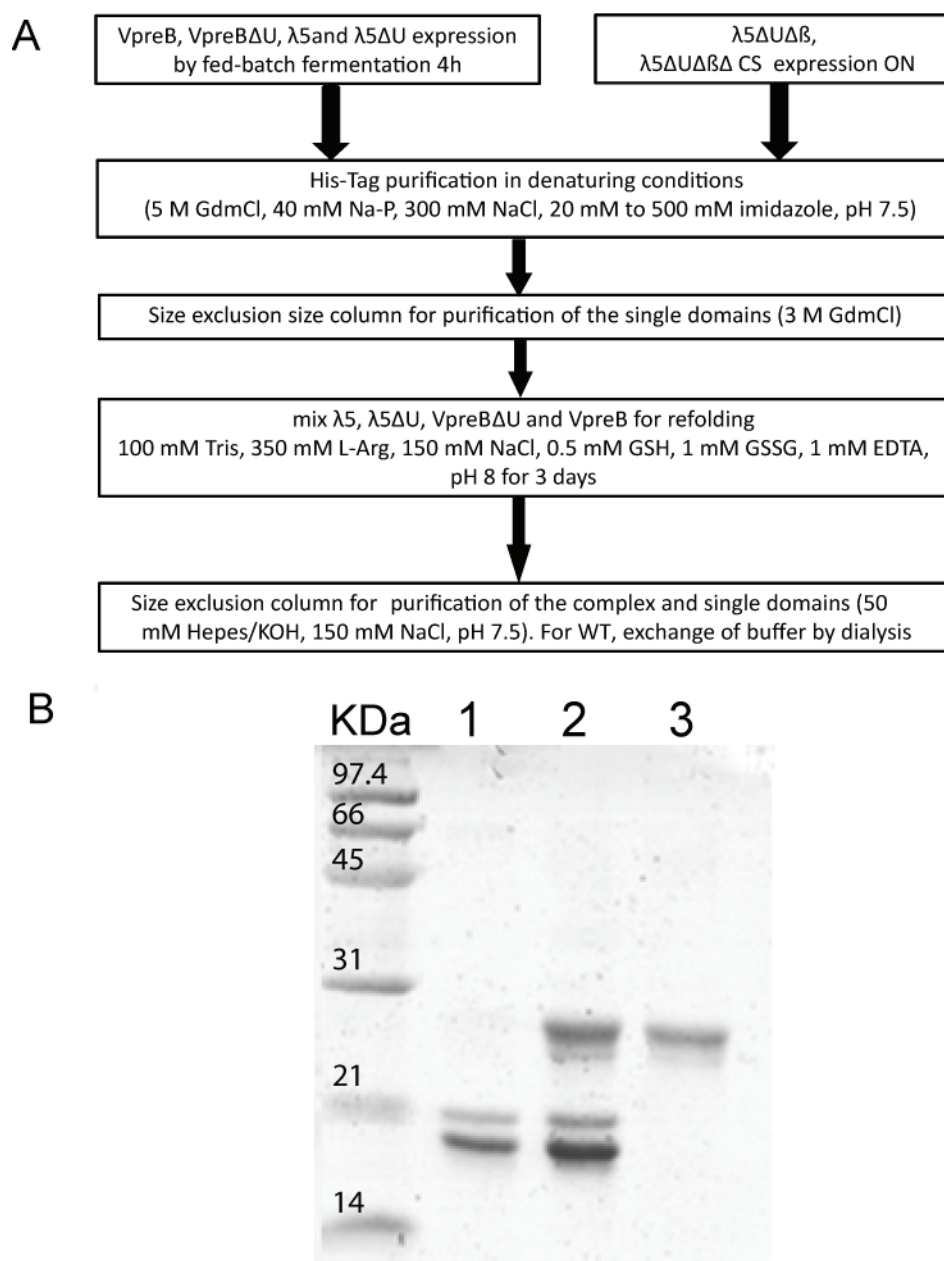


Figure 15: Expression and purification scheme of SLC proteins WT and mutants. (A) Expression was carried out at 37 °C for 4 h after induction. The inclusion body preparation was followed by the first step of purification, nickel affinity chromatography in denaturing conditions. Then, a gel filtration was performed followed by refolding of the proteins separated or in complex. Finally, the mutants were polished by gel filtration and eluted fractions were pooled, concentrated and stored at -80 °C. For the WT proteins, a final His-tag purification was performed and buffer exchange in Hepes buffer was achieved by dialysis. The proteins were concentrated and stored at -80 °C. (B) Representative gel of the final purified SLC proteins 1: VpreB, 2: SLC ($\lambda 5$ +VpreB), 3: $\lambda 5$.

3.1.4 Characterization of human SLC proteins

Different methods were used to validate our purification protocol and gain insight into the structure of the individual proteins and protein complex. These are described in this section.

3.1.4.1 *Structural characterization of the SLC proteins*

Circular dichroism (CD) spectroscopy was used to analyze the secondary and tertiary structure of the SLC proteins. CD spectra of the two separate proteins (VpreB and $\lambda 5$) and SLC complex were recorded (Figure 17) as described in section 2.4. The spectra obtained for the wild type complex and $\lambda 5$ were dominated by β -sheet spectra characterized by a minimum at around 218 nm, in agreement with the crystal structure. The VpreB spectra was dominated by unfolded segments, consistent with the unique region being unstructured (Figure 17 A). To obtain a more detailed picture of the structure of the single proteins and in complex, we used near-UV (NUV) CD and fluorescence spectroscopy. These spectroscopic techniques can be used to garner tertiary structural information about the environment of the aromatic amino acids Phe, Tyr, and predominantly Trp. The single protein $\lambda 5$ and the SLC complex showed well defined NUV-CD spectra indicative of a defined structure around the aromatic reporter groups. In accordance with the FUV-CD spectra, VpreB did not show a defined NUV-CD signal, but a featureless spectrum typical of an unfolded protein (Figure 17 B).

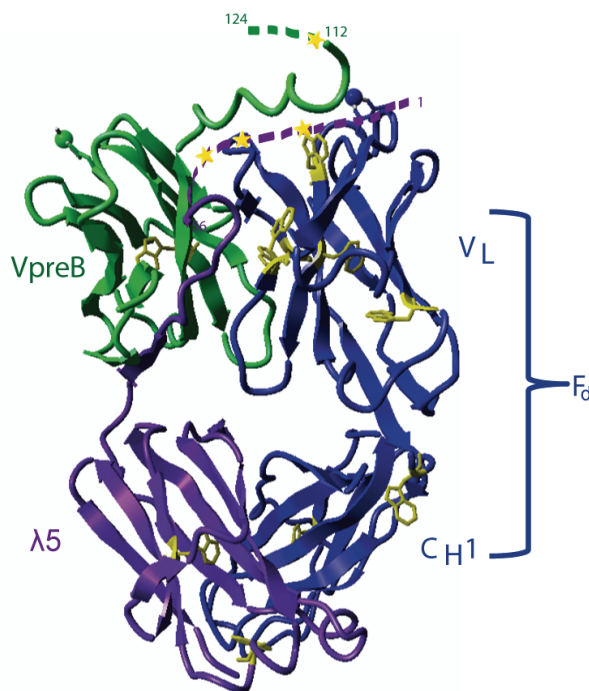


Figure 16: Tryptophan residues in the Fd-SLC complex structure. Ribbon representation of the Fab pre-BCR structure, PDB: 2H32 (Bankovich et al, 2007). Three proteins chains are included: VpreB (green), $\lambda 5$ (violet), and Fd (blue). Fab fragment shows the conserved Ig fold including the tryptophan residues in yellow. Missing portion of the unique regions are indicated with residue numbers and dashed lines at N terminus of $\lambda 5$ (48 amino acids) and C terminus of VpreB (15 amino acids). The tryptophan residues present in the unique region of $\lambda 5$ (3 Trp) and VpreB (1 Trp) are represented by yellow stars.

The fluorescence spectra of the single proteins and the complex corroborate the findings from FUV-CD and NUV-CD measurements for $\lambda 5$ and SLC. The Trp fluorescence is usually quenched in the native state of folded antibody domains due to the local proximity of the buried intrinsic disulfide bridge to an adjacent buried Trp residue of hydrophobic core. Therefore, changes in the fluorescence intensity provide means to follow structural changes, from the folded to unfolded (by GdmCl) state. The fluorescence intensity of the unfolded proteins was significantly higher than in the native state (Figure 17 C) in accordance with the defined secondary and tertiary structure of both proteins (Figure 16). This argues for structural rearrangements moving the Trp residues away from the internal disulphide bridge in the unfolded state. For VpreB, the fluorescence spectra of the unfolded state were also higher than the native state. This contrasts with the partially folded structural state of VpreB, which was reflected by the increase in fluorescence intensity. The difference in signal between the native and denatured state is higher for the complex compare to the single domains (Figure 17 C). This suggest that the tryptophan residues present in the unique region

Results and Discussion

(Figure 16) are more surface exposed in the isolated proteins compared to the complex, proposing a rearrangement of the unique region when the SLC complex is formed. As VpreB and $\lambda 5$ possess unstructured amino acids at their C and N termini, respectively, the β -sheet characteristics of the FUV-CD spectra can be less defined.

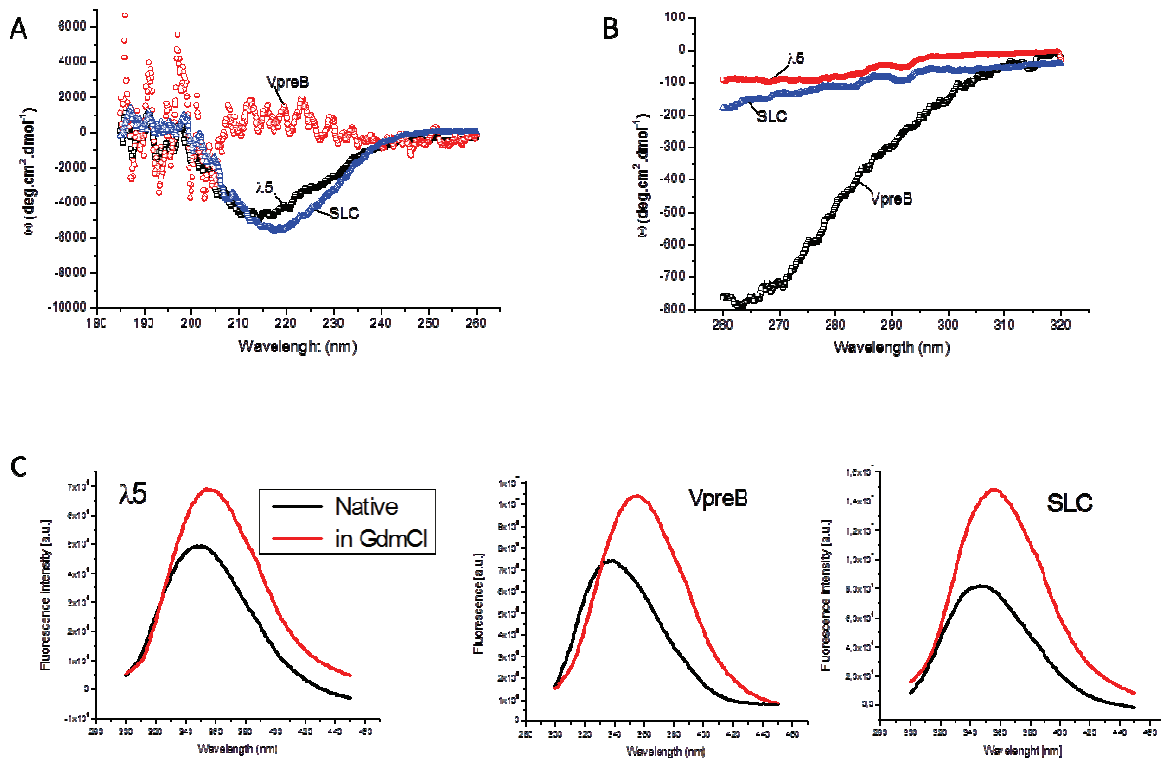


Figure 17: CD and fluorescence analysis of SLC proteins. (A) Far UV and (B) near UV CD spectra of human recombinant VpreB (red line), $\lambda 5$ (black line) and SLC (blue line). Spectra were obtained in 50 mM HEPES buffer at pH 7.5. (C) Fluorescence spectra in native conditions (50 mM HEPES, 150 mM KCl, pH 7.5) and under denaturing condition (5 M GdmCl buffer). Protein fluorescence was excited at 280 nm. All measurements were performed at 20 °C.

3.1.4.2 Chemical and thermal stability of the SLC proteins

To investigate the stability of the SLC proteins, thermal and GdmCl-induced unfolding transitions were performed. Temperature-induced unfolding was monitored by FUV-CD spectroscopy to follow the secondary structure changes, and the increase in hydrophobic patches was followed using sypro orange fluorescence (TSA). In contrast, GdmCl-induced unfolding was monitored by fluorescence spectroscopy. Therefore, for GdmCl-induced transitions, no secondary changes but rearrangements within the environment of the aromatic amino acids were observable. The reactions were not reversible, thus thermodynamic stabilities of the SLC proteins could not be determined.

In Figure 18 A and B, the thermal transitions of the SLC proteins isolated and in complex are shown. VpreB is the least stable of the domains with the lower melting temperature under 30 °C (Table 2), while $\lambda 5$ and the SLC complex showed a similar transition midpoint in temperature-induced experiments of around 50 °C. The midpoint values obtained by following the secondary structure or hydrophobic patches were similar (Table 2).

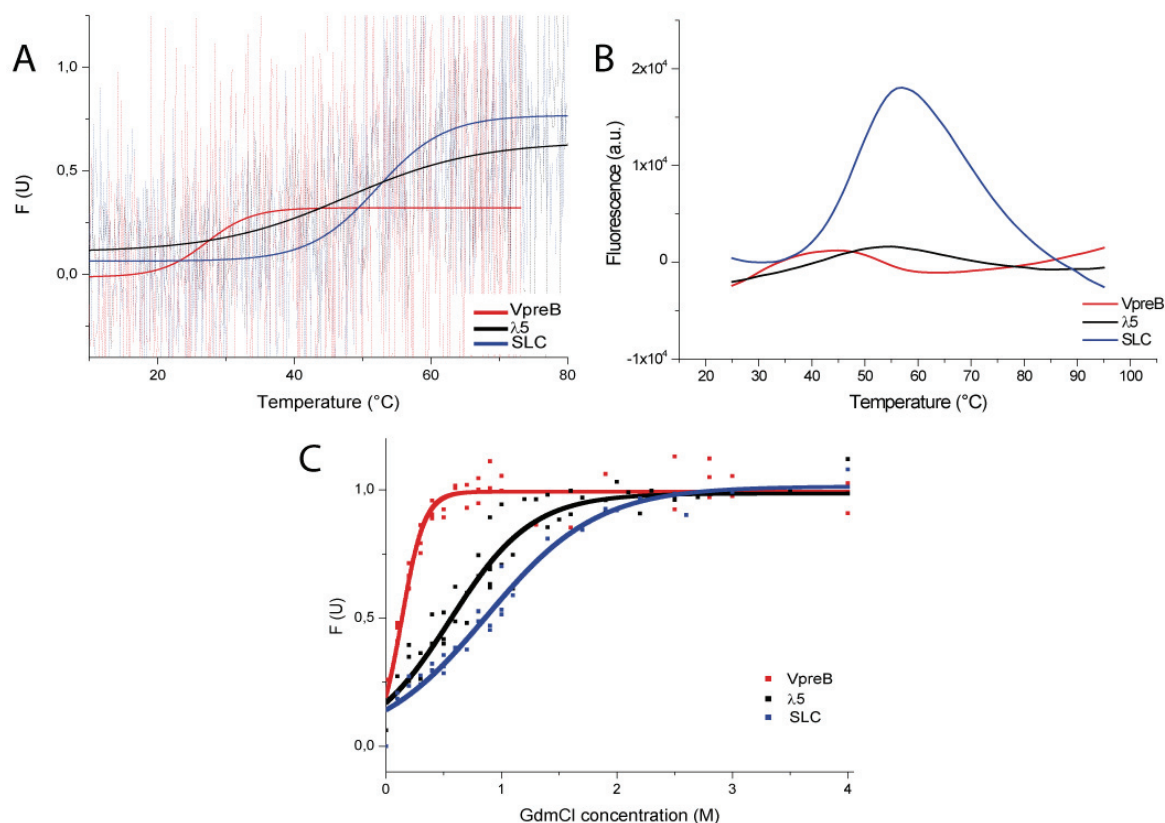


Figure 18: Stability of the SLC proteins in their native state. To assess the stability of the SLC proteins, temperature-induced (top) and GdmCl (bottom) unfolding experiments were performed. Data for the temperature-induced (A and B) and GdmCl-induced transitions (C) are shown. (A) temperature-induced unfolding transitions followed by CD spectroscopy and (B) by sypro orange fluorescence (TSA). Temperature-induced unfolding was monitored by FUV-CD spectroscopy at a fixed wavelength with a heating rate of 20 °C h⁻¹. For TSA, the heating rate was 1 °C min⁻¹ and fluorescence changes were monitored by real-time PCR. (C) GmCl transitions were measured by fluorescence spectroscopy. Chemical denaturation of proteins was induced by different concentration of GdmCl and structural changes were monitored at a fixed wavelength (360 nm). Three measurements were averaged to improve the signal quality. Data were fitted to a Boltzmann function to obtain transitions midpoints.

The GdmCl-induced unfolding experiments (Figure 18 C) showed a different trend as proteins unfolded at rather low concentrations of GdmCl. On the other hand, the stability distribution matched the observations from the thermal-induced transition with the stability of VpreB < $\lambda 5$ ≤ SLC (Table 2) quite well.

Table 2: Thermal and chemical stabilities of SLC proteins.

Protein	T _{melt} (°C)	T _{melt} (°C)	D _{1/2} (M)
	FUV-CD	TSA	
VpreB	28.3 ± 3.5	29.6 ± 0.3	0.14 ± 0.01
λ5	47.7 ± 2.7	47.7 ± 0.8	0.56 ± 0.03
SLC	50.1 ± 1.5	47.6 ± 0.1	0.87 ± 0.04

Stabilities against the thermal and chemical denaturation (GdmCl) of the SLC proteins. Midpoints of thermal (T_{melt}) and chemical (D_{1/2}) transitions are shown. Values are average ± standard deviation.

3.1.4.3 Quaternary structure analysis

In order to obtain the SLC complex, the denatured WT proteins were mixed and refolded together. To examine the quaternary structure of the proteins, analytical ultracentrifugation (aUC) was used (Figure 19 A). In the sedimentation velocity runs, the absorption at 230 nm of 10 μM of proteins was measured against a reference buffer. These experiments consistently revealed a shift of the s-values for the single domains towards larger values corresponding to the heterodimer SLC. The calculated molecular mass of the SLC complex was 41.4 KDa compatible with the theoretical mass of 40.4 KDa. The calculated mass of λ5 was 20 KDa in agreement with the isolated protein (theoretical mass 23.5 KDa). The VpreB domain displayed an asymmetric distribution indicative of the presence of monomer with a calculated mass of 18.4 KDa (theoretical mass 18.5 KDa) and homodimers with a slightly smaller apparent molecular mass of 34.4 KDa. The propensity to form stable homodimers may be a result for the stabilization of the partially folded state. These results demonstrate the successful *in vitro* production of the soluble and folded SLC complex as well as the single proteins.

In order to confirm the quaternary structure of the SLC and single isolated proteins, samples were subjected to analytical size exclusion chromatography (SEC). Elution profiles are shown in Figure 19 B. Surprisingly, elution profiles for the VpreB and λ5 proteins were identical, and an additional peak appear in the SLC elution profile, most

likely from the complex. Notably, the proteins interacted with the column resin, as their elution was out of range of the calibration curve (Figure 19 B inset), obtained with standard proteins of defined molecular weights. These results are in accordance with SEC data obtained from the purification of the proteins after refolding, as the proteins did not elute from the standard SEC (HiLoadsuperdex 75 26/60) at the expected molecular weight. As the molecular weight could not be calculated from the elution obtained, other HPLC columns were tested. The TSK-G 3000 PW (Tosoh Bioscience) and YMC Pack Diol (YMC) column showed the same or stronger interactions of the proteins with the material (data not show). Taken together, this interaction limits the application of SEC to determine the molecular weight of the proteins.

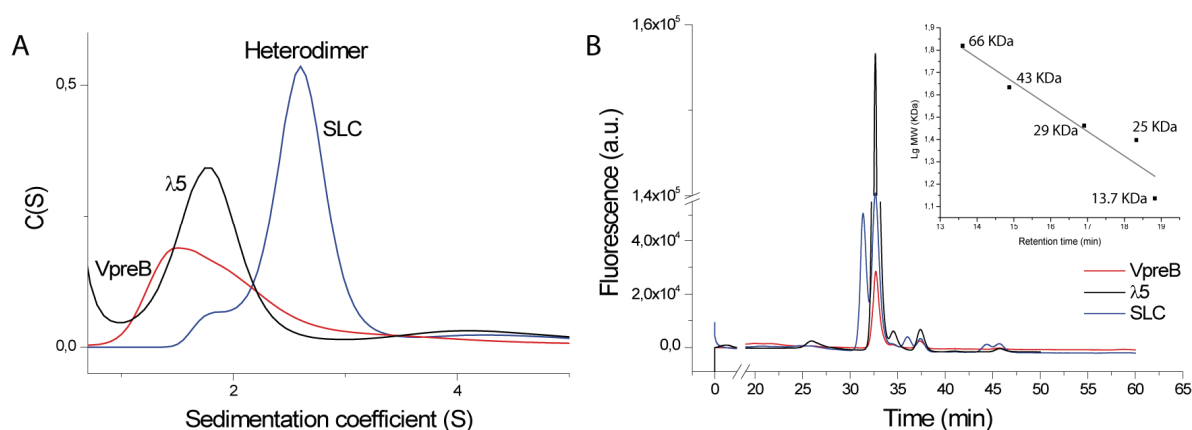


Figure 19: Quaternary structural study of SLC proteins. (A) aUC sedimentation velocity experiments at 45,000 rpm. The three proteins were tested against the reference buffer in a four whole Beckman-Coulter AN60-Ti rotor. The data were analyzed using the dc/dt method. (B) Analytical gel filtration analysis. A Superdex 75 10/300 GL column (GE Healthcare) was equilibrated with buffer containing 50 mM HEPES-KOH, 150 mM KCl, pH 7.5. Prior to loading of 50 μ l of 10 μ M SLC proteins, 25 μ l of various standard proteins with different size at a concentration of 4 mg/ml were applied to obtain a calibration curve (see inset: albumin, ovalbumin, carbonic anhydrase, chymotrypsinogen A and ribonuclease). The flow rate was set to 0.5 ml/min and elution profiles were recorded at 350 nm (Excitation wavelength: 280 nm). Gain settings were adjusted for each analyzed protein.

3.1.5 Discussion

A source of pure and functional SLC proteins in complex and isolated is required to elucidate the molecular determinants for the SLC formation and its interaction with the HC. Despite several attempts, soluble expression of the proteins were not obtained from *E. coli* and the expressed proteins accumulated in an insoluble form. However, the stepwise optimization of refolding buffer developed by Dashivets et al (2009) in

Results and Discussion

combination with the TSA allowed the purification of recombinant SLC protein as isolated proteins and in complex. The purity of VpreB was not 100 %, as a second band was present which mass spectrometry revealed to be VpreB as well. This phenomenon has been shown previously in *E. coli* (Hirabayashi et al, 1995) and baculovirus (Bankovich et al, 2007; Gauthier et al, 1999). This could be explained by a partially expressed VpreB which decrease in the presence of the partners $\lambda 5$ /HC, or it could represent the human counterpart of a murine protein product from the VpreB3 gene (\approx 4 KDa smaller compare to VpreB), which has been found to be transiently associated with the HC in murine pre-B cells (Lassoued et al, 1996). $\lambda 5$ protein is slightly degraded which was also encountered when expressed in the baculovirus system with the unique region present (Bankovich et al, 2007). Nevertheless, the isolated and in complex proteins had a reasonable purity level with the following yields: VpreB = 0.76 mg, $\lambda 5$ = 3.36 mg and SLC = 3.57 mg for \approx 30 g of cells. The SLC complex and the $\lambda 5$ protein showed secondary structure of β -sheet characteristic of functional antibodies domain and in accordance with the crystal structure. On the other hand, VpreB did not show a defined secondary structure and the temperature-induced and GdmCl-induced unfolding experiment revealed a more unstable protein. While SLC and $\lambda 5$ have a thermal midpoint of \approx 50 °C, comparable to other antibodies domain (Feige et al, 2010b), no significant stabilization by complex formation was observed in the thermal denaturation. Although a slight increase in the stability was observed in the chemical denaturation for the complex. Despite the lower chemical stability of the three proteins the folding behavior could not be fitted to a two state equation and the reaction was not reversible. The homodimers observed for the VpreB domain in the aUC runs reinforce the hypothesis that the domain is less stable, as shown by CD and fluorescence spectroscopy, and dimerize to gain the stability normally brought by its partner, the $\lambda 5$ domain.

In summary, we obtained the two human proteins forming the SLC, by producing them separately in *E. coli*. They were non-covalently associated with the connected heterodimer *in vitro* during refolding as demonstrated by the aUC velocity run. The expression and purification of the SLC proteins with their unique region is an ideal

starting point to analyze the complex formation and its interaction in more details using biochemical and biophysical methods.

3.2 Effect of the unique region in the isolated proteins and the SLC complex

As a first step, to analyze the determinants influencing the stability and assembly of the SLC, we produced different variants of VpreB and $\lambda 5$ in *E. coli* (Figure 20 A and B). These included variants in which the unique region sequences were deleted. The SLC mutants were expressed and purified as described in 3.1.3. The deletion of the VpreB unique tail resulted in an unstable single domain, limiting its characterization in complex with $\lambda 5$ with deleted unique region. In order to obtain the SLC complexes, as for the WT proteins, variants were mixed and complexes were then purified by SEC. The complex form by VpreB with its unique region deleted and $\lambda 5$ lead to an unstable protein, therefore no further characterization was performed. The purification of SLC variants was more successful compared to the WT proteins with a higher purity grade ($\approx 90\%$, Figure 20 C) and the following yields: $\lambda 5\Delta U = 3.5$ mg; $\lambda 5\Delta U\Delta\beta = 3$ mg; $\lambda 5\Delta U$ -VpreB = 2 mg and $SLC\Delta U = 3.7$ mg for 20 g of cells. Expression and purification of the mutated SLC proteins allowed a detailed characterization of the proteins in the absence of the unique region to get an insight of its importance. The purification scheme is described in Figure 15.

Results and Discussion

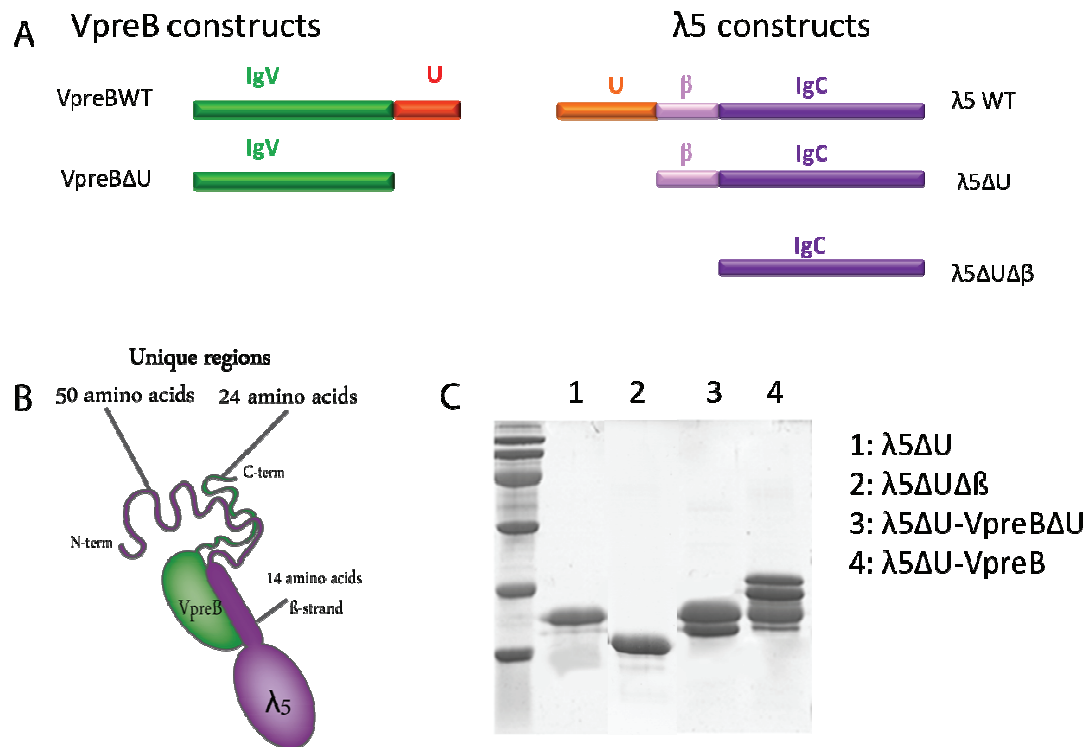


Figure 20: Scheme SLC constructs: (A) Schematic diagram of wild-type and mutant proteins included in this study. The $\lambda 5\Delta U$ and $\lambda 5\Delta U\Delta\beta$ mutants lack the 50 amino acids unique region and the 14 amino acids β -sheet, respectively. The mutant VpreB ΔU lacks the 24 amino acids unique region. (B) Schematic of a conventional SLC composed of VpreB and $\lambda 5$ proteins with their unique regions. VpreB is lacking a β -sheet which is provided by $\lambda 5$, allowing the non-covalently link between the two proteins. The unique regions of VpreB and $\lambda 5$ are shown schematically. (C) Representative gel of the final purified SLC mutants isolated (1 and 2) and in complex (3 and 4).

Complex formation was validated by aUC (Figure 21) and analytical HPLC (data not shown). For all different combinations, sedimentation coefficient were obtained in accordance with the expected complex sizes. Alone the $\lambda 5\Delta U$ sedimented with 1.5 S with a calculated molecular weight of 13.7 KDa (theoretical = 16.34 KDa) and for the complex of SLC ΔU , the peak shifted to 2.6 S for a calculated molecular weight of 31.7 KDa (theoretical = 38.5 KDa), despite the presence of some “free” $\lambda 5\Delta U$ (Figure 21 A). In the same direction, the complex of the $\lambda 5\Delta U$ -VpreB sedimented at 3 S with a calculated molecular mass of 35.5 KDa, similar to the theoretical one, 33.2 KDa (Figure 21 B). Consistently, experiments revealed a shift of the s-values from the single domains towards higher s-values in agreements with the heterodimer formation. This shows that the refolding of the two domains resulted in heterodimer complexes and its formation does not depend on the presence of the unique regions.

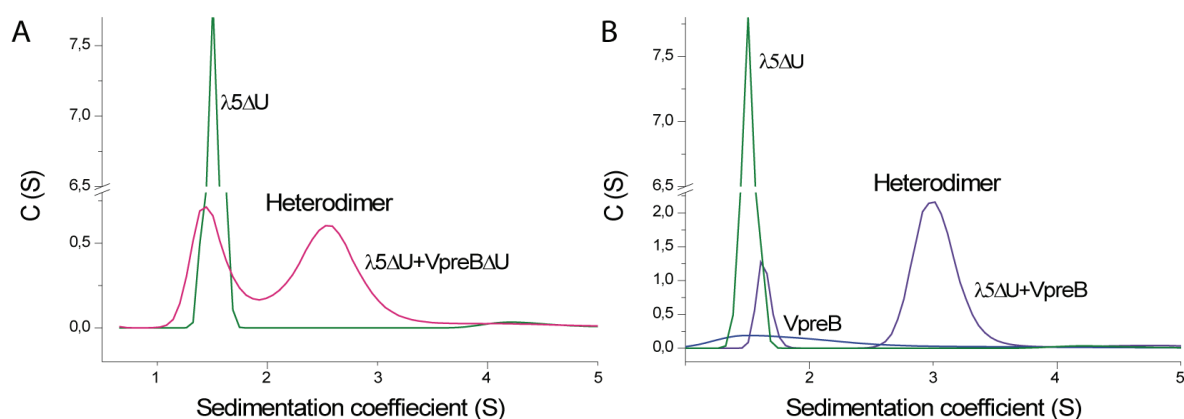


Figure 21: Quaternary structural study of SLC variants. aUC sedimentation velocity experiments at 45,000 rpm. The three proteins were tested against the reference buffer in a four hole Beckman-Coulter AN60-Ti rotor. The obtain data were analyzed using dc/dt method. (A) SLC Δ U complex in pink and isolated λ 5 Δ U protein in green. (B) λ 5 Δ U-VpreB complex in purple and isolated proteins VpreB in blue and λ 5 Δ U in green. Measurements were performed at 20 °C in 50 mM Hepes, 150 mM KCl, pH 7.5.

3.2.1 The role of the unique region in chemical and thermal stability

To address the influence of the unique regions on the overall stability of the single proteins and complexes, we measured temperature- and GdmCl-induced unfolding transitions. Thermal melting curves were monitored by changes in the far-UV CD signal at 208 nm and the fluorescence signal increase of sypro orange (Roche) (Figure 22 A and B). As for the WT proteins, no significant difference was obtained between the melting temperature measured by change in the secondary structure or dye binding to hydrophobic patches. The λ 5 Δ U-VpreB and SLC Δ U complexes have a higher melting temperature (± 10 °C) in the TSA measurement which indicates a stable complex in which the hydrophobic patches are buried in the interface. The GdmCl-induced unfolding experiments exhibited a similar trend. λ 5 Δ U and λ 5 Δ U $\Delta\beta$ have a higher $D_{1/2}$ compared to λ 5. In contrast, the complex showed a similar stability as the WT complex (Table 3 and Figure 22 C). Taken together, we observed a significant thermodynamic stability difference between λ 5 WT and the variant with the unique region and β -sheet deleted. The deletion results in a two-fold increase in the chemical stability. Additionally, the chimeric complexes with or without the unique region have a higher thermal and chemical stability.

Results and Discussion

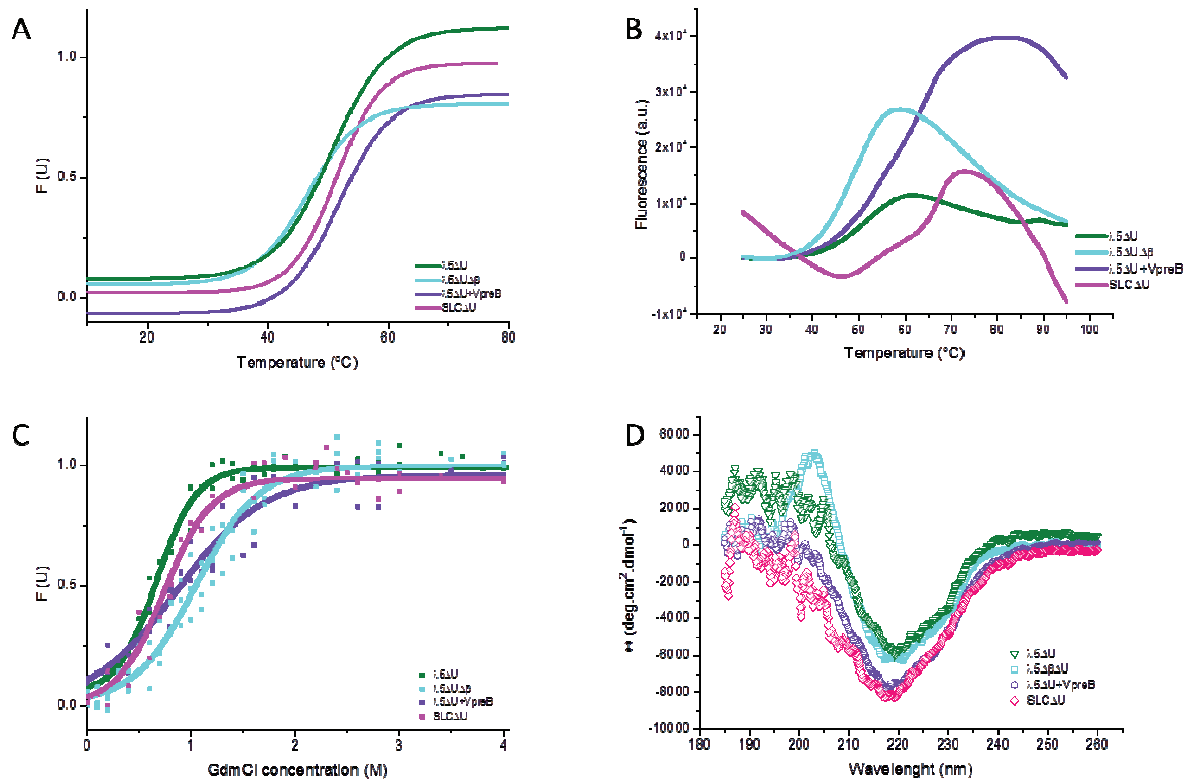


Figure 22: Stability of the SLC mutants in their native state. To assess the stability of the SLC proteins, temperature-induced (A and B) and GdmCl (C and D) unfolding experiments were performed for all variants. Temperature-induced unfolding transition followed by CD spectroscopy (A) or by sypro orange fluorescence (TSA) (B). Temperature-induced unfolding was monitored by FUV-CD spectroscopy at a fixed wavelength with a heating rate of $20\text{ }^{\circ}\text{C h}^{-1}$. For TSA, the heating rate was $1\text{ }^{\circ}\text{C min}^{-1}$ and fluorescence changes were monitored. Data were fitted to a Boltzmann function to obtain mid points. (D) Far UV CD spectra of human recombinant SLC variants. Spectra were obtained in 50 mM HEPES, 150 mM KCl buffer at pH 7.5, all measurements were performed at $20\text{ }^{\circ}\text{C}$. Isolated proteins and complexes show a typical all- β FUV CD spectrum.

The secondary structures of all variants, isolated or in complex, are shown in Figure 22 D. The constructs with deleted unique regions showed a predominantly β -sheet structure characterized by a minimum around 218 nm in agreement with the dominant secondary structure in antibody domains.

Table 3: Thermal and chemical stabilities of SLC mutants.

Protein	T _{melt} (°C)	T _{melt} (°C)	D _{1/2} (M)
	FUV-CD	TSA	GdmCl
λ5	47.7 ± 2.7	47.7 ± 0.8	0.56 ± 0.03
VpreB	28.3 ± 3.5	29.6 ± 0.3	0.14 ± 0.01
SLC	50.1 ± 1.5	47.6 ± 0.1	0.87 ± 0.04
λ5ΔU	47.4 ± 0.9	47.7 ± 0.8	0.74 ± 0.02
λ5ΔUΔβ	47.6 ± 0.4	48.1 ± 0.1	1.05 ± 0.03
SLCΔU	52.5 ± 2.8	69.1 ± 4.5	0.74 ± 0.04
λ5ΔU+ VpreB	51.8 ± 0.2	59.2 ± 0.1	0.87 ± 0.05

Stabilities against the thermal and chemical denaturation (GdmCl) of the SLC mutants compared to the WT proteins. Midpoints of thermal (T_{melt}) and chemical (D_{1/2}) transitions are shown. *Values are average ± standard deviation.*

3.2.2 The role of the unique region in SLC complex formation

The physicochemical interactions between λ5 and VpreB that form the non-covalent complex of the SLC are poorly understood. To provide further evidence for heterodimer formation between λ5 and VpreB, aUC analysis with fluorescence detection using Atto488-labeled λ5 and unlabeled VpreB was performed. When increasing amounts of unlabeled VpreB were added to labeled λ5, the size distribution gradually shifted towards the distribution observed for the SLC (Figure 23 A). As the use of the fluorescence optics permitted the selective monitoring of the labeled λ5 domain, this shift is the result of heterodimer formation. The titrations allowed us to determine the K_D of the interactions. The dissociation constant of the two WT domains was determined to be 0.06 ± 0.02 μM (Figure 23 B), whereas the K_D for the λ5ΔU-VpreB complex was determined to be 1.5 ± 0.3 μM, by monitoring labeled λ5ΔU (Figure 23 C). We did, however, observe differences compared to the WT complex. Surprisingly, the WT domain has a lower K_D (60 nM) correlated to a higher affinity compared to the complex in which the unique region of λ5 was deleted. When both unique regions were

Results and Discussion

deleted, the determination of K_D was more difficult as VpreB Δ U cannot be obtained in an isolated form. In order to analyze the dissociation, the complex with labeled λ 5 Δ U was diluted (Figure 23 D). In this case, the limiting factor was the concentration of the labeled protein, as the limit of detection is when the signal to noise ratio is in a range of 200 nM of label. Additionally, we encountered some problems of aggregation, as once the complex was dissociated the isolated proteins, most likely VpreB Δ U, seemed to be unstable; thus, shifting the equilibrium. Despite the exact K_D not being determined, we could limit the range as being between 0.5 and 1 μ M. These results show a stabilization of the complex by the presence of the unique regions. Furthermore, these results prove the importance of the unique region for complex formation. Their deletion decreases the affinity, suggesting that their negative and positive charges contribute to the non-covalent interaction. Taken together these experiments suggest that the unique regions have opposite effects: the complex formation is stabilized by the unique regions while the thermal and chemical stability is decreased.

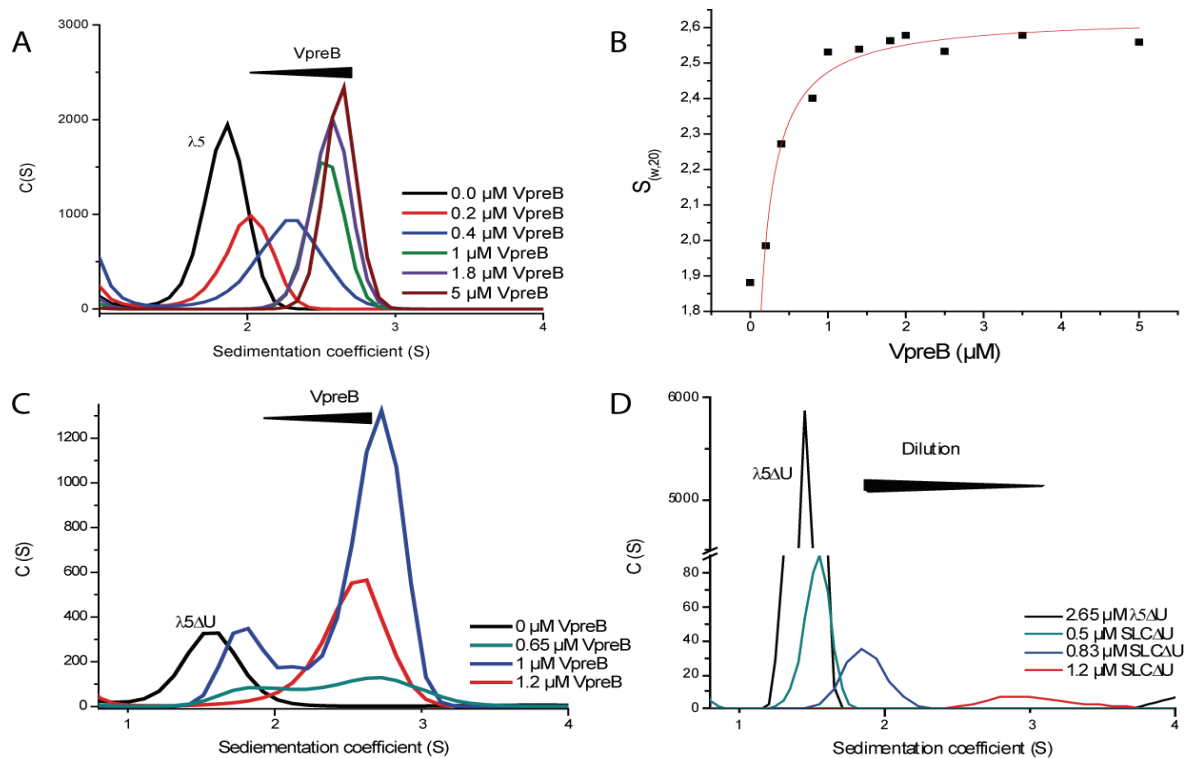


Figure 23: Study of complex formation in the presence or absence of the unique regions. aUC sedimentation velocity experiments with constant concentration of labeled λ 5 (A) or λ 5 Δ U (C and D) and increasing concentrations of VpreB. (A) complex formation of the SLCWT. (B) The K_D is obtained by the shift of $S_{20,w}$ -values plotted against the VpreB concentration added. Data was fit to a one binding site equation. (C) Complex formation of the λ 5 Δ U-VpreB. (D) Complex dissociation of the SLC Δ U by dilution. Measurements were performed at 20 $^{\circ}$ C in 50 mM Hepes, 150 mM KCl, pH 7.5.

3.2.3 Interaction mechanism between V_H and SLC proteins

The capacity of the VpreB domain to pair with V_H or HC in the absence of the λ5 domain has been previously shown (Gauthier et al, 1999; Hirabayashi et al, 1995; Seidl et al, 2001). Despite these insights, our understanding of the mechanism by which the additional β sheet brought in by λ5, and the presence of the unique regions, influence this interaction is still at an early stage. Interaction of SLC domains with V_H were analyzed by Surface Plasmon Resonance (for details see 2.6.4). The V_H domains were immobilized, on a CM5 sensor chip via an introduced cysteine at the N-terminus, and the different constructs were injected at a constant flow rate of 30 μl min⁻¹.

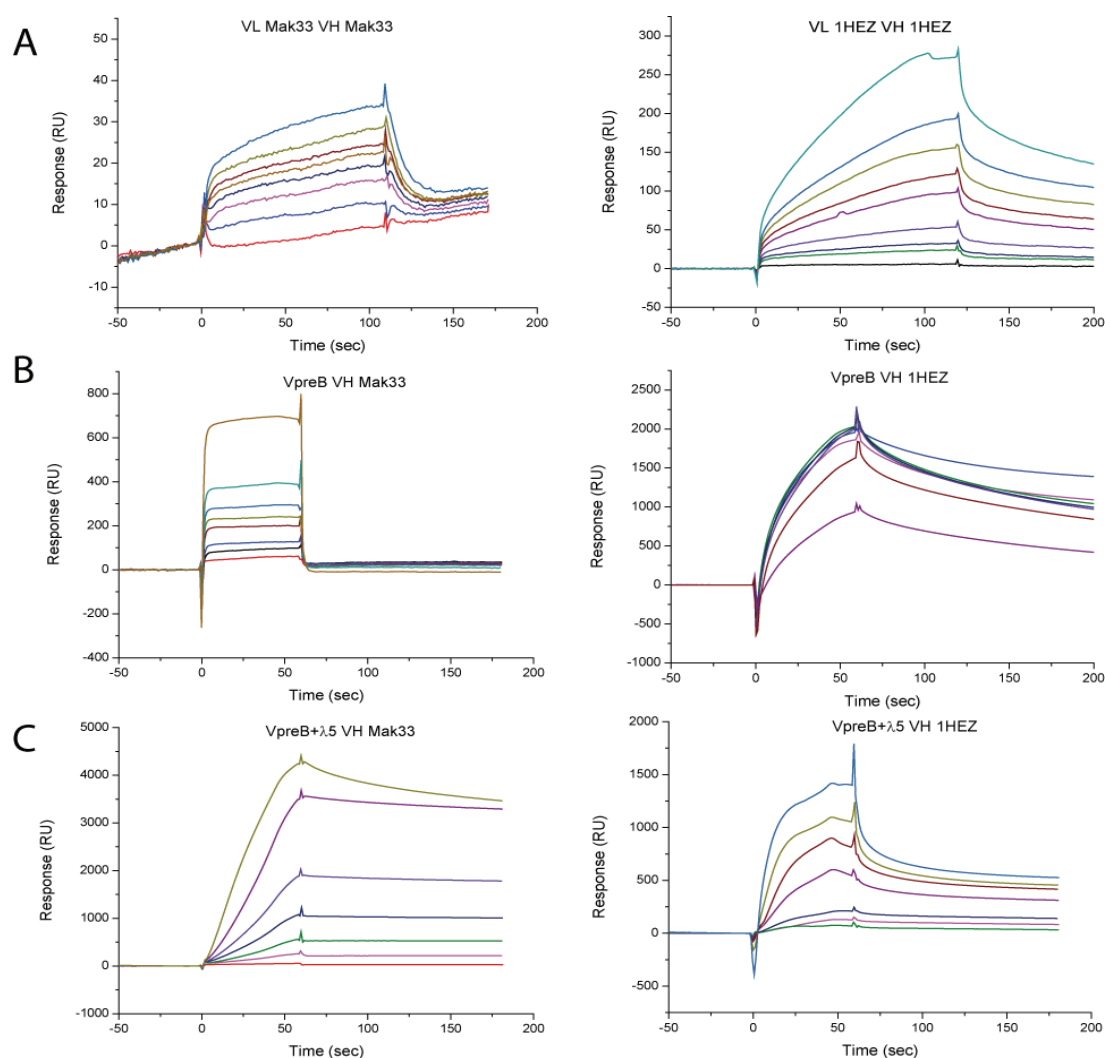


Figure 24: Kinetic analysis of the V_H interaction with VpreB and SLC. Superimposed sensorgrams obtained at different concentration of construct with immobilized V_H Mak33 (right side) or V_H 1HEZ (left side). (A) Injection at different concentrations of WT V_L MAK33 (right side) and V_L 1HEZ (left side) as a control. (B) Injection at different concentrations of VpreB. (C) Injection at different concentrations of SLC complex (λ5+VpreB). All above experiments were performed at 20 °C.

Results and Discussion

The superimposed sensogrammes in Figure 24, show examples of the titration of the analyte over immobilized ligand V_H . Despite the binding and dissociation variation from one combination to another, an increase in the signal can be observed in all cases correlating with the increase in concentration of the analytes. The binding levels were plotted against the concentration for all sensograms and data were fitted assuming a 1:1 interaction to obtain the K_D using the Biacore X100 Evaluation software (Figure 25). Mean K_D values are shown in Table 4. VpreB and V_H Mak33 domains associate with each other with an apparent K_D of $2.75 \times 10^{-6} \pm 0.28$ M; consistent with values for the positive control the Mak33 V_L domain ($1.68 \times 10^{-6} \pm 0.67$ M). Surprisingly, for the V_H 1HEZ the affinity of VpreB domain is much higher ($K_D = 3.37 \times 10^{-6} \pm 0.34$ M) than the positive control V_L 1HEZ ($K_D = 30.4 \times 10^{-6} \pm 2.97$ M). In the case of V_H 1HEZ K_D values are higher due to the homodimers form by this domain in isolation. The WT $\lambda 5$ protein showed a higher K_D alone than in complex with the VpreB protein, in the same range as VpreB alone, while the affinity decreased with the deletion of the unique region by at least three-fold. Values followed the same tendency when using human IgM or Mak IgG V_H (Figure 25 B). These results showed the importance of the unique region to obtain a higher affinity for the VpreB partner, V_H domain.

Due to problems with the stability of VpreB and its low concentration, the interaction with an immobilized VpreB on the chip could not be performed.

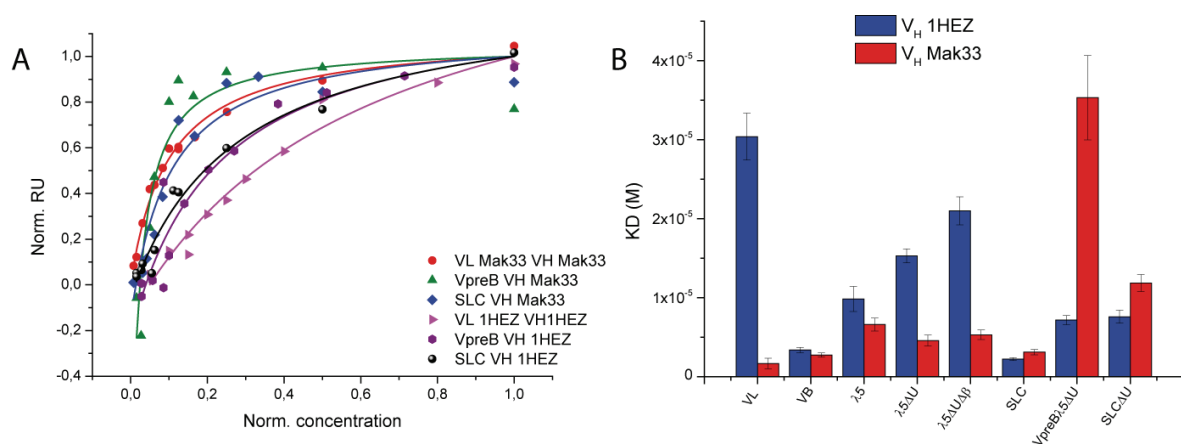


Figure 25 K_D values for different combinations of variable domains and SLC components. Affinities of the different constructs towards V_H Mak33 and V_H 1HEZ determined by SPR using V_H -coupled chips. (A) Normalized titration of VL, VpreB and SLC to the two V_H . (B) K_D values for the different interactions with the fitting error are shown.

Table 4: K_D determination by SPR.

Apparent K_D (μM)	V_H Mak33	V_H 1HEZ
V_L	1.68 ± 0.67	30.4 ± 2.97
$\lambda 5$	6.61 ± 0.82	9.83 ± 1.59
VpreB	2.75 ± 0.28	3.37 ± 0.34
SLC	3.11 ± 0.34	2.23 ± 0.19
SLC Δ U	11.9 ± 1.08	7.59 ± 0.82
$\lambda 5\Delta$ U+VpreB	35.3 ± 5.33	7.16 ± 0.57
$\lambda 5\Delta$ U	4.58 ± 0.69	15.30 ± 0.89
$\lambda 5\Delta$ U Δ β	5.30 ± 0.60	21.0 ± 1.77

SPR experiments were performed at 20 °C with a Biacore X100 (GE, Healthcare, Uppsala, Sweden). Ligand was immobilized via an introduced cysteine at the N-terminus. Measurements were performed at least 3 times with different chips and different concentrations of immobilized ligand. K_D values were determined using the Biacore X100 Evaluation software. Values are average \pm standard deviation.

3.2.4 Discussion

In order to further analyze the determinants influencing the stability and assembly of the SLC, different variants were produced. This included constructs in which the unique sequences were deleted or in which the β -strand involved in the intermolecular β -sheet complementation of $\lambda 5$ was deleted. The extensive optimization of the purification of the WT proteins allowed pure variants to be obtained. All variants individually isolated, or in complex, showed the expected β -sheet secondary structure characteristic of functional antibodies domains in accordance with the crystal structure. Compared to the WT, $\lambda 5$ and VpreB domains which possess an unstructured amino acids at N and C

Results and Discussion

terminus, respectively, the β -sheet spectra is more pronounced for the deleted unique region constructs. Additionally, the complex stability did not significantly vary, while the thermal and chemical denaturation of isolated variants reveal an increase in stability (Figure 26). This increase in stability is more pronounced for the isolated variants of $\lambda 5$ domain. Considering that $\lambda 5$ homologue C_L is a very stable domain that can fold autonomously to a monomeric state (Goto et al, 1979), and the " C_L " of $\lambda 5$ is the variants $\lambda 5\Delta U\Delta\beta$, is not surprising that this variant shows a high chemical stability. This suggests that the β -strand and the unique region have a destabilization effect on the proteins, which may be a mechanism to insure the interaction of $\lambda 5$ and VpreB before encountering the HC. This hypothesis is in accordance with Minegishi et al., as $\lambda 5$ cannot be secreted without the VpreB, in the presence of its unique region (Minegishi et al, 1999). The complex formation of the variants was validated by aUC. In agreement with previously published *in vivo* data (Minegishi et al, 1999), complex formation is possible in the presence or absence of the unique region. However, our kinetic studies of the complex formation revealed an important effect of the unique region which was not described before. Indeed, their presence increased the stability of the complex with a dissociation constant being 20-fold lower ($K_D = 0.06 \pm 0.02 \mu\text{M}$), compared to the $\lambda 5\Delta U$ -VpreB complex ($K_D = 1.5 \pm 0.3 \mu\text{M}$), or the complex with both unique regions deleted ($0.5 \mu\text{M} < K_D < 1 \mu\text{M}$). These results reveal that the importance of the unique region is not limited to signaling as suggested previously (Knoll et al, 2012; Ohnishi & Melchers, 2003). They also have a considerable effect in maintaining the non covalently-linked complex. Additionally, the 24 amino acid unique tail of VpreB contains six negatively charged residues and the 50 amino acids unique tail of $\lambda 5$; eight positively charged arginine/lysine residues (Bradl et al, 2003; Guelpa-Fonlupt et al, 1994). The opposite charges may also explain the strong interaction of the complex in the presence of the unique regions (Figure 26).

Furthermore, it has been shown that the unique region have a plasticity that could permit them to adapt to diverse CDR3s (Martin et al, 2003). However, its interaction with and selection of CDRs remains unknown. Our biophysical study of the interaction of V_H with the SLC variants reveals a lower affinity, a K_D apparent in the μM range, compared to the data from Gauthier (Gauthier et al, 1999) in which K_D were reported in

the nM range. This difference may be explained by the different approaches used, as not only were proteins expressed in the baculovirus system but the immobilized protein was the VpreB or the single chain of SLC (3X (GSSSS) linker between VpreB and $\lambda 5$) or the F_d (V_H-C_H1). Considering the data from Ubelhart et al (2010), who demonstrated the importance of the glycosylation of an asparagine at position 46 of the V_H domain for interaction with SLC and expression of the preBCR in the cell surface, the lack of glycosylation in our domains expressed in *E. coli* can decrease the affinity. Additionally, SPR requires the immobilisation of the ligand which can be disadvantageous for the accessibility of the binding partner. However, in the SPR study from Hirabayashi et al (1995), in which VpreB was expressed in *E. coli*, the apparent K_D values are within the μ M range that were observed here. Furthermore, previous work has demonstrated that the K_D range of conventional V_H-V_L association is in the μ M, in accordance with our results (Glockshuber et al, 1990). On the one hand, the interaction of the additional β -sheet present in the $\lambda 5$ domain could interact with the V_H domain in the absence of the VpreB protein. On the other hand, we cannot rule out the binding being a result of the hydrophobic interaction between domain as the $\lambda 5\Delta U\Delta\beta$ variant could also interact with the V_H domain, which does not occur in nature. Moreover, we found that the presence of the unique region of VpreB increased the affinity for the V_H domain by at least three-fold. The difference encountered between the V_H Mak33 from IgG and the V_H 1HEZ from human IgM are caused by the homodimerization of the human domain. Thus, the K_D measured includes an exchange of the homodimers to heterodimer with the analyte. Isolated VpreB has a slightly higher affinity for the V_H compared to the SLC complex, but a significant difference is observable when the unique regions are deleted (Figure 26). These results show the importance of the unique regions in the interaction with the V_H domain.

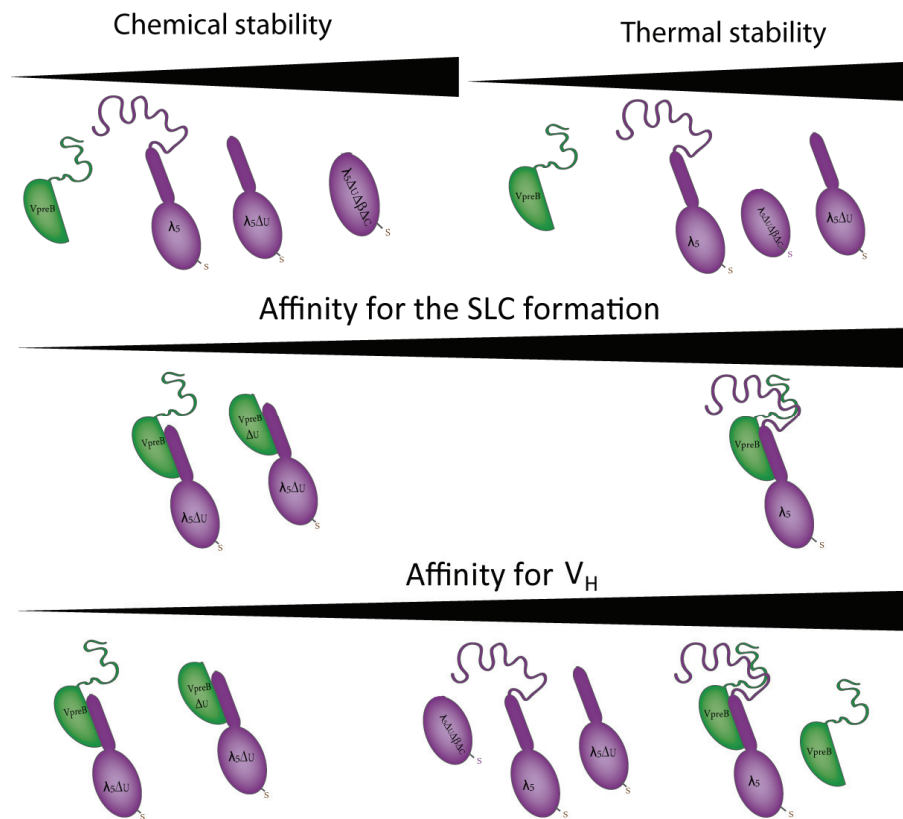


Figure 26: Overview of the different variants effects. Comparison of the chemical and thermal stability between the isolated variants (upper panel). SLC complex formation stability depending on the unique regions presence (middle panel); and the affinity for V_H domain depending on the different isolated or in complex variants (lower panel). $\lambda 5$ WT and variants in violet and VpreB WT and variant in green.

Taken together the findings indicate that the unique regions do not only play an opposite role in the surface representation of the pre-BCR, VpreB unique region fixes the pre-BCRs on the surface, while the non-Ig part of $\lambda 5$ crosslinks for the down regulation of the receptor (Knoll et al, 2012), but they also have an opposite effect in the stability, formation and interaction with the HC. More precisely, their presence is enough to decrease the thermal and chemical stability, but also increased the complex formation stability and the affinity for the V_H domain.

3.3 Effect of SLC proteins on the folding of the antibody C_H1 domain

SLC is an important component of the immune system as it checks the quality of HCs before the expression of LCs. Moreover, the SLC-HC interaction is a prerequisite for the continuation of B-cell development (Melchers, 2005; Nishimoto et al, 1991). To address

the function of the SLC in HC selection, we reconstituted the C_H1 domain interaction with the SLC proteins *in vitro*.

3.3.1 Association of the C_H1 domains with SLC proteins

It was shown previously that the C_H1 domain is a limiting factor in antibody secretion (Hendershot et al, 1987a) and that it is unfolded in the absence of the C_L domain (Feige et al, 2009). Additionally, reduced C_H1 is not able to assemble with C_L (Feige et al, 2009). Therefore, oxidized C_H1 was used in all experiments as a prerequisite for the association of C_H1 with C_L domain and consequently for inducing structure formation in C_H1.

Folding of the C_H1 domain can be monitored by CD spectroscopy. The CD signal for all proteins was monitored over time for all proteins until it reached a plateau, which corresponds to the folded C_H1 domain. In the absence of its C_L partner, C_H1 showed the characteristic signal of an unfolded protein (Figure 27 B). In the presence of C_L, folding of the C_H1 domain was induced (Figure 27 A) in agreement with the literature (Feige et al, 2009). The presence of $\lambda 5\Delta U\Delta\beta$ instead of C_L, we also observed a folding reaction (Figure 27). The rate constant of this reaction was around 30 min, consistent with previously determined values (Feige et al, 2009). Adding VpreB to unfolded C_H1 did not change the CD signal indicating that the VpreB was not able to influence the conformational state of C_H1 (Figure 27 A). In contrast, in the presence of the $\lambda 5\Delta U\Delta\beta$, a change on the signal was detected, and the spectrum for the folded C_H1 could be calculated after subtracting the $\lambda 5\Delta U\Delta\beta$ spectrum to the $\lambda 5\Delta U\Delta\beta$ -C_H1 spectrum (Figure 27 B). These results are in accordance with the folding model of the C_H1 domain in the presence of SLC, where the C_H1 domain requires the SLC to displace BiP (Vettermann et al, 2006), allowing the domain to fold and be further secreted. Due to the unfolded region in the WT domains, we could not determine the folding constant of C_H1 by far-UV CD in their presence.

Results and Discussion

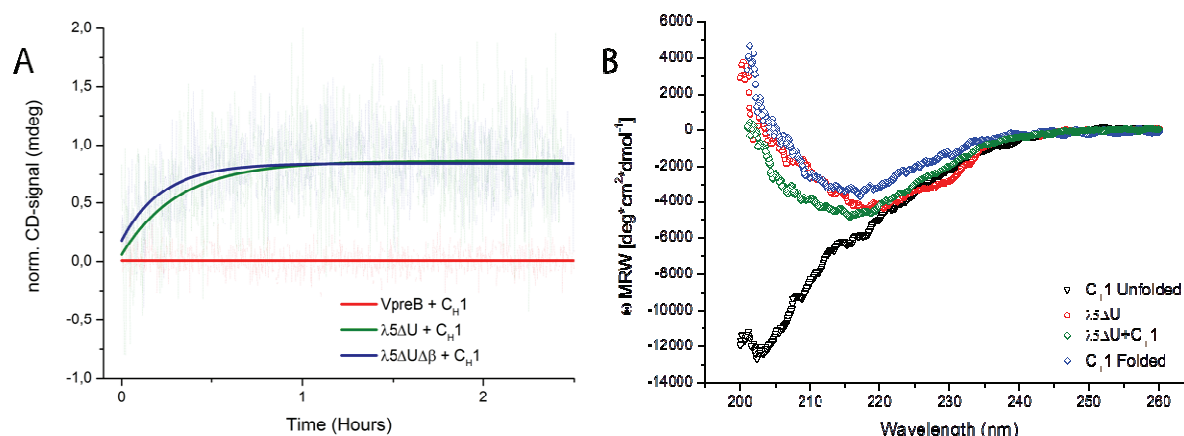


Figure 27: Folding of the human C_H1 domain. (A) The folding upon binding of C_H1 and λ5ΔU or λ5ΔUΔβ was monitored by the changes in signal at 205 nm by FUV-CD spectroscopy (10 μM CH1, 10 μM of partner, 25 °C). A single exponential trace was observed and fit to an exponential decay to obtain the folding rate and K_{obs} of the reaction. (B) The CD spectra of the folded C_H1 can be acquired by subtracting the λ5ΔU spectrum from the λ5ΔU-C_H1 spectrum.

The secondary structure formation in the association-coupled folding of the C_H1 domain of murine IgG Mak33 and human C_H1 were determined in the presence of different variants. The folding rate (τ) and K_{obs} for all variants are summarized in Table 5. The SLC variants, as isolated proteins or in complex, share the associated-coupled folding of C_H1 in their presence (murine Mak33 or human). The K_{obs} values are in good agreement with the murine C_H1 which shows a folding rate of 0.07 min⁻¹. Hence, the SLC variants share the same features as murine or human C_L for folding the unstructured, isolated C_H1 domain. The K_{obs} are in a similar range and no considerable difference was observed between the folding of C_H1 in the presence of the isolated proteins or in complex.

To verify the quaternary structure of the complex formed by the association of C_H1 with the SLC proteins, aUC was used. Consistently, the experiment revealed a shift of the s-values of the single labeled protein (λ5 or λ5ΔU), when increasing amount of unlabeled C_H1 was added (Figure 28). These experiments confirmed the concentration-dependent formation of C_H1-SLC variant heterodimers.

Table 5: τ and K_{obs} determination by FUV-CD spectroscopy.

	C_{H1} Mak 33		C_{H1} Human	
	τ (min)	K_{obs} (min^{-1})	τ (min)	K_{obs} (min^{-1})
C_I Mak33	15 ± 0.7	0.07	18.5 ± 3.5	0.054
C_I Human	ND	ND	25.1 ± 1.5	0.04
$\lambda 5\Delta U$	22 ± 3.6	0.05	23.5 ± 1.3	0.75
$\lambda 5\Delta U\Delta Cyst$	52 ± 7.4	0.02	31 ± 6.5	0.035
$\lambda 5\Delta U\Delta\beta$	38 ± 4.5	0.03	23 ± 1.8	0.05
$\lambda 5\Delta U\Delta\beta\Delta Cyst$	27 ± 3.3	0.04	18.5 ± 4.3	0.057
$\lambda 5\Delta U$ -VpreB	30 ± 3.1	0.06	8 ± 0.6	0.13
$\lambda 5\Delta U$ -VpreB ΔU	16 ± 1.5	0.03	18.8 ± 1.2	0.053

τ rate of the reaction and $K_{obs} = (1/\tau)$ were determined by CD measurement as described in Figure 27. The experiments were performed at least 3 times. ND indicates that no signal difference could be observed. Values are average \pm standard deviation.

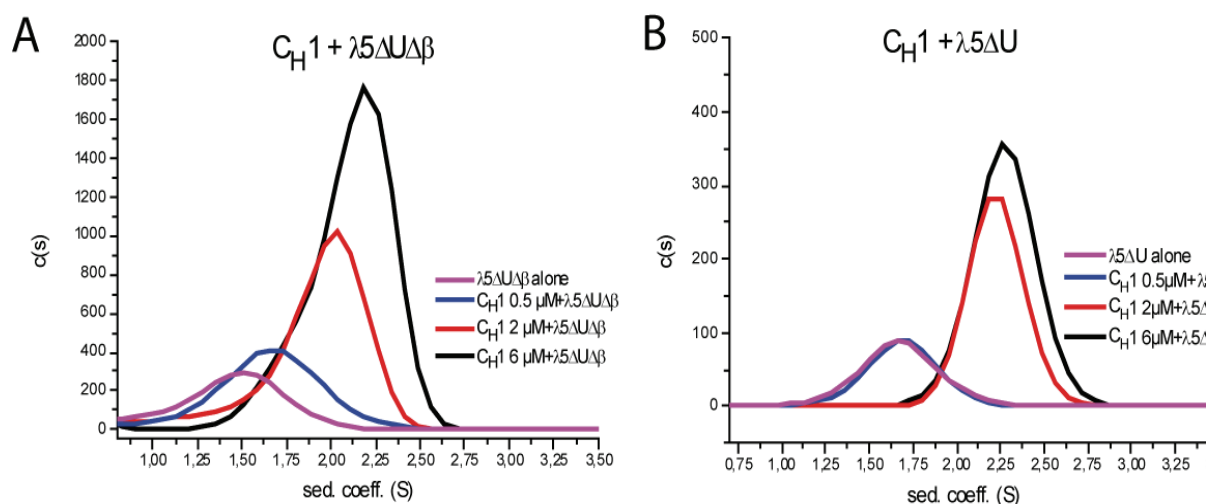


Figure 28: Binding of CH1 to $\lambda 5\Delta U\Delta\beta$ and $\lambda 5\Delta U$. aUC sedimentation velocity experiments with constant concentration of $\lambda 5\Delta U\Delta\beta$ (A) and $\lambda 5\Delta U$ (B), and increasing concentration of C_{H1} Mak33. Measurements were performed at 20 °C in 50 mM Hepes, 150 mM KCl, pH 7.5.

3.3.2 Atomic level description of the C_{H1} folding pathway

To resolve folding of the C_{H1} domain with atomic-level resolution, NMR experiments were performed. The isolated ¹⁵N labeled C_{H1} showed a ¹H-¹⁵N HSQC spectrum which is characteristic of an unstructured protein. Based on previous studies (Feige et al, 2009), a comparison of the C_{H1} folding in association with either C_L or λ5ΔUΔβ was carried out (Figure 29). The folding was followed by real time ¹⁵N HSQC spectra. Results showed the dispersion of the spectra which confirmed the complete folding of C_{H1} in the presence of C_L or λ5ΔUΔβ.

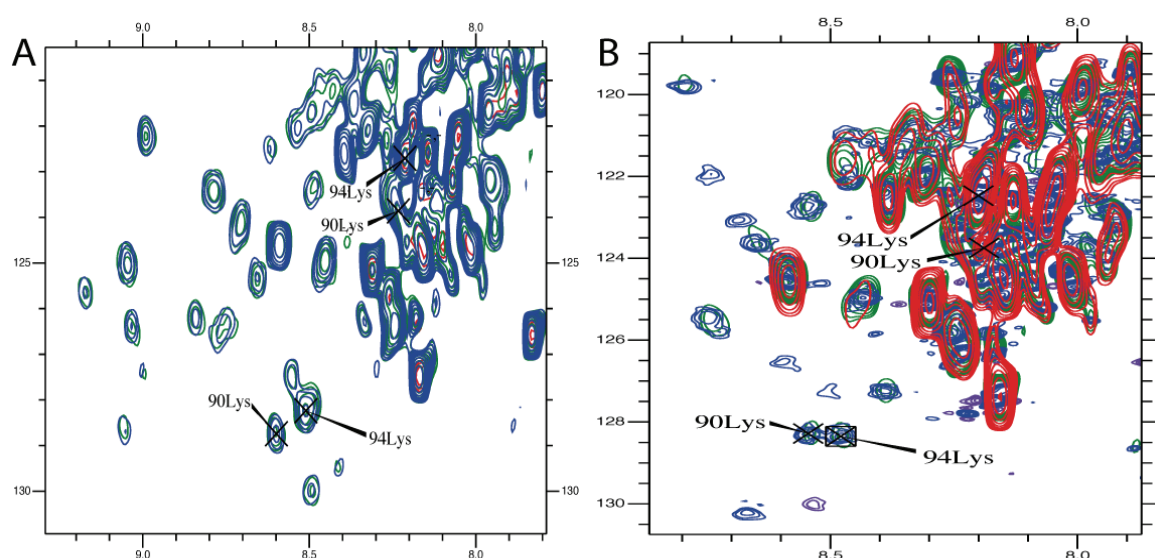


Figure 29: NMR spectroscopic characterization of λ5ΔUΔβ-induced C_{H1} folding. ¹⁵N-HSQC spectra of the C_{H1} domain in the presence of C_L (A) or λ5ΔUΔβ (B). ¹⁵N-HSQC spectra recorded every 14 min at 12.5 °C immediately after mixing. Shown here is an example of changes in the intensities, upon addition of unlabeled C_L (A) or λ5ΔUΔβ (B) (molar ratio of 1:2). Intrinsically disordered C_{H1} alone in red, 700 min (in green) and 2210 min (in blue) after addition of protein.

Based on a previous study (Feige et al, 2009), the amplitude change over time could be described by a single exponential function in the presence of the SLC variant, which is slightly faster than the C_L-C_{H1} reaction (Figure 30). This further supported the idea that the C_{H1} folds upon binding to the SLC in the same manner as demonstrated by Feige and coworkers (Feige et al, 2009; Feige et al, 2010a). Thus, as for C_L and C_{H1}, the interaction of C_{H1} with SLC initiates the formation of a hydrophobic cluster leading to the association-coupled folding reaction.

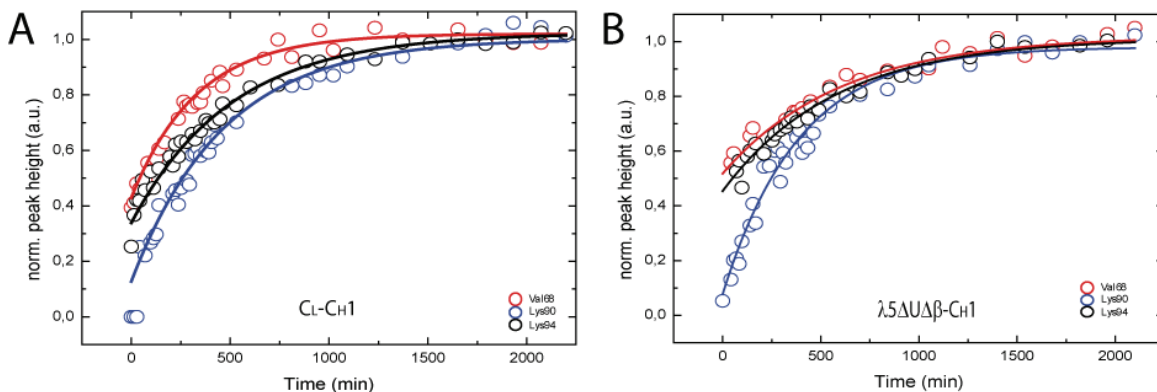


Figure 30: Folding kinetics of the C_{H1} domain. To characterize the folding of the intrinsically-disordered C_{H1} domain in the presence of $\lambda 5\Delta U\Delta\beta$, time-dependent HSQC intensities were measured upon addition of C_L (A) or $\lambda 5\Delta U\Delta\beta$ (B) to ¹⁵N-labeled C_{H1} and fitted by single exponential function. Three representative traces for Val 68 (red), Lys90 (blue) and Lys94 (black) of C_{H1} are shown. Measurements were carried out at 12.5 °C.

3.3.3 Discussion

Secretion of mature antibody molecules is controlled by the assembly of the C_{H1} domain with the C_L domain to adopt the characteristic immunoglobulin fold (Feige et al, 2010a). This association-coupled folding reaction of C_{H1} in complex with C_L additionally requires disulfide bridge formation and peptidyl-prolyl-isomerization: both reactions are readily accelerated by the ER folding machinery (Feige et al, 2009; Lee et al, 1999; Lilie et al, 1993). This comprehensive model puts the intrinsically unfolded nature of the C_{H1} domain at the center of the secretion control mechanism and, by correlation, as a limiting factor for transport of preBCR to the cell surface. The *in vitro* reconstitution of the C_{H1} complex with the SLC variants revealed the folding of the C_{H1} upon binding to the SLC variants ($K_{obs} \approx 0.04 \text{ min}^{-1}$). Additionally, concentration-dependent formation of a stable complex between the C_{H1} and SLC variants were confirmed by aUC experiments. The kinetic parameters of C_{H1} binding SLC variants agree well with previous analysis (Feige et al, 2009). The NMR spectroscopic analysis demonstrated that the folding reaction of C_{H1} in the presence of the SLC, at atomic-level resolution, is similar to the C_{H1}-C_L reaction. In the cell, folding, assembly and subsequent secretion or transport to the cell surface of preBCR involves additional factors (Meunier et al, 2002). The molecular chaperone BiP, present in high concentrations in the ER, is part of the SEC-translocon and interacts co-translationally with the nascent chain (Alder et al, 2005;

Brodsky et al, 1995). Hence, BiP plays an important role in retaining the unassembled HC in the ER (Haas & Wabl, 1983; Lee et al, 1999). Based on Feige et al results, where the C_H1 domain is released from BiP in presence of the C_L domain (Feige et al, 2009), our results confirm the hypothesis that the λ 5 domain releases the μ -chain from its interaction with BiP (Melchers, 1999). The interaction with the SLC initiates the formation of a hydrophobic cluster in the C_H1 domain and subsequent the prolyl-isomerization leads to covalent bond between λ 5 and C_H1. Taken together, our data demonstrate the detailed by which SLC interaction with the C_H1 domain allows the transport of the preBCR to the cell surface. Accordingly, the nature of the reaction that governs C_H1 folding and assembly with SLC allows the efficient and accurate assembly of the preBCR prior to transport to the cell surface as a general mechanism of quality control of the HC.

3.4 Interaction of SLC proteins with F_d fragment of the HC: preliminary results

The overall architecture of the pre-BCR is shown in Figure 10. The SLC/HC pair contains a similar architecture of Ig-like domains to a Fab fragment, but the non-covalent interaction of VpreB and λ 5 relies on divergent β -strands. In this arrangement, the λ 5 unique region substitutes for the J region of a normal V_L that follows LC CDR3 (CDR3-L) and is involved in the V_H/V_L interface. Thus, the two non Ig-like regions would protrude in the same position as the CDR3 of V_L (Figure 31). The interaction of the SLC unique regions with the CDR3 of V_H, was suggested by Bankovich et al (2007). This mechanism is in agreement with the selection function of the HC by the SLC (Melchers, 2005). Here, we set out to study the position of the SLC unique regions in the complex F_d-SLC, to confirm the model by which the flexible regions are involved in the signaling and the quality control of the V_H domain, and, more precisely, its CDR3.

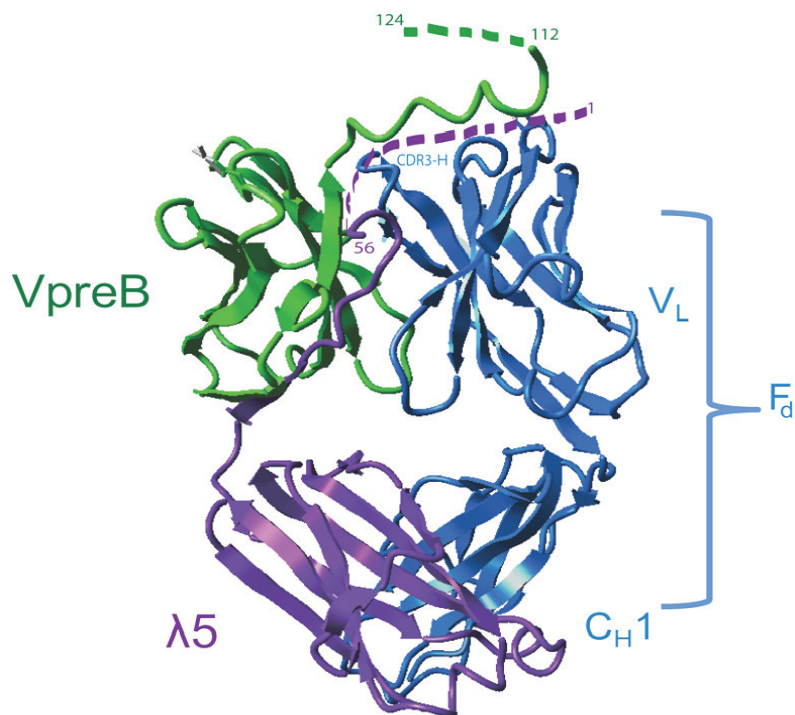


Figure 31: The F_d-SLC complex structure. Ribbon representation of the pre-BCR structure, PDB: 2H32 (Bankovich et al, 2007). Three proteins chains are included in the model: VpreB (green), λ5 (violet), and F_d (blue). Missing portions of the molecule are indicated with residue numbers and dashed lines at N terminus of λ5 (48 amino acids) and C terminus of VpreB (15 amino acids).

3.4.1 Basic structural characterization of the F_d-SLC

In order to gain a more detail insight of the F_d-SLC complex, the sequence of F_d from the crystal structure (PDB. 2H32) was synthesized by GeneArt® (Thermo Fisher Scientific) with codon optimization for expression in *E. coli* in pET28b vector, and a C-terminal Flag-tag added to facilitate the purification. Previous work has shown that the isolated F_d fragment can only be handled in the presence of high concentrations of denaturants (Buchner & Rudolph, 1991). It is however possible to obtain the F_{ab} complex by adding the LC to F_d to achieve F_{ab} refolding and association (Buchner & Rudolph, 1991). Based on this approach, the F_d was expressed overnight in BL21 cells and isolated from IBs as described previously (2.3.3). The IBs were then dissolved in 5 M urea buffer A (2.1.8.1) and loaded onto a Q-sepharose column (for detail see 2.3.4.2). The F_d fragment was collected in the low salt buffer and contaminants remained bound to the column. Subsequently, a size exclusion column was performed in denaturing conditions (3 M GdmCl buffer). Protein refolding was achieved by dialysis in the optimal buffer for the SLC proteins (see 3.1.2 for details), adding F_d, λ5 and VpreB or F_d, λ5ΔU and VpreBΔU

Results and Discussion

(with a concentration of 0.1 mg/ml). After refolding some contaminating proteins were still present, so further purification was needed. The complex was loaded onto a His Trap FF column with native buffers, but this was not sufficient to remove contaminating proteins. Therefore, SEC was tested but no protein peak was detected. The use of Anti-Flag® M2 Magnetic beads (Sigma, St. Louis, USA) resulted in the loss of the complex during the acidic elution (0.1 M Glycine HCl, pH 3.0). However, the use of ultracentrifugation at 45 000 rpm overnight or the HPLC SEC column (Superdex 75 10/300 GL, GE Healthcare, Freiburg, Germany) resulted in a purer protein preparation (Figure 32). It is important to note that the F_d -SLC complex interacted with this column, as observed before (section 3.1.3), and so the complex size could not be determined by this method. The presence of the purified protein was verified by mass spectroscopy.

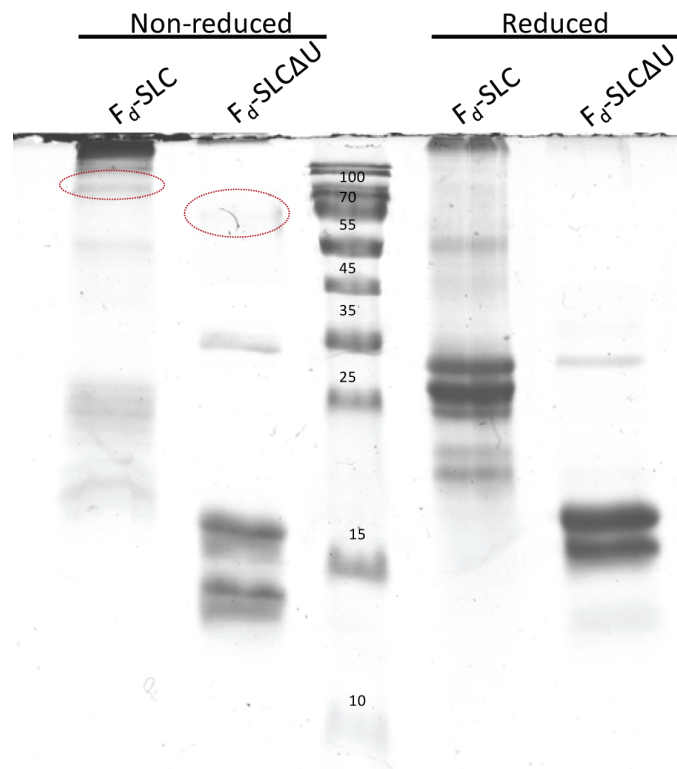


Figure 32: Representative gel of the final purified F_d -SLC and F_d -SLCAU complex. *E. coli* expressed F_d , SLC and SLCAU were purified from IBs in denaturing condition (FF his-trap and SEC) and refolded together. After optimization of the native purification condition (as described in the text) the final purification is shown in this gel. Non-reducing condition on the left side and reducing condition on the right side. The complexes of F_d -SLC and F_d -SLCAU with the disulfide bond formation are indicated by the red circles.

CD spectroscopy was used to validate our purification protocol and gain insight into the structure of the F_d -SLC complex and the influence of the unique regions. The secondary structure of F_d -SLC and F_d -SLCAU was dominated by β -sheet spectra in the FUV

measurements, in agreement with the crystal structure (Figure 33 A). Furthermore, compared to the SLC complex with or without unique region the spectra in the presence of the unique region showed a less pronounced minimum for F_d-SLC compare to F_d-SLCΔU. This can be explained by the unstructured amino acids unique regions. To garner tertiary structural information NUV-CD spectroscopy was performed. The two complexes showed defined and similar finger print NUV-CD spectra (Figure 33 B). We then measured the temperature-induced unfolding to address the influence of the unique regions on the overall stability of the complexes. Thermal melting curves were monitored by changes in the FUV-CD signal at 220 nm, and the midpoints of thermal transition determined to be: F_d-SLC = 57 ± 1.3 °C and F_d-SLCΔU = 54 ± 6.2 °C. There was no significant difference between the melting temperatures measured.

Complex formation was validated by aUC (Figure 33 C and D). For both complexes sedimentation coefficients were obtained in accordance with the expected complex sizes. The F_d-SLC sedimented with 3.4 S with a calculated molecular mass of 58.8 KDa (theoretical = 66.0 KDa) and the F_d-SLCΔU sedimented with 3.2 S for a calculated molecular mass of 54.1 KDa (theoretical = 57.9 KDa). In comparison to the SLC and SLCΔU complexes, the peak shifted towards higher s values in agreement with F_d-SLC and F_d-SLCΔU complex formation independent of the unique regions.

Results and Discussion

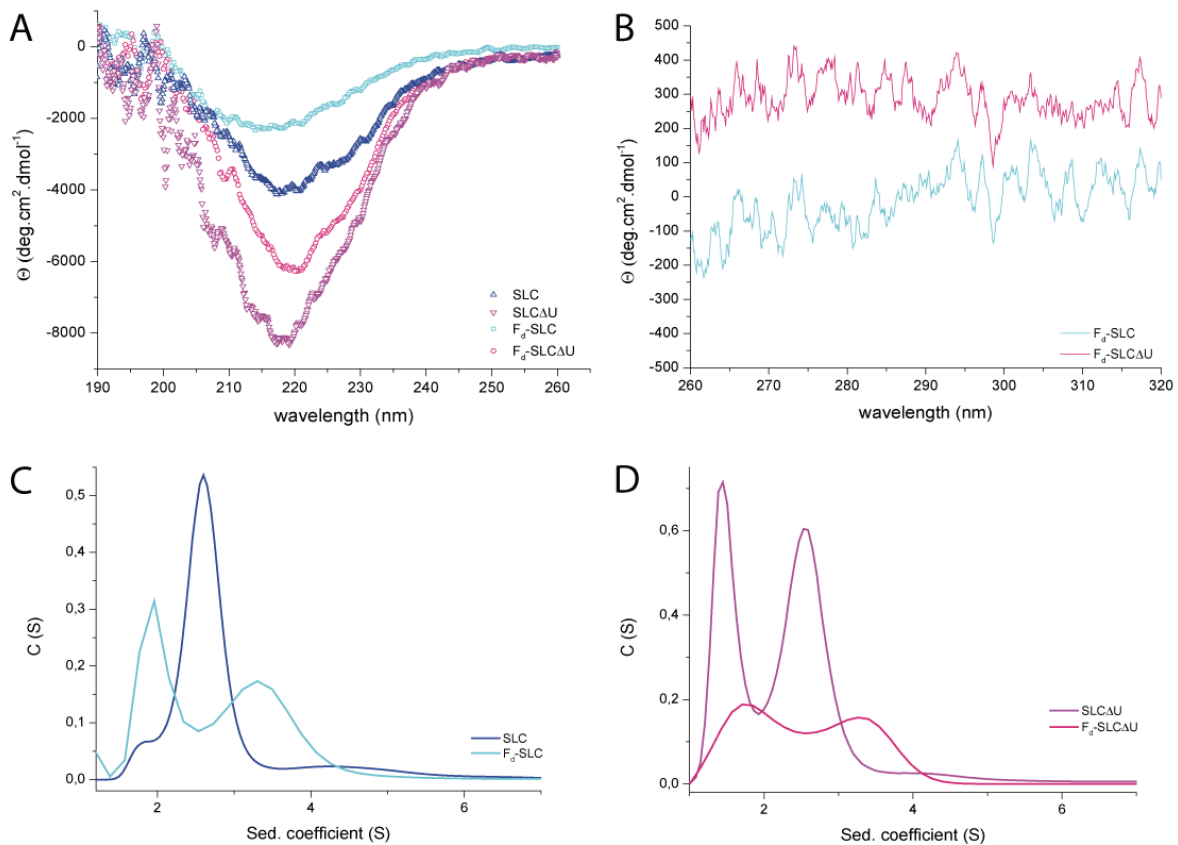


Figure 33 : Secondary, tertiary and quaternary structure of Fd-SLC and Fd-SLCΔU complexes. (A) FUV-CD spectra of F_d-SLC (light blue), F_d-SLCΔU (pink) in comparison to the complexes alone SLC (blue) and SLCΔU (magenta) are shown. (B) NUV-CD spectra of F_d-SLC (light blue) and F_d-SLCΔU (pink) are shown. For the spectra 16 accumulations each were recorded and buffer-corrected. (C) and (D) aUC sedimentation velocity experiments at 45 000 rpm as described in Figure 19. All measurements were performed at 20 °C in 50 mM Hepes, 150 mM KCl, pH 7.5.

3.4.2 Structural model of the SLC-Fab

To address whether the pre-BCR is capable of recognizing an antigen, we combined the SLC variants with the V_H domain against creatine kinase (V_H Mak33). The biotinylated antigen was immobilized to a streptavidin-coated 96-microwell plate and the V_H domain was labeled with a FLAG-tag at the C-terminus for detection. The tag does not influence the interaction between the V_H-V_L interactions as shown by Dr. Eva-Maria Herold. An anti-FLAG antibody coupled to horseradish peroxidase allowed detection of the bound domains. This method allows a qualitative read out of the interaction of the SLC variants pair to the V_H domain for antigen recognition. The binding ability of the V_H-Flag-V_L was our positive control for efficient binding to the antigen, while V_H-Flag alone was the negative control (Figure 34). The binding capacity of the pair V_H-SLC and V_H-λ5 at low

concentrations was less than the negative control, which meant that no substantial interactions with the antigen were detected. Interestingly, V_H - $\lambda 5$ shows an activity at high concentrations while V_H -VpreB exhibited a strong interaction even at low concentrations. The binding ability of V_H -SLC Δ U and V_H - $\lambda 5\Delta$ UVpreB was stronger, but still two-fold less compared to the positive control. This preliminary data demonstrated the negative influence of the unique region on antigen binding, as a decrease was observed in their presence. However, the unique region of VpreB alone did not appear to block antigen binding.

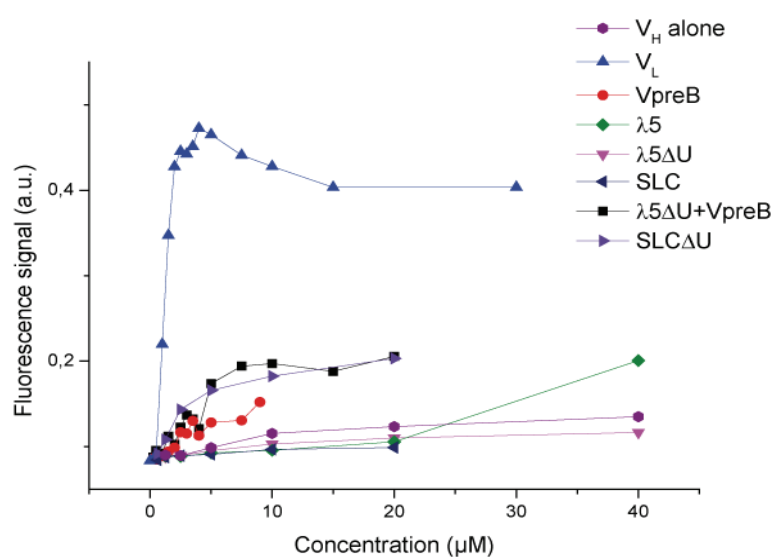


Figure 34: ELISA with SLC variants to determine the influence of the unique regions on antigen binding.

To determine the position of the unique region in the complex of SLC variants and V_H domain, an ELISA was performed. Biotinylated human creatine kinase was coupled to a streptavidin-coated microwell plate. Wild type V_H was labeled with a FLAG-tag at the C-terminus and could be detected with an anti-FLAG antibody couple to horseradish peroxidase. The couple V_H - V_L in blue is a representative of an active antigen recognition coupling. V_H was the negative control. The absorption was recorded at 405 nm at the signal maximum (after 15 min). Experiments were performed at 20 °C.

3.4.3 Discussion

The biophysical study of the F_d -SLC is at an early stage as the pure F_d -SLC complex is required to elucidate the molecular determinants of preBCR formation. Here, we describe the purification protocol used to obtain the SLC- F_{ab} fragment in the presence or absence of the unique regions. The yield obtained for F_d -SLC was 0.23 mg and for the F_d -SLC Δ U it was 0.098 mg for approximately 10 g of cells. But the purity decreased in the presence of the unique regions similar to the results obtained with the isolated SLC complex. Nevertheless, the F_d -SLC and F_d -SLC Δ U displayed a β -Sheet secondary

Results and Discussion

structure characteristic of functional antibodies and a similar finger print in their tertiary structure. The thermal midpoint of approximate 55 °C for both complexes did not show significant destabilization in the presence of the unique regions, as observed with the isolated SLC proteins, but a slight increase in the thermal stability in their presence (+ 3 °C). Formation of the SLC-F_{ab} complex was demonstrated by aUC velocity run. In non-reducing gel, we observed that approximately 70 % of the F_d-SLC complex formed the disulfide bond between λ5 and C_H1, while for F_d-SLCΔU it was the case in 15 % of the complexes. Despite this substantial difference, the complexes were still formed based on the hydrophobic interface between the SLC-F_d as for LC-HC previously described (Azuma & Hamaguchi, 1976; Lappalainen et al, 2008; Lilie & Buchner, 1995). The aUC data showed that a disulfide bridge and the unique regions are not essential for the “SLC-Fab” complex formation, in accordance with the literature (Bankovich et al, 2007; Minegishi et al, 1999). The successful refolding and purification of the F_d-SLC and F_d-SLCΔU allows further analysis into the positioning of the unique region using small-angle X-ray scattering (SAXS).

Furthermore, it has been shown that the unique region has plasticity that could permit the SLC to adapt to diverse CDR3s (Bankovich et al, 2007; Martin et al, 2003). Our preliminary data on the antigen recognition of V_H Mak in the presence of the different SLC variants showed an important decrease of the binding compared to the positive control V_H-V_L. This effect was reinforced in the presence of the two unique regions, as the SLC-V_H was not able to bind the antigen. These results demonstrated that the unique regions most likely interfere with the CDR3s which are contributing significantly to the binding of antibodies to their antigens (Ewert et al, 2003). This is the most flexible region regarding length and sequence (Morea et al, 1998). Surprisingly, the VpreB-V_H complex had a binding comparable to the SLCΔU-V_H suggesting that the unique region of VpreB alone is not sufficient to block antigen recognition. This is in accordance with previously published data (Smith & Roman, 2010) as the λ5 domain and its unique region are sufficient to select and discriminate SLC-incompatible HCs. Nevertheless, these are preliminary data and further analysis and experiments are needed to validate this hypothesis. This finding will make it possible to correlate the function of the non-Ig regions to its unique structure.

Conclusion and perspectives

In this thesis, the expression, refolding and purification of the SLC proteins VpreB and $\lambda 5$ was established with a view to analyze mechanistic aspects of pre-BCR formation. New insights into the folding and association behavior of the SLC were gained: on the one hand, the effect of the unique regions for SLC association and folding were demonstrated, and their effect on SLC interaction with the natural partners; V_H , C_H1 and F_d were studied. Taken together, the mechanism of the interaction between the different components of the pre-BCR was described on the single domain level for the first time.

Analysis of the single proteins of the SLC demonstrated surprising differences between the single domains and complexes. Despite a common Ig motif in the unique SLC, the non-Ig regions play an important role for the formation and stability of the SLC complex. The mechanism of folding and complex formation seems more complex than previously presumed and involves not only protein interactions, but also folding events. CD analysis of the isolated proteins and the complex gave a deeper insight into the folding behavior of SLC. We could determine that the VpreB domain is in a partially folded state while the SLC shows a defined β -sheet structure. This suggests that the partially unfolded VpreB may interact with the molecular chaperone BiP. As described in Figure 35, a model of VpreB interaction with BiP before folding in the presence of $\lambda 5$ is considered. This hypothesis needs to be confirmed with further interaction studies of VpreB, BiP and $\lambda 5$ in comparison with the VpreB Δ U+ β construct. The folding behavior of VpreB could be compared with that of the C_H1 domain, as VpreB seems to get folded in presence of its partner the $\lambda 5$ protein. Additionally, the low thermal and chemical stability of the SLC appear to be a step in assuring its interaction with the HCs. Surprisingly, deletion of the non-Ig part increased the thermal and chemical stability of $\lambda 5$ and SLC complexes. The complex formation study revealed stabilization in the presence of both unique regions. An opposite effect was found for the unique region as their presence results in a decrease of the chemical and thermal stability while increasing complex stability. These results are the first evidence of a new mechanism for SLC formation whereby VpreB

Conclusion

folds in presence of its partner and the unique regions stabilize the non-covalent association of the heterodimer.

To address the function of the SLC in HC selection, we first reconstituted the C_H1 domain interaction with the SLC proteins. CD and NMR experiments confirmed the hypothesis that the C_H1 domain folds upon interaction with the SLC in a manner similar to that shown by Feige et al (2009). These results are the first evidence that the SLC is required for the folding of the C_H1 domain. Thus, evolution of a C_H1 domain that absolutely requires assembly with a SLC for folding, allows the cells to ensure that newly produced HCs in pre-B cells will be retained unless they are able to pass that first important test: they can combine with the SLC and are transported to the cell surface only after passing this test. Future work should focus on obtaining more detailed parameters of the folding kinetics of C_H1 in the presence of the SLC; this appears to be slightly faster than C_H1 folding in presence of C_L in our NMR experiments. For this studies the folded C_H1 will have to be assigned in the presence of the SLC constructs as well as the K_D has to be determined. The model of the requirement for assembly-assisted folding of C_H1 in presence of the SLC is shown in Figure 35. The VpreB may be retained by the molecular chaperone BiP and release in presence of λ5 protein to form the SLC. In parallel, the HC protein is retained by BiP though the unfolded C_H1 in the absence of the SLC. This is a crucial step for controlling the assembly and transport of Ig proteins. Then BiP is displaced by the SLC and the folding of C_H1 occurs. The quality-control measures also the ability of the HC protein to associate with the SLC, if this association fails the apoptosis signaling starts in the cell. Those HC that fit to the SLC can have their C_H1 folded and form a disulfide bridge between the SLC and HC which allows the transport of the pre-BCR to the cell surface.

The crystal structure of the SLC-Fab fragment (Bankovich et al, 2007) suggests that the two non-Ig like regions protrude at the same position as the CDR3 of V_L. To confirm the model by which the flexible regions, that could not be crystallized, are involved in the selection of V_H domain, we established the purification of the F_d-SLC complex in the presence and absence of the unique region. Our kinetic study of the isolated proteins or complexes interacting with the V_H domain revealed an increase in affinity in the presence of the unique region. Furthermore, our ELISA study showed that the presence

of the unique region of $\lambda 5$ blocks the antigen binding of V_H ; its deletion was sufficient to restore antigen binding. Further studies on the unique regions with different length, tryptophan deletion and a mutant of the C_L domain with the β -sheet and unique region of $\lambda 5$ will allow to have a better insight on their function. This preliminary data allowed to not only dissect the mechanism of selection of HCs at the single domain level, but also to obtain a better understanding of the unique region function as well as their positioning.

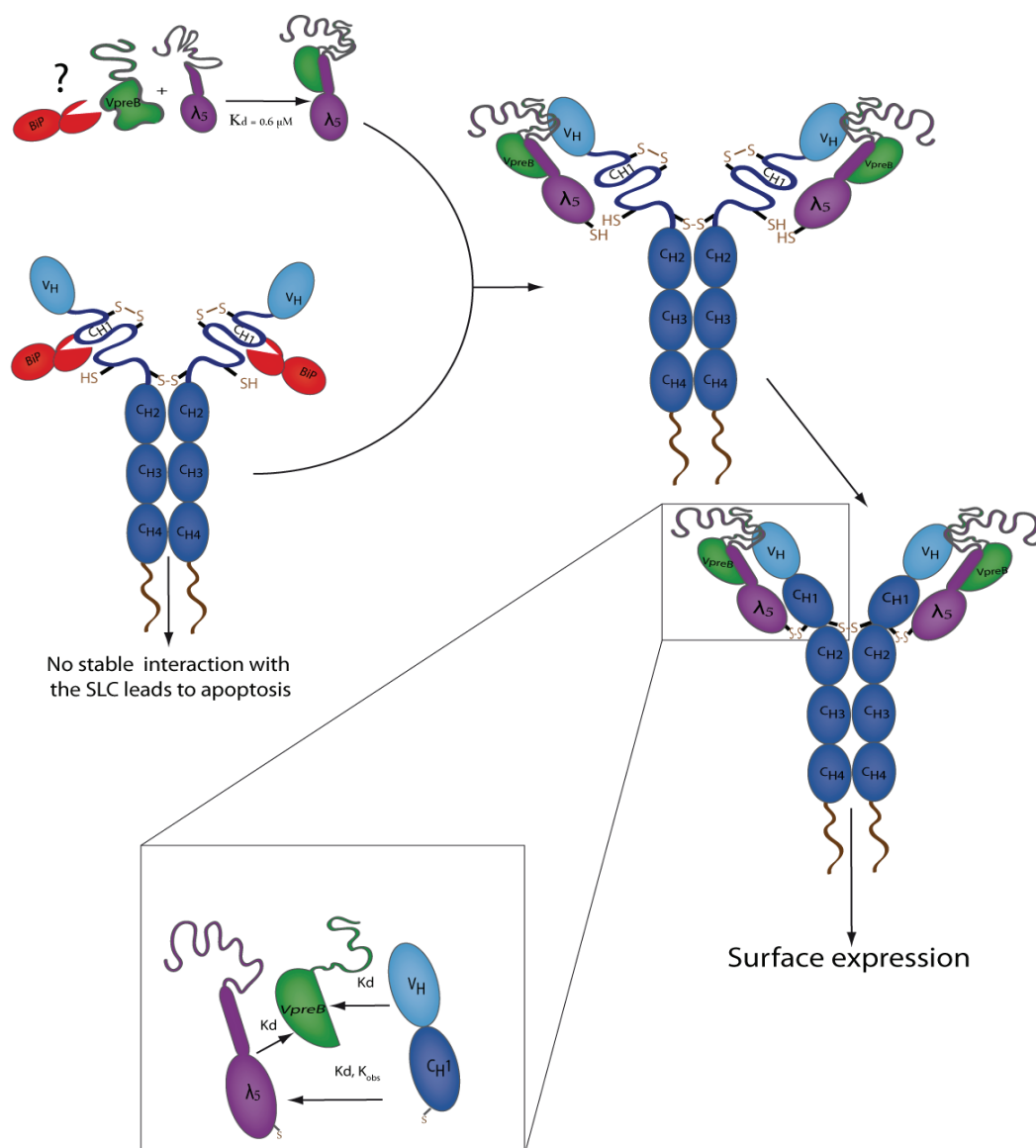


Figure 35: Mechanism of folding and assembly of the pre-BCR. The scheme indicates the possible pathway of folding, assembly and disulfide formation for the SLC and the SLC-HC complex. The partially unfolded VpreB (green) may be retained by the molecular chaperone BiP before its folding is completed by interaction with the $\lambda 5$ (violet) protein. The C_{H1} domain of the HCs (blue) remains unfolded and stably bound to BiP until the SLC displaces BiP and the SLC induces folding of the C_{H1} domain. Once all C_{H1} is folded, a disulfide bridge between the SLC and HC forms which allows the transport to the cell surface. HC membrane anchor are shown in brown. In the magnification square the different rates obtained in this work by dissecting the Fab of the pre-BCR to the isolated domain level are shown.

Conclusion

Taken together, this work provides significant new insights into the B cell development quality control, especially the folding and assembly of the SLC-Fab fragment, and paves the path for understanding the detailed mechanism of HCs selection by a unique SLC.

Abbreviations

aa	Amino acids
aUC	Analytical ultracentrifugation
BCR	B cell receptor
BiP	Heavy chain binding protein
CD	Circular dichroism
CDR	Complementary determining region
CDR-H3	CDR-3 of the heavy chain variable domain
C _H 1	First constant domain of heavy chain
C _H 2	Second constant domain of heavy chain
C _H 3	Third constant domain of heavy chain
CM5	Carboxymethylated dextran
CV	Column volume
CypB	Cyclophilin B
DNA	Deoxyribonucleic acid
DTT	Di-thiothreitol
<i>E. coli</i>	<i>Escherichia coli</i>
EDC	N,N'-1-ethyl-3-(3-dimethylaminopropyl)-carbodiimide
EDTA	ethylenedinitrilotetraacetic acid
ELISA	Enzyme linked immunosorbent assay
ER	Endoplasmic reticulum
ERAD	Endoplasmic reticulum associated protein degradation
<i>et al.</i>	And others
Fab	Fragment, antigen binding
Fc	Fragment, crystallizable
Fd	Fragment V _H +C _H 1
Fv	Fragment of variable domains
g	Gram
GdmCl	Guanidinium chloride
GSH	L-Glutathione reduced
GSSG	L-Glutathione oxidized
h	Hour
HEPES	N-(2-Hydroxyethyle)-piperazine-N'-2-ethanesulfonic acid
HPLC	High-performance liquid chromatography
HRP	Horse reddish peroxidase
Hsp	Heat shock protein
Ig	Immunoglobulin
IPTG	Isopropyl-β-D-thiogalactopyranoside
K _D	Dissociation constant

Abbreviations

KDa	Kilodalton
l	Liter
LB	Lysogeny Broth
M	Molar
min	Minute
ml	Milliliter
nM	Nanomolar
NMR	Nuclear magnetic resonance
OD ₆₀₀	Optical density at 600 nm
PBS	Phosphate buffered saline
PCR	Polymerase chain reaction
PDB ID	Protein data bank identification
PDI	Protein disulphide isomerase
PPIase	Peptidyl-prolyl- <i>cis-trans</i> isomerase
pre-BCR	Pre B cell receptor
rpm	Revolutions per minute
RT	Room temperature
SAXS	Small-angle X-ray scattering
SDS	Sodium dodecyl sulphate
SDS-PAGE	Sodium dodecylsulfate polyacrylamide gel electrophoresis
SEC	Size exclusion chromatography
SLC	Surrogate light chain
SLC Δ U	Surrogate light chain with the unique regions deleted
SOB	Super Optimal Broth
SPR	Surface Plasmon resonance
SV	Sedimentation velocity
TCEP	Tris(2-carboxyethyl) phosphine hydrochloride
TEMED	<i>N,N,N',N'</i> -Tetramethylethylenediamin
Tris	Tris(hydroxymethyl)-aminomethan
μ l	Microliter
μ M	Micromolar
UPR	Unfolded protein response
UV	Ultraviolet
V	Volt
V _L	Variable domain of light chain
V _H	Variable domain of heavy chain
v/v	Volume per volume
WT	Wild type
w/v	Weight per volume
x g	Multiple of the acceleration of gravity
Θ_{MRW}	Mean residue ellipticity

References

Alder NN, Shen Y, Brodsky JL, Hendershot LM, Johnson AE (2005) The molecular mechanisms underlying BiP-mediated gating of the Sec61 translocon of the endoplasmic reticulum. *The Journal of cell biology* **168**: 389-399

Allman D, Li J, Hardy RR (1999) Commitment to the B lymphoid lineage occurs before DH-JH recombination. *The Journal of experimental medicine* **189**: 735-740

Anfinsen CB (1973) Principles that govern the folding of protein chains. *Science* **181**: 223-230

Arnold JN, Wormald MR, Sim RB, Rudd PM, Dwek RA (2007) The impact of glycosylation on the biological function and structure of human immunoglobulins. *Annual review of immunology* **25**: 21-50

Avalos AM, Meyer-Wentrup F, Ploegh HL (2014) B-cell receptor signaling in lymphoid malignancies and autoimmunity. *Advances in immunology* **123**: 1-49

Azuma T, Hamaguchi K (1976) The mechanism of reassembly of immunoglobulin G. *Journal of biochemistry* **80**: 1023-1038

Baldwin RL (1996) Why is protein folding so fast? *Proceedings of the National Academy of Sciences of the United States of America* **93**: 2627-2628

Bankovich AJ, Raunser S, Juo ZS, Walz T, Davis MM, Garcia KC (2007) Structural insight into pre-B cell receptor function. *Science* **316**: 291-294

Baumal R, Potter M, Scharff MD (1971) Synthesis, assembly, and secretion of gamma globulin by mouse myeloma cells. 3. Assembly of the three subclasses of IgG. *The Journal of experimental medicine* **134**: 1316-1334

Boes M (2000) Role of natural and immune IgM antibodies in immune responses. *Molecular immunology* **37**: 1141-1149

Bolen DW, Santoro MM (1988) Unfolding free energy changes determined by the linear extrapolation method. 2. Incorporation of delta G degrees N-U values in a thermodynamic cycle. *Biochemistry* **27**: 8069-8074

Bork P, Holm L, Sander C (1994) The immunoglobulin fold. Structural classification, sequence patterns and common core. *Journal of molecular biology* **242**: 309-320

References

Bradford MM (1976) A rapid and sensitive method for the quantitation of microgram quantities of protein utilizing the principle of protein-dye binding. *Analytical biochemistry* **72**: 248-254

Bradl H, Wittmann J, Milius D, Vettermann C, Jack HM (2003) Interaction of murine precursor B cell receptor with stroma cells is controlled by the unique tail of lambda 5 and stroma cell-associated heparan sulfate. *Journal of immunology* **171**: 2338-2348

Brodsky JL, Goeckeler J, Schekman R (1995) BiP and Sec63p are required for both co- and posttranslational protein translocation into the yeast endoplasmic reticulum. *Proceedings of the National Academy of Sciences of the United States of America* **92**: 9643-9646

Buchner J, Rudolph R (1991) Renaturation, purification and characterization of recombinant Fab-fragments produced in *Escherichia coli*. *Bio/technology* **9**: 157-162

Bukau B, Weissman J, Horwich A (2006) Molecular chaperones and protein quality control. *Cell* **125**: 443-451

Burrows P, LeJeune M, Kearney JF (1979) Evidence that murine pre-B cells synthesise mu heavy chains but no light chains. *Nature* **280**: 838-840

Burrows PD, Stephan RP, Wang YH, Lassoued K, Zhang Z, Cooper MD (2002) The transient expression of pre-B cell receptors governs B cell development. *Seminars in immunology* **14**: 343-349

Calfon M, Zeng H, Urano F, Till JH, Hubbard SR, Harding HP, Clark SG, Ron D (2002) IRE1 couples endoplasmic reticulum load to secretory capacity by processing the XBP-1 mRNA. *Nature* **415**: 92-96

Casadevall A, Pirofski LA (2012) A new synthesis for antibody-mediated immunity. *Nature immunology* **13**: 21-28

Clark PL (2004) Protein folding in the cell: reshaping the folding funnel. *Trends in biochemical sciences* **29**: 527-534

Conley ME, Burrows PD (2010) Plugging the leaky pre-B cell receptor. *Journal of immunology* **184**: 1127-1129

Cooper MD (2015) The early history of B cells. *Nature reviews Immunology*

Dalziel M, Crispin M, Scanlan CN, Zitzmann N, Dwek RA (2014) Emerging principles for the therapeutic exploitation of glycosylation. *Science* **343**: 1235681

- Dashivets T, Wood N, Hergersberg C, Buchner J, Haslbeck M (2009) Rapid matrix-assisted refolding of histidine-tagged proteins. *ChemBiochem : a European journal of chemical biology* **10**: 869-876
- Decker DJ, Boyle NE, Koziol JA, Klinman NR (1991) The expression of the Ig H chain repertoire in developing bone marrow B lineage cells. *Journal of immunology* **146**: 350-361
- Dill KA (1990) Dominant forces in protein folding. *Biochemistry* **29**: 7133-7155
- Dill KA, Chan HS (1997) From Levinthal to pathways to funnels. *Nature structural biology* **4**: 10-19
- Dobson CM (2002) Getting out of shape. *Nature* **418**: 729-730
- Dobson CM, Karplus M (1999) The fundamentals of protein folding: bringing together theory and experiment. *Current opinion in structural biology* **9**: 92-101
- Ehlich A, Schaal S, Gu H, Kitamura D, Muller W, Rajewsky K (1993) Immunoglobulin heavy and light chain genes rearrange independently at early stages of B cell development. *Cell* **72**: 695-704
- Elantak L, Espeli M, Boned A, Bornet O, Bonzi J, Gauthier L, Feracci M, Roche P, Guerlesquin F, Schiff C (2012) Structural basis for galectin-1-dependent pre-B cell receptor (pre-BCR) activation. *The Journal of biological chemistry* **287**: 44703-44713
- Ellgaard L, Helenius A (2003) Quality control in the endoplasmic reticulum. *Nature reviews Molecular cell biology* **4**: 181-191
- Ellis RJ, Hartl FU (1999) Principles of protein folding in the cellular environment. *Current opinion in structural biology* **9**: 102-110
- Ellis RJ, Minton AP (2003) Cell biology: join the crowd. *Nature* **425**: 27-28
- Ericsson UB, Hallberg BM, Detitta GT, Dekker N, Nordlund P (2006) Thermofluor-based high-throughput stability optimization of proteins for structural studies. *Analytical biochemistry* **357**: 289-298
- Espeli M, Mancini SJ, Breton C, Poirier F, Schiff C (2009) Impaired B-cell development at the pre-BII-cell stage in galectin-1-deficient mice due to inefficient pre-BII/stromal cell interactions. *Blood* **113**: 5878-5886
- Ewert S, Huber T, Honegger A, Pluckthun A (2003) Biophysical properties of human antibody variable domains. *Journal of molecular biology* **325**: 531-553

References

Fairbank G, Steck TL, Wallach DFH (1971) Electrophoretic Analysis of Major Polypeptides of Human Erythrocyte Membrane. *Biochemistry* **10**: 2606-&

Feige MJ, Buchner J (2014) Principles and engineering of antibody folding and assembly. *Biochimica et biophysica acta* **1844**: 2024-2031

Feige MJ, Groscurth S, Marcinowski M, Shimizu Y, Kessler H, Hendershot LM, Buchner J (2009) An unfolded CH1 domain controls the assembly and secretion of IgG antibodies. *Molecular cell* **34**: 569-579

Feige MJ, Groscurth S, Marcinowski M, Yew ZT, Truffault V, Paci E, Kessler H, Buchner J (2008) The structure of a folding intermediate provides insight into differences in immunoglobulin amyloidogenicity. *Proceedings of the National Academy of Sciences of the United States of America* **105**: 13373-13378

Feige MJ, Hagn F, Esser J, Kessler H, Buchner J (2007) Influence of the internal disulfide bridge on the folding pathway of the CL antibody domain. *Journal of molecular biology* **365**: 1232-1244

Feige MJ, Hendershot LM (2011) Disulfide bonds in ER protein folding and homeostasis. *Current opinion in cell biology* **23**: 167-175

Feige MJ, Hendershot LM, Buchner J (2010a) How antibodies fold. *Trends in biochemical sciences* **35**: 189-198

Feige MJ, Simpson ER, Herold EM, Bepperling A, Heger K, Buchner J (2010b) Dissecting the alternatively folded state of the antibody Fab fragment. *Journal of molecular biology* **399**: 719-730

Feige MJ, Walter S, Buchner J (2004) Folding mechanism of the CH2 antibody domain. *Journal of molecular biology* **344**: 107-118

Ferreon AC, Deniz AA (2011) Protein folding at single-molecule resolution. *Biochimica et biophysica acta* **1814**: 1021-1029

Fersht A (1999) *Structure and mechanism in protein science: a guide to enzyme catalysis and protein folding*: W H Freeman and Company.

Fink AL (2005) Natively unfolded proteins. *Current opinion in structural biology* **15**: 35-41

Fra AM, Fagioli C, Finazzi D, Sitia R, Alberini CM (1993) Quality control of ER synthesized proteins: an exposed thiol group as a three-way switch mediating assembly, retention and degradation. *The EMBO journal* **12**: 4755-4761

- Frydman J, Nimmesgern E, Ohtsuka K, Hartl FU (1994) Folding of nascent polypeptide chains in a high molecular mass assembly with molecular chaperones. *Nature* **370**: 111-117
- Gauthier L, Lemmers B, Guelpa-Fonlupt V, Fougereau M, Schiff C (1999) Mu-surrogate light chain physicochemical interactions of the human preB cell receptor: implications for VH repertoire selection and cell signaling at the preB cell stage. *Journal of immunology* **162**: 41-50
- Gauthier L, Rossi B, Roux F, Termine E, Schiff C (2002) Galectin-1 is a stromal cell ligand of the pre-B cell receptor (BCR) implicated in synapse formation between pre-B and stromal cells and in pre-BCR triggering. *Proceedings of the National Academy of Sciences of the United States of America* **99**: 13014-13019
- Gazumyan A, Reichlin A, Nussenzweig MC (2006) Ig beta tyrosine residues contribute to the control of B cell receptor signaling by regulating receptor internalization. *The Journal of experimental medicine* **203**: 1785-1794
- Glockshuber R, Malia M, Pfitzinger I, Pluckthun A (1990) A comparison of strategies to stabilize immunoglobulin Fv-fragments. *Biochemistry* **29**: 1362-1367
- Goto Y, Azuma T, Hamaguchi K (1979) Refolding of the immunoglobulin light chain. *Journal of biochemistry* **85**: 1427-1438
- Goto Y, Hamaguchi K (1982) Unfolding and refolding of the constant fragment of the immunoglobulin light chain. *Journal of molecular biology* **156**: 891-910
- Guelpa-Fonlupt V, Bossy D, Alzari P, Fumoux F, Fougereau M, Schiff C (1994) The human pre-B cell receptor: structural constraints for a tentative model of the pseudo-light (psi L) chain. *Molecular immunology* **31**: 1099-1108
- Guo B, Kato RM, Garcia-Lloret M, Wahl MI, Rawlings DJ (2000) Engagement of the human pre-B cell receptor generates a lipid raft-dependent calcium signaling complex. *Immunity* **13**: 243-253
- Gupta D, Tuteja N (2011) Chaperones and foldases in endoplasmic reticulum stress signaling in plants. *Plant signaling & behavior* **6**: 232-236
- Haas IG, Wabl M (1983) Immunoglobulin heavy chain binding protein. *Nature* **306**: 387-389
- Harding HP, Zhang Y, Ron D (1999) Protein translation and folding are coupled by an endoplasmic-reticulum-resident kinase. *Nature* **397**: 271-274
- Hartl FU (1996) Molecular chaperones in cellular protein folding. *Nature* **381**: 571-579

References

Haslbeck M, Franzmann T, Weinfurtner D, Buchner J (2005) Some like it hot: the structure and function of small heat-shock proteins. *Nature structural & molecular biology* **12**: 842-846

Hauser J, Verma-Gaur J, Grundstrom T (2013) Broad feedback inhibition of pre-B-cell receptor signaling components. *Molecular immunology* **54**: 247-253

Helenius A, Aebi M (2004) Roles of N-linked glycans in the endoplasmic reticulum. *Annual review of biochemistry* **73**: 1019-1049

Hellman R, Vanhove M, Lejeune A, Stevens FJ, Hendershot LM (1999) The in vivo association of BiP with newly synthesized proteins is dependent on the rate and stability of folding and not simply on the presence of sequences that can bind to BiP. *The Journal of cell biology* **144**: 21-30

Hendershot L, Bole D, Kohler G, Kearney JF (1987a) Assembly and Secretion of Heavy-Chains That do Not Associate Posttranslationally with Immunoglobulin Heavy-Chain Binding-Protein. *Journal of Cell Biology* **104**: 761-767

Hendershot L, Bole D, Kohler G, Kearney JF (1987b) Assembly and secretion of heavy chains that do not associate posttranslationally with immunoglobulin heavy chain-binding protein. *The Journal of cell biology* **104**: 761-767

Hendershot L, Wei J, Gaut J, Melnick J, Aviel S, Argon Y (1996) Inhibition of immunoglobulin folding and secretion by dominant negative BiP ATPase mutants. *Proceedings of the National Academy of Sciences of the United States of America* **93**: 5269-5274

Hendershot LM (1990) Immunoglobulin heavy chain and binding protein complexes are dissociated in vivo by light chain addition. *The Journal of cell biology* **111**: 829-837

Herzog S, Reth M, Jumaa H (2009) Regulation of B-cell proliferation and differentiation by pre-B-cell receptor signalling. *Nature reviews Immunology* **9**: 195-205

Hetz C (2012) The unfolded protein response: controlling cell fate decisions under ER stress and beyond. *Nature reviews Molecular cell biology* **13**: 89-102

Hirabayashi Y, Lecerf JM, Dong Z, Stollar BD (1995) Kinetic analysis of the interactions of recombinant human VpreB and Ig V domains. *Journal of immunology* **155**: 1218-1228

Horwich AL, Fenton WA (2009) Chaperonin-mediated protein folding: using a central cavity to kinetically assist polypeptide chain folding. *Quarterly reviews of biophysics* **42**: 83-116

Huber R, Deisenhofer J, Colman PM, Matsushima M, Palm W (1976) Crystallographic structure studies of an IgG molecule and an Fc fragment. *Nature* **264**: 415-420

Iisenman DE, Lancet D, Pecht I (1979) Folding pathways of immunoglobulin domains. The folding kinetics of the Cgamma3 domain of human IgG1. *Biochemistry* **18**: 3327-3336

Janeway C (2005) *Immunobiology : the immune system in health and disease*, 6th edn. New York: Garland Science.

Kabat EA, Wu TT, Bilofsky H (1977) Unusual distributions of amino acids in complementarity-determining (hypervariable) segments of heavy and light chains of immunoglobulins and their possible roles in specificity of antibody-combining sites. *The Journal of biological chemistry* **252**: 6609-6616

Karasuyama H, Kudo A, Melchers F (1990) The proteins encoded by the VpreB and lambda 5 pre-B cell-specific genes can associate with each other and with mu heavy chain. *The Journal of experimental medicine* **172**: 969-972

Karlin S, Brocchieri L (1998) Heat shock protein 70 family: multiple sequence comparisons, function, and evolution. *Journal of molecular evolution* **47**: 565-577

Kelly SM, Jess TJ, Price NC (2005) How to study proteins by circular dichroism. *Biochimica et biophysica acta* **1751**: 119-139

Kim PS, Baldwin RL (1982) Specific intermediates in the folding reactions of small proteins and the mechanism of protein folding. *Annual review of biochemistry* **51**: 459-489

Kitamura D, Roes J, Kuhn R, Rajewsky K (1991) A B cell-deficient mouse by targeted disruption of the membrane exon of the immunoglobulin mu chain gene. *Nature* **350**: 423-426

Kline GH, Hartwell L, Beck-Engeser GB, Keyna U, Zaharevitz S, Klinman NR, Jack HM (1998) Pre-B cell receptor-mediated selection of pre-B cells synthesizing functional mu heavy chains. *Journal of immunology* **161**: 1608-1618

Knoll M, Yanagisawa Y, Simmons S, Engels N, Wienands J, Melchers F, Ohnishi K (2012) The non-Ig parts of the VpreB and lambda5 proteins of the surrogate light chain play opposite roles in the surface representation of the precursor B cell receptor. *Journal of immunology* **188**: 6010-6017

Kozmik Z, Wang S, Dorfler P, Adams B, Busslinger M (1992) The promoter of the CD19 gene is a target for the B-cell-specific transcription factor BSAP. *Molecular and cellular biology* **12**: 2662-2672

Kozutsumi Y, Segal M, Normington K, Gething MJ, Sambrook J (1988) The presence of malfolded proteins in the endoplasmic reticulum signals the induction of glucose-regulated proteins. *Nature* **332**: 462-464

References

- Laemmli UK (1970) Cleavage of Structural Proteins during Assembly of Head of Bacteriophage-T4. *Nature* **227**: 680-&
- Lang K, Schmid FX, Fischer G (1987) Catalysis of protein folding by prolyl isomerase. *Nature* **329**: 268-270
- Lappalainen I, Hurley MG, Clarke J (2008) Plasticity within the obligatory folding nucleus of an immunoglobulin-like domain. *Journal of molecular biology* **375**: 547-559
- Lassoued K, Illges H, Benlagha K, Cooper MD (1996) Fate of surrogate light chains in B lineage cells. *Journal of Experimental Medicine* **183**: 421-429
- Lee YK, Brewer JW, Hellman R, Hendershot LM (1999) BiP and immunoglobulin light chain cooperate to control the folding of heavy chain and ensure the fidelity of immunoglobulin assembly. *Molecular biology of the cell* **10**: 2209-2219
- Levinthal C. (1969) How to fold graciously. . In DeBrunner I, JTP ME, Eds. (eds.), Mossbauer spectroscopy in biological systems. Allerton House, Monticello, Illinois: University of Illinois Press, pp. 22–24.
- Lilie H, Buchner J (1995) Domain interactions stabilize the alternatively folded state of an antibody Fab fragment. *FEBS letters* **362**: 43-46
- Lilie H, Lang K, Rudolph R, Buchner J (1993) Prolyl isomerases catalyze antibody folding in vitro. *Protein science : a publication of the Protein Society* **2**: 1490-1496
- Lindquist S, Craig EA (1988) The heat-shock proteins. *Annual review of genetics* **22**: 631-677
- Mains PE, Sibley CH (1983) The requirement of light chain for the surface deposition of the heavy chain of immunoglobulin M. *The Journal of biological chemistry* **258**: 5027-5033
- Marcinowski M, Holler M, Feige MJ, Baerend D, Lamb DC, Buchner J (2011) Substrate discrimination of the chaperone BiP by autonomous and cochaperone-regulated conformational transitions. *Nature structural & molecular biology* **18**: 150-158
- Martin DA, Bradl H, Collins TJ, Roth E, Jack HM, Wu GE (2003) Selection of Ig mu heavy chains by complementarity-determining region 3 length and amino acid composition. *Journal of immunology* **171**: 4663-4671

- Maurel M, Chevet E, Tavernier J, Gerlo S (2014) Getting RIDD of RNA: IRE1 in cell fate regulation. *Trends in biochemical sciences* **39**: 245-254
- Melchers F (1999) Fit for life in the immune system? Surrogate L chain tests H chains that test L chains. *Proceedings of the National Academy of Sciences of the United States of America* **96**: 2571-2573
- Melchers F (2005) The pre-B-cell receptor: selector of fitting immunoglobulin heavy chains for the B-cell repertoire. *Nature reviews Immunology* **5**: 578-584
- Melchers F, Karasuyama H, Haasner D, Bauer S, Kudo A, Sakaguchi N, Jameson B, Rolink A (1993) The surrogate light chain in B-cell development. *Immunology today* **14**: 60-68
- Melchers F, ten Boekel E, Seidl T, Kong XC, Yamagami T, Onishi K, Shimizu T, Rolink AG, Andersson J (2000) Repertoire selection by pre-B-cell receptors and B-cell receptors, and genetic control of B-cell development from immature to mature B cells. *Immunological reviews* **175**: 33-46
- Melchers F, ten Boekel E, Yamagami T, Andersson J, Rolink A (1999) The roles of preB and B cell receptors in the stepwise allelic exclusion of mouse IgH and L chain gene loci. *Seminars in immunology* **11**: 307-317
- Meunier L, Usherwood YK, Chung KT, Hendershot LM (2002) A subset of chaperones and folding enzymes form multiprotein complexes in endoplasmic reticulum to bind nascent proteins. *Molecular biology of the cell* **13**: 4456-4469
- Minegishi Y, Coustan-Smith E, Wang YH, Cooper MD, Campana D, Conley ME (1998) Mutations in the human lambda5/14.1 gene result in B cell deficiency and agammaglobulinemia. *The Journal of experimental medicine* **187**: 71-77
- Minegishi Y, Hendershot LM, Conley ME (1999) Novel mechanisms control the folding and assembly of lambda5/14.1 and VpreB to produce an intact surrogate light chain. *Proceedings of the National Academy of Sciences of the United States of America* **96**: 3041-3046
- Montero D, Tachibana C, Rahr Winther J, Appenzeller-Herzog C (2013) Intracellular glutathione pools are heterogeneously concentrated. *Redox biology* **1**: 508-513
- Morea V, Tramontano A, Rustici M, Chothia C, Lesk AM (1998) Conformations of the third hypervariable region in the VH domain of immunoglobulins. *Journal of molecular biology* **275**: 269-294

References

- Morstadt L, Bohm A, Yuksel D, Kumar K, Stollar BD, Baleja JD (2008) Engineering and characterization of a single chain surrogate light chain variable domain. *Protein science : a publication of the Protein Society* **17**: 458-465
- Munro S, Pelham HR (1987) A C-terminal signal prevents secretion of luminal ER proteins. *Cell* **48**: 899-907
- Murphy KMea (2008) *Janeway's Immunobiology*, 7th edition edn.: Garland Science, (New York).
- Nishimoto N, Kubagawa H, Ohno T, Gartland GL, Stankovic AK, Cooper MD (1991) Normal pre-B cells express a receptor complex of mu heavy chains and surrogate light-chain proteins. *Proceedings of the National Academy of Sciences of the United States of America* **88**: 6284-6288
- Nutt SL, Heavey B, Rolink AG, Busslinger M (1999) Commitment to the B-lymphoid lineage depends on the transcription factor Pax5. *Nature* **401**: 556-562
- Ogawa M, ten Boekel E, Melchers F (2000) Identification of CD19(-)B220(+)c-Kit(+)Flt3/Flk-2(+)cells as early B lymphoid precursors before pre-B-I cells in juvenile mouse bone marrow. *International immunology* **12**: 313-324
- Ohnishi K, Melchers F (2003) The nonimmunoglobulin portion of lambda5 mediates cell-autonomous pre-B cell receptor signaling. *Nature immunology* **4**: 849-856
- Pantoliano MW, Petrella EC, Kwasnoski JD, Lobanov VS, Myslik J, Graf E, Carver T, Asel E, Springer BA, Lane P, Salemme FR (2001) High-density miniaturized thermal shift assays as a general strategy for drug discovery. *Journal of biomolecular screening* **6**: 429-440
- Pelanda R, Schwers S, Sonoda E, Torres RM, Nemazee D, Rajewsky K (1997) Receptor editing in a transgenic mouse model: site, efficiency, and role in B cell tolerance and antibody diversification. *Immunity* **7**: 765-775
- Radford SE (2000) Protein folding: progress made and promises ahead. *Trends in biochemical sciences* **25**: 611-618
- Reth M, Petrac E, Wiese P, Lobel L, Alt FW (1987) Activation of V kappa gene rearrangement in pre-B cells follows the expression of membrane-bound immunoglobulin heavy chains. *The EMBO journal* **6**: 3299-3305
- Reth MG, Ammirati P, Jackson S, Alt FW (1985) Regulated progression of a cultured pre-B-cell line to the B-cell stage. *Nature* **317**: 353-355
- Richter K, Haslbeck M, Buchner J (2010) The heat shock response: life on the verge of death. *Molecular cell* **40**: 253-266

- Rolink A, Grawunder U, Winkler TH, Karasuyama H, Melchers F (1994) IL-2 receptor alpha chain (CD25, TAC) expression defines a crucial stage in pre-B cell development. *International immunology* **6**: 1257-1264
- Rolink A, Melchers F (1991) Molecular and cellular origins of B lymphocyte diversity. *Cell* **66**: 1081-1094
- Ron D, Walter P (2007) Signal integration in the endoplasmic reticulum unfolded protein response. *Nature reviews Molecular cell biology* **8**: 519-529
- Rudolph R, Lilie H (1996) In vitro folding of inclusion body proteins. *FASEB journal : official publication of the Federation of American Societies for Experimental Biology* **10**: 49-56
- Rutkowski DT, Hegde RS (2010) Regulation of basal cellular physiology by the homeostatic unfolded protein response. *The Journal of cell biology* **189**: 783-794
- Sambrook J, Russell DW (2011) *Molecular cloning a laboratory manual*, 3. edn. Cold Spring Harbor, NY: Cold Spring Harbor Laboratory Press.
- Saphire EO, Stanfield RL, Crispin MD, Parren PW, Rudd PM, Dwek RA, Burton DR, Wilson IA (2002) Contrasting IgG structures reveal extreme asymmetry and flexibility. *Journal of molecular biology* **319**: 9-18
- Schanda P, Brutscher B (2005) Very fast two-dimensional NMR spectroscopy for real-time investigation of dynamic events in proteins on the time scale of seconds. *Journal of the American Chemical Society* **127**: 8014-8015
- Scheibel T, Buchner J (2006) Protein aggregation as a cause for disease. *Handbook of experimental pharmacology*: 199-219
- Schmid FX (2005) *Spectroscopic techniques to study protein folding and stability*, in *The Protein Folding Handbook*,: Wiley-VCH Verlag GmbH & Co. KGaA.
- Schroeder HW, Jr., Cavacini L (2010) Structure and function of immunoglobulins. *The Journal of allergy and clinical immunology* **125**: S41-52
- Schuck P (2000) Size-distribution analysis of macromolecules by sedimentation velocity ultracentrifugation and lamm equation modeling. *Biophysical journal* **78**: 1606-1619
- Seckler R, Jaenicke R (1992) Protein folding and protein refolding. *FASEB journal : official publication of the Federation of American Societies for Experimental Biology* **6**: 2545-2552

References

Seidl T, Rolink A, Melchers F (2001) The VpreB protein of the surrogate light-chain can pair with some mu heavy-chains in the absence of the lambda 5 protein. *European journal of immunology* **31**: 1999-2006

Selkoe DJ (2003) Folding proteins in fatal ways. *Nature* **426**: 900-904

Shen Y, Hendershot LM (2005) ERdj3, a stress-inducible endoplasmic reticulum DnaJ homologue, serves as a cofactor for BiP's interactions with unfolded substrates. *Molecular biology of the cell* **16**: 40-50

Simpson ER, Herold EM, Buchner J (2009) The folding pathway of the antibody V(L) domain. *Journal of molecular biology* **392**: 1326-1338

Smith BP, Roman CA (2010) The unique and immunoglobulin-like regions of surrogate light chain component lambda5 differentially interrogate immunoglobulin heavy-chain structure. *Molecular immunology* **47**: 1195-1206

Sone M, Akiyama Y, Ito K (1997) Differential in vivo roles played by DsbA and DsbC in the formation of protein disulfide bonds. *The Journal of biological chemistry* **272**: 10349-10352

Stevens FJ, Argon Y (1999) Protein folding in the ER. *Seminars in cell & developmental biology* **10**: 443-454

Su Q, Wang S, Gao HQ, Kazemi S, Harding HP, Ron D, Koromilas AE (2008) Modulation of the eukaryotic initiation factor 2 alpha-subunit kinase PERK by tyrosine phosphorylation. *The Journal of biological chemistry* **283**: 469-475

ten Boekel E, Melchers F, Rolink AG (1997) Changes in the V(H) gene repertoire of developing precursor B lymphocytes in mouse bone marrow mediated by the pre-B cell receptor. *Immunity* **7**: 357-368

Thies MJ, Mayer J, Augustine JG, Frederick CA, Lilie H, Buchner J (1999) Folding and association of the antibody domain CH3: prolyl isomerization precedes dimerization. *Journal of molecular biology* **293**: 67-79

Thomas HI, Morgan-Capner P (1990) The avidity of specific IgM detected in primary rubella and reinfection. *Epidemiology and infection* **104**: 489-497

Tirasophon W, Welihinda AA, Kaufman RJ (1998) A stress response pathway from the endoplasmic reticulum to the nucleus requires a novel bifunctional protein kinase/endoribonuclease (Ire1p) in mammalian cells. *Genes & development* **12**: 1812-1824

- Tonegawa S (1983) Somatic generation of antibody diversity. *Nature* **302**: 575-581
- Tsubata T, Reth M (1990) The products of pre-B cell-specific genes (λ 5 and VpreB) and the immunoglobulin mu chain form a complex that is transported onto the cell surface. *The Journal of experimental medicine* **172**: 973-976
- Ubelhart R, Bach MP, Eschbach C, Wossning T, Reth M, Jumaa H (2010) N-linked glycosylation selectively regulates autonomous precursor BCR function. *Nature immunology* **11**: 759-765
- van Anken E, Braakman I (2005) Endoplasmic reticulum stress and the making of a professional secretory cell. *Critical reviews in biochemistry and molecular biology* **40**: 269-283
- Vettermann C, Herrmann K, Jack HM (2006) Powered by pairing: the surrogate light chain amplifies immunoglobulin heavy chain signaling and pre-selects the antibody repertoire. *Seminars in immunology* **18**: 44-55
- Wagner C, Kiefhaber T (1999) Intermediates can accelerate protein folding. *Proceedings of the National Academy of Sciences of the United States of America* **96**: 6716-6721
- Walter S, Buchner J (2002) Molecular chaperones--cellular machines for protein folding. *Angewandte Chemie* **41**: 1098-1113
- Wandinger SK, Richter K, Buchner J (2008) The Hsp90 chaperone machinery. *The Journal of biological chemistry* **283**: 18473-18477
- Wang YH, Nomura J, Faye-Petersen OM, Cooper MD (1998) Surrogate light chain production during B cell differentiation: differential intracellular versus cell surface expression. *Journal of immunology* **161**: 1132-1139
- Wickner S, Maurizi MR, Gottesman S (1999) Posttranslational quality control: folding, refolding, and degrading proteins. *Science* **286**: 1888-1893
- Williams AF, Barclay AN (1988) The immunoglobulin superfamily--domains for cell surface recognition. *Annual review of immunology* **6**: 381-405
- Woehlbier U, Hetz C (2011) Modulating stress responses by the UPRosome: a matter of life and death. *Trends in biochemical sciences* **36**: 329-337
- Wu TT, Kabat EA (1970) An analysis of the sequences of the variable regions of Bence Jones proteins and myeloma light chains and their implications for antibody complementarity. *The Journal of experimental medicine* **132**: 211-250

References

Xu Z, Zan H, Pone EJ, Mai T, Casali P (2012) Immunoglobulin class-switch DNA recombination: induction, targeting and beyond. *Nature reviews Immunology* **12**: 517-531

Yasukawa T, Kanei-Ishii C, Maekawa T, Fujimoto J, Yamamoto T, Ishii S (1995) Increase of solubility of foreign proteins in *Escherichia coli* by coproduction of the bacterial thioredoxin. *The Journal of biological chemistry* **270**: 25328-25331

Yoshida H, Haze K, Yanagi H, Yura T, Mori K (1998) Identification of the cis-acting endoplasmic reticulum stress response element responsible for transcriptional induction of mammalian glucose-regulated proteins. Involvement of basic leucine zipper transcription factors. *The Journal of biological chemistry* **273**: 33741-33749

Yoshida H, Matsui T, Yamamoto A, Okada T, Mori K (2001) XBP1 mRNA is induced by ATF6 and spliced by IRE1 in response to ER stress to produce a highly active transcription factor. *Cell* **107**: 881-891

Yoshida H, Okada T, Haze K, Yanagi H, Yura T, Negishi M, Mori K (2000) ATF6 activated by proteolysis binds in the presence of NF-Y (CBF) directly to the cis-acting element responsible for the mammalian unfolded protein response. *Molecular and cellular biology* **20**: 6755-6767

Young JC, Agashe VR, Siegers K, Hartl FU (2004) Pathways of chaperone-mediated protein folding in the cytosol. *Nature reviews Molecular cell biology* **5**: 781-791

Zimmerman SB, Trach SO (1991) Estimation of macromolecule concentrations and excluded volume effects for the cytoplasm of *Escherichia coli*. *Journal of molecular biology* **222**: 599-620

Zimmermann R, Eyrisch S, Ahmad M, Helms V (2011) Protein translocation across the ER membrane. *Biochimica et biophysica acta* **1808**: 912-924

Acknowledgements

First of all I would like to thank my supervisor Prof. Dr. Johannes Buchner for a stimulating and challenging PhD project, for all the ideas and advice he has given me over the past years, encouraging me in frustrating moments, providing excellent scientific equipment, and for the freedom he granted me in my fields of interest. I want to thank my thesis committee members: Prof. Dr. Michael Sattler and Dr. Andreas Bracher for taking the time and for interesting discussions. For financial support I would like to thank the IMPRS program and its members for the pleasant time during the workshops and seminars.

I thank also the members of the antibody group, past and present, Roger Müller, Eva Herold and Moritz Marcinowski for their practical advice and fruitful discussions, Mathias Rosam and Christine John who also gave me good advice and company and Christina Stutzer who will succeed me. It was a pleasure to work with you! I am also very grateful to Matthias Feige, thanks for never getting tired to answer my questions about C_H1 folding and your technical advises. To the aUC responsible Katrin Back, Jirka Peschek and Christine John thank you for your help with the aUC experiments and data analysis, it is a tricky project but your patience and investment made it possible. I want to thank Diana Gomez and Bernd Reif for their cooperation on the folding of C_H1 upon binding the λ 5 protein variant.

A special thanks goes to Dr. Martin Haslbeck for all the helpful discussions, for answering all my questions, for encouraging me and for keeping things running in the lab. Thanks to all the admins for resolving all computer problems and specially Mathias Rosam for his tireless effort! Furthermore, I would like to thank our secretaries Mrs. Hilber and Mrs. Rubinstein for their friendly support with all aspects of office work, visa and their extraordinary patience. Many thanks our technicians Bettina Richter, Ruby Khan, Anja Liebscher and Helmut Krause for their support through-out the daily routine.

I am indebted to my colleagues in the JB's lab for their laughs and the really nice time we have spend together throughout these last years and which have now become friends; especially Tanya D., Julia R., Alexandra, Jirka, Vroni, Eva H., Priyanka, Sandrine, Christoph, Hannah, Mati, Katha and Katrin. Of course not to forget thanking, fellow PhD students which whom I have developed a wonderful friendship and were there for me in the good and bad times; Nerea, Marcelino, Jo, Vane, Vale, Linda, Victor and Dianis.

I would like to thank my parents for their never-ending belief in me and their continuous support. Last but not least, I would like to thank my boyfriend Thomas Antoine for his patience, love and for always being there.

Declaration

I, Natalia Catalina Sarmiento Alam, hereby declare that this thesis was prepared by me independently. I was using only the references and resources stated here. The work has so far not been submitted to any audit commission.

Hiermit erkläre ich, Natalia Catalina Sarmiento Alam, dass ich die vorliegende Arbeit selbständig verfasst und keine anderen als die angegebenen Quellen und Hilfsmittel verwendet habe. Die Arbeit wurde bisher keiner Prüfungskommission vorgelegt.

Natalia Catalina Sarmiento Alam

München